CENTER FOR DRUG EVALUATION AND RESEARCH

APPLICATION NUMBER:

125554Orig1s000

PHARMACOLOGY REVIEW(S)

MEMORANDUM

OPDIVO (nivolumab)

Date: December 4, 2014
To: File for BLA 125554
From: John K. Leighton, PhD, DABT
Acting Director, Division of Hematology Oncology Toxicology
Office of Hematology and Oncology Products

I have examined pharmacology/toxicology supporting review for Opdivo conducted by Drs. Weis and Putman, and secondary memorandum and labeling provided by Dr. Helms. I concur with Dr. Helms' conclusion that Opdivo may be approved and that no additional nonclinical studies are needed for the proposed indication.

This is a representation of an electronic record that was signed electronically and this page is the manifestation of the electronic signature.

/s/

JOHN K LEIGHTON
12/04/2014

MEMORANDUM

Date: December 4, 2014
From: Whitney S. Helms, Ph.D.
Pharmacology Supervisor
Division of Hematology Oncology Toxicology for Division of Oncology Products 2
To: File for BLA # 125554
OPDIVO (nivolumab)
Re: Approvability of Pharmacology and Toxicology

On, July 30, 2014 Bristol-Myers Squibb (BMS) completed the submission of biological license application (BLA) 125554 for nivolumab for the treatment of patients with unresectable or metastatic melanoma and disease progression following ipilimumab, and, if BRAF V600 mutation positive, a BRAF inhibitor. Nivolumab was granted breakthrough designation for this indication on September 11, 2014. Non-clinical studies examining the pharmacology and toxicology of nivolumab provided to support BLA 125554 were reviewed in detail by Shawna L. Weis, Ph.D. and Alexander H. Putman, Ph.D. The findings of these studies are summarized in the "Executive Summary" of the BLA review and reflected in the product label.

Nivolumab is a fully human IgG4 monoclonal antibody targeting programmed cell death 1 (PD-1). BMS submitted pharmacology studies demonstrating that nivolumab is able to bind PD-1 from both humans and cynomolgus monkeys and to prevent the interaction of PD-1 with its ligands, PD-L1 and PD-L2. This interaction plays an important role in the maintenance of self-tolerance and the prevention of unnecessary tissue damage following immune activation after acute infection by downregulating the immune response. Blocking this signaling pathway thus enhances immune reactivity and, by extension, can serve to enhance tumor immunosurveillance and the anti-tumor immune response. A murine surrogate of nivolumab was able to delay or prevent tumor cell growth in several syngeneic murine xenograft tumor models. Nivolumab did not mediate complement dependent cytotoxicity, antibody dependent cellular cytotoxicity, or to directly elicit cytokine release from cells in the absence of TCR activation.

General toxicology studies of nivolumab administered either weekly (4 week study) or twice weekly (13-week study) were conducted in cynomolgus monkeys to investigate the safety of the antibody. In both monkey studies, exposure of nivolumab at all dose levels tested exceeded that measured in humans at the intended clinical dose and schedule of 3 mg/kg once every 2 weeks. Toxicities noted in both of these studies were limited to mild increases in monocytic and lymphocytic infiltration of tissues. These changes are consistent with the pharmacologic activity of the antibody: blocking signaling through the immunoinhibitory PD-1 pathway. Immunophenotyping performed on samples from monkeys administered nivolumab during the 13-week study did show a trend towards increases in the percentage of CD4+ and CD8+ effector and central memory cells; this trend was clearer for the CD8+ T cell population. Monkeys did not develop any clear signs of the autoimmune toxicity seen in clinical trials with nivolumab, however, the generalized lymphocytic infiltration and increases in memory T cells do hint at the possibility of these types of toxicities. Given nivolumab's mechanism of action, the possibility

exists that greater exposure to environmental influences in treated monkeys would result in a more serious inflammatory pattern closer to that seen clinically.

Consistent with the ICH S6 guidance, genetic toxicology studies were not conducted or required for nivolumab. Carcinogenicity studies were not required to support the licensing application for a product to treat advanced human cancer and are neither planned nor expected as post-marketing requirements at this time.

The Applicant conducted an enhanced pre- and post-natal development study in cynomolgus monkeys to assess the potential of nivolumab to cause reproductive toxicity. Consistent with literature reports describing a key role for the PD-1 signaling pathway in the maintenance of allogeneic pregnancy through maintenance of maternal tolerance to the fetus, treatment of dams with nivolumab resulted in dose-related increases in first- and third-trimester pregnancy losses as well as infant death relative to concurrent or historical controls. Thus, the use of an antibody inhibiting this pathway during pregnancy represents a risk to the fetus. Nivolumab is, therefore, not recommended for use during pregnancy unless the benefits to the mother outweigh the risks to a fetus, and, based on the long half-life of the drug, use of contraception for (b)(4) months following the final dose of nivolumab is recommended for females of reproductive potential.

In mouse PD-1 knockout models, no clear physical malformations have been reported, however, late onset of or potentiation of autoimmune disorders have been associated with the loss of PD-1 signaling. Blocking PD-1 signaling during development may, therefore, result in alterations in the developing immune system. In surviving cynomolgus monkey infants from nivolumab treated dams (18 of 32 combining both dose levels used in the study), no malformations were observed. In addition there were no clear effects on neurobavioral or clinical pathology parameters observed during the 182 day post-natal phase of the study despite evidence of continued nivolumab exposure in the infants of high-dose group animals throughout the study. Prenatal exposure to nivolumab did not affect lymphocyte subsets or the primary response to antigens upon immunization with either hepatitis B surface antigen (HBsAg) or tetanus toxoid (TT), though there was a trend toward an increased response to HBsAg upon second exposure in infants from nivolumab treated dams compared to controls.

In addition to the antigen response study included in the pre- and postnatal development study, the Applicant conducted additional ex vivo and in vivo investigations into the mechanism of action of nivolumab and potential effects on immune function following primary and secondary antigen exposure in the presence of the antibody. Ex vivo studies using human PBMCs demonstrated increased antigen responsiveness in the presence of nivolumab. Increases were noted not only following primary immune activation, demonstrated in mixed lymphocyte reaction studies, but also in response to previously recognized antigens including cytomegalovirus and chronic hepatitis virus. An increase in sensitivity to pulmonary rechallenge by ovalubumin was also demonstrated in a mouse PD-1 knockout model. Finally, there are published reports showing that the absence of PD-1 signaling can result in detrimental alterations in the immune response to pathogens. Notably, infection of PD-1 deficient mice with tuberculosis was associated with a decrease in survival compared to wild type animals[1]. Similarly, decreases in survival have been reported in mouse models of lymphocytic choriomeningitis virus (LCMV) infection, though the etiology of these decreases is different

between the types of infection[2-3]. Collectively the data from the rechallenge and infection models is consistent with the potential for increased nivolumab-mediated toxicity following second exposure to an antigen in the presence of the antibody or following administration of nivolumab to virally-infected patients. Data describing these animal models of infection are recommended for inclusion in Section 13.2 of the label.

Recommendations: I concur with the conclusions of Drs. Weis and Putman that the pharmacology and toxicology data support the approval of BLA 125554 for Opdivo for the treatment of patients with unresectable or metastatic melanoma and disease progression following ipilimumab, and, if BRAF V600 mutation positive, a BRAF inhibitor. There are no outstanding nonclinical issues that would prevent the approval of Opdivo for the treatment of the intended patient population.

---

[1] Lazar-Molnar, et al., 2010, Programmed death-1 (PD-1)–deficient mice are extraordinarily sensitive to tuberculosis, PNAS, 107(30):13402-13407.

[2] Frebel, H., et. al., 2012, Programmed death 1 protects from fatal circulatory failure during systemic virus infection of mice. J. Exp. Med., 209(13): 2485-2499

[3] Mueller, S.N., et. al., 2010, PD-L1 has distinct functions in hematopoietic and nonhematopoietic cells in regulating T cell responses during chronic infection in mice, J. Clin. Invest., 120: 2508-2515.

This is a representation of an electronic record that was signed electronically and this page is the manifestation of the electronic signature.

/s/

WHITNEY S HELMS
12/04/2014

DEPARTMENT OF HEALTH AND HUMAN SERVICES
PUBLIC HEALTH SERVICE
FOOD AND DRUG ADMINISTRATION
CENTER FOR DRUG EVALUATION AND RESEARCH

PHARMACOLOGY/TOXICOLOGY BLA REVIEW AND EVALUATION

Application number:	BLA 125,554
Supporting document/s:	000
Applicant's letter date:	30 April 2014
CDER stamp date:	30 April 2014
Product:	Opdivo (Nivolumab)
Indication:	Unresectable or metastatic melanoma in patients previously treated with ipilimumab, regardless of BRAF status
Applicant:	Bristol Meyers Squibb Co
	Route 206 & Province Line Rd Rm D3 218
	Po Box 4000
	Princeton, New Jersey 085434000
	UNITED STATES
Review Division:	DHOT / DOP2
Reviewer:	Shawna L. Weis, PhD
	Alexander H. Putman, PhD
Supervisor/Team Leader:	Whitney S. Helms, PhD
Division Director:	John K. Leighton, PhD, DABT (DHOT) / Patricia Keegan, MD (DOP2)
Project Manager:	Meredith Libeg

Disclaimer

Except as specifically identified, all data and information discussed below and necessary for approval of BLA 125,554 are owned by BMS or are data for BMS has obtained a written right of reference. Any information or data necessary for approval of BLA 125,554 that BMS does not own or have a written right to reference constitutes one of the following: (1) published literature, or (2) a prior FDA finding of safety or effectiveness for a listed drug, as reflected in the drug's approved labeling. Any data or information described or referenced below from reviews or publicly available summaries of a previously approved application is for descriptive purposes only and is not relied upon for approval of BLA 125,554.

TABLE OF CONTENTS

Table of Tables

Table of Figures

1 Executive Summary

1.1 Introduction

Nivolumab is an IgG_4 monoclonal antibody directed against human programmed cell death 1 (PD-1), a receptor belonging to the immunoglobulin superfamily that is expressed primarily on activated CD4+ and CD8+ T cells, NK cells, B cells, and monocytes. PD-1 interaction with its ligands, PD-L1 and PD-L2, leads to down-regulation of T cell responses, including T cell proliferation and cytokine production, and limits immune-destruction of tissues. The interaction between PD-1 and its ligands, thus plays a role in maintaining the balance between immune activation and tolerance, potentially including tumor tolerance. Bristol-Meyers Squibb (BMS) has submitted the current BLA to support the use of nivolumab, for the treatment of unresectable or metastatic melanoma in patients previously treated with ipilimumab, and, if BRAF V600 mutation positive, a BRAF inhibitor.

1.2 Brief Discussion of Nonclinical Findings

Nivolumab bound to PD-1 from humans and cynomolgus monkeys to a similar extent and blocked the interaction of PD-1 with its ligands. Nivolumab did not bind to PD-1 from rodents or rabbits. In vitro, there was no evidence of a direct effect of nivolumab on cytokine release, as assessed by measuring cytokine levels following incubation of the antibody with peripheral blood mononuclear cells (PBMCs) collected from human donors. The ability of nivolumab to mediate antibody dependent cellular cytotoxicity (ADCC) and complement dependent cytotoxicity (CDC) was also examined; as reported with other IgG_4 antibodies, nivolumab was unable to mediate either effect. Because nivolumab was unable to bind to PD-1 from rodents, the Applicant developed a murine surrogate anti-PD-1 antibody to investigate the effects of PD-1 pathway inhibition on tumor growth. This murine surrogate for nivolumab exhibited anti-tumor activity in multiple murine syngeneic tumors models.

Nivolumab was evaluated in 4- and 13-week repeat dose studies in the cynomolgus monkey and was well-tolerated at doses of up to 50 mg/kg. A diffuse pattern of inflammatory infiltration was observed in organs and tissues, but no target organ toxicity was identified by clinical pathology or histological analysis. Similar findings were observed whether nivolumab was administered by weekly or twice-weekly IV injection to cynomolgus monkeys for up to 13 weeks. Consistent with its mechanism of action, there was a trend towards increases in CD4+ and CD8+ memory T cells in the high dose group (50 mg/kg).

In patients receiving nivolumab, autoimmune disturbances are the most commonly reported adverse events including, among others, immune-mediated pneumonitis, colitis, hepatotoxicity, thyroid toxicity, and nephritis. Though exposures in the monkey studies were up to 42-fold higher than the clinical AUC of 25500 µg*hr/mL determined when nivolumab was administered at the recommended dose of 3 mg/kg on a once every two week schedule, no evidence of autoimmune disease was observed in the monkey toxicology studies. The relationship between PD-1 pathway deficiency and many major autoimmune diseases is, however, supported by the pharmacologic

mechanism of action and by data obtained both in PD-1 pathway deficient animals and from human epidemiology studies.

In an enhanced pre- and post-natal development study in cynomolgus monkeys, nivolumab was administered to pregnant dams twice weekly at dose levels of 10 or 50 mg/kg resulting in maternal exposures (AUC) of between 9.1 and 42-fold greater than those observed clinically at the recommended dose of 3 mg/kg every 2 weeks, and in fetal exposures of between 2.3 and 9.6-fold above the average clinical Cmax of 116 µg/mL. Consistent with literature reports of increased rates of allogeneic pregnancy loss in PD-1-deficient mouse models (both PD-1 pathway genetic mutants and mice that received PD-1 neutralizing antibodies), there were dose-related increases in first- and third-trimester pregnancy losses in nivolumab-treated monkeys relative to concurrent and/or historical controls, including an increase in the incidence of infant loss among dams in the low dose (10 mg/kg) group compared with either concurrent or historical controls. There are no reports of fetal malformations associated with PD-1 deficiency in mice though the risk of malformations does not appear to have been rigorously examined in published assessments. In the submitted study, there were no malformations in surviving infants of nivolumab treated dams observed and, aside from one finding of thyroid follicular hypertrophy/hyperplasia in a fetus in the 10 mg/kg dose group that was aborted on Gestational Day 124, there were no gross or histopathological lesions in infants that died prior to scheduled termination. The cause of death for infants in the 10 mg/kg dose group was ascribed to prematurity and failure to thrive. Overall, these findings harmonize with the reported role of PD-1 in promoting maternal tolerance to fetal antigens at the placental/fetal interface and in draining uterine lymph nodes of pregnant dams. Pregnancy Category (b) (4) is recommended.

In surviving infants of nivolumab treated dams, there were no clear effects of prenatal nivolumab exposure on neurobehavioral, or clinical pathology parameters throughout the postnatal observation period, and no gross or histopathological findings associated with nivolumab administration at scheduled termination. Nivolumab was detectable in the serum of infants from high-dose (50 mg/kg) treated dams through at least Postnatal Day 182. Pre-natal exposure to nivolumab did not prevent the ability of surviving infant monkeys to mount a T-cell-dependent antigen response (TDAR) to either hepatitis B surface antigen (HBsAg) or tetanus toxoid (TT). There was no clear effect of nivolumab in this study as antibody responses in treated infants were comparable to controls for both antigens evaluated, although the mean response to a second antigen challenge by HBsAg was consistently higher in animals from nivolumab-treated groups suggesting some pharmacologic effect of the antibody on the enhancement of the immune response.

The ability of nivolumab to enhance immune responsiveness was further demonstrated in both in vitro and in vivo models. In a mixed lymphocyte reaction assay using human PBMCs, the presence of nivolumab resulted in increases in T cell proliferation and IFNγ production compared to an isotype control. Similarly when human PBMCs from cytomegalovirus (CMV)-positive donors were restimulated with CMV lysate in the presence of nivolumab, there were clear increases in immune activation as measured

by IFNγ production compared that seen with an isotype control antibody. In vivo, a bronchopharyngeal challenge assay was conducted comparing the pulmonary reactivity of wild-type versus PD-1 deficient mice to restimulation by ovalubumin (OVA) following an initial peripheral sensitization to the same antigen. PD-1 knockout animals demonstrated increased sensitivity to pulmonary OVA rechallenge, with increased cellularity of bronchial associated lymphatic tissue (BALF) as well as increased cytokine production and IgG_1 compared to wild-type OVA-treated animals. These data suggest that patients who are vaccinated or re-vaccinated while undergoing treatment with nivolumab may have an enhanced immune response to the vaccine or, if encountered, the pathogen, potentially resulting in more frequent vaccine-related or bystander toxicity.

Due to its mechanism of action, treatment with nivolumab has the potential not only increase tissue injury by suppressing the ability to downregulate the immune reaction but also impair appropriate antimicrobial immune responses. Evidence exists to suggest that blocking the PD-1 pathway can influence the immune response towards a TH1 phenotype (Amaranth et. al., 2011). PD-1-deficient mice (C57BL/6) infected with *M. tuberculosis* exhibited a dramatic decrease in survival, which correlated with uncontrolled bacterial proliferation and a larger inflammatory response in the lungs of PD-1-deficient mice compared with wild type controls. Similarly, in assays of cultured primary T cells isolated from HCV-infected patients, re-stimulation with HCV-4H peptide in the presence of nivolumab led to antigen-specific increases in cytokine production. Finally, in mice infected with lymphocytic choriomeningitis virus (LCMV), PD-1 deficiency led to cardiovascular collapse resulting from immune-mediated endothelial cell injury. Because of the seriousness of the outcomes in some animal models of infection in the absence of PD-1 signaling, these reports are recommended for inclusion in the Nonclinical section of the label for Opdivo.

1.3 Recommendations

1.3.1 Approvability

From the nonclinical perspective, nivolumab is approvable for the treatment of patients with unresectable or metastatic melanoma in patients previously treated with ipilimumab, regardless of BRAF status.

1.3.2 Additional Non Clinical Recommendations

None

2 Drug Information

2.1 Drug

CAS Registry Number
946414-94-4

Generic Name
Nivolumab

Code Name
- MDX-1106
- BMS-936558

Chemical Name
None

Molecular Formula/Molecular Weight
The Applicant states that the molecular formula of the predominant drug product is: $C_{6462}H_{9990}N_{1714}O_{2074}S_{42}$ (b) (4) and has a calculated molecular weight of 146,221 Da.

Structure or Biochemical Description
Nivolumab is a fully human IgG_4 monoclonal antibody that binds PD-1. The molecule consists of (b) (4)

Pharmacologic Class
Nivolumab is a monoclonal antibody that blocks the activity of programmed cell-death-1 (PD-1).

2.2 Relevant INDs, NDAs, BLAs and DMFs

IND	Indication
100,052	NSCLC
104,225	Melanoma (combination with ipilimumab)
(b) (4)	
113,463	Renal cell carcinoma
115,195	***Melanoma***
(b) (4)	

2.3 Drug Formulation

Nivolumab is formulated as a 10 mg/mL solution for intravenous administration. The composition of the formulation is provided in Applicant-Table 1

Table 1: Composition of nivolumab 10 mg/mL formulation (100 mg vial)

Component	Quality Standard	Function	Quantity per Vial[a]
Nivolumab (BMS-936558)	BMS specification[b]	Active ingredient	(b) (4)
Sodium Citrate, Dihydrate	USP, Ph.Eur.	(b) (4)	(b) (4)
Sodium Chloride	USP, Ph.Eur.		
Mannitol	USP, Ph.Eur.		
Pentetic Acid[c]	USP		
Polysorbate 80	NF, Ph.Eur.		
Hydrochloric Acid[d]	NF, Ph.Eur.		
Sodium Hydroxide[d]	NF		
Water for Injection	USP, Ph.Eur.		
(b) (4)	NF, Ph.Eur.		

(b) (4)

[b] BMS specifications for nivolumab is provided in Section 3.2.S.4.1, *Specification*.

[c] Also known as diethylenetriaminepentaacetic acid (DTPA)

[d] Diluted solutions of hydrochloric acid and sodium hydroxide may be used for pH adjustment.

(b) (4)

USP = United States Pharmacopoeia
Ph.Eur. = European Pharmacopoeia
NF = National Formulary
q.s. = quantity sufficient
NA = Not applicable

2.4 Comments on Novel Excipients

None

2.5 Comments on Impurities/Degradants of Concern

The Applicant conducted an analysis of potential impurities that might be extracted during the manufacturing process or leach from the container or closure systems. The majority of the potential impurities of concern were present at levels of (b) (4) /dose, which is consistent with levels considered acceptable under the ICH S9 guideline for impurities in drug products intended to treat patients with advanced cancer. For one potential leachate, (b) (4), the estimated maximum exposure is (b) (4) /dose. (b) (4) has undergone toxicological assessment by the US EPA (http://www.epa.gov/chemrtk/pubs/summaries/cibaspec/c12667b3rs.pdf). Based on a NOEL of 500 mg/kg/day obtained in a 13-week GLP toxicology study in the rat, the PDE is 100 mg/day; thus, the proposed exposure level of is (b) (4) dose is considered acceptable for the proposed indication.

2.6 Proposed Clinical Population and Dosing Regimen

- Indication: Unresectable or metastatic melanoma in patients previously treated with ipilimumab , and, if BRAF V600 mutation positive, a BRAF inhibitor.
- Dosing Regimen: 3 mg/kg IV every 2 weeks (Q2Wk)

2.7 Regulatory Background

13 June 2012	IND 115,195
17 July 2012	End of Phase 2 meeting (Type A)
03 October 2012	Fast –Track/rolling-review granted
06 December 2012	End of Phase 2 meeting (Type B)
11 September 2014	Breakthrough designation granted
09 July 2014	Pre-BLA meeting

3 Studies Submitted

3.1 Studies Reviewed

❖ In Vitro Characterization of a Fully Human Anti-PD-1 Monoclonal Antibody (MDX-1106-025-R)
❖ PD-1 Epitope Sequence Analysis by Mass Spectrometry (b) (4) -1106-321)
❖ Effect of MDX-1106 on CD4+ T Cells during an Allogeneic Mixed Lymphocyte Reaction (MLR) (MDX-1106-026-R)
❖ Effect of MDX-1106 on Recall Antigen-Activated T-Cell Secretion of Interferon-Gamma In Vitro (MDX-1106-042-R)
❖ Effect of PD-1 Antibody on the Function of Hepatitis C Virus (HCV)-specific Human CD8+ T cells (MDX-1106-228-R)
❖ Effect of MDX-1106 on Ex Vivo Cytokine Expression in Human Peripheral Blood Cells (MDX-1106-201-R)
❖ Binding and Blocking Characteristics of Chimeric Anti-Mouse-PD-1 Antibody, 4H2 (MDX-1106-028-R)
❖ Effects of Anti-PD-1 Monoclonal Antibody in a J558 Myeloma Model (MDX 1106-034-R)
❖ Effect of Anti-PD-1 Monoclonal Antibody Administration on Unstaged MC38 Tumor Growth Rates in Mice (MDX 1106-023-R)
❖ Effects of Varying Anti-PD-1 Doses on Staged MC38 Tumors in Mice (MDX 1106-200-R)
❖ Dose-Response Effects of Anti-PD-1 Monoclonal Antibody on Unstaged SA1/N Tumor Growth Rate and Immune Response at Tumor Re-Challenge (MDX 1106-006-R)
❖ Dose-Response Effects of Anti-PD-1 Monoclonal Antibody in a Therapeutic SA1/N Tumor Model (MDX 1106-022-R)
❖ A Single-Dose Pharmacokinetic Study of MDX-1106 Administered by Intravenous Injection to Cynomolgus Monkeys (SUV00027)
❖ A 30-day toxicity study of MDX-1106 administered by once weekly intravenous injection to cynomolgus monkeys, followed by an appropriate 4-week recovery

period (SUV00025)
❖ A 3-month intravenous toxicity study of MDX-1106 With a 28-day recovery period in cynomolgus monkeys (b) (4)-552003)
❖ Intravenous Study of Pre- and Postnatal Development in Cynomolgus Monkeys with a 6-Month Postnatal Evaluation ((b) (4) Study: 20012606)
❖ Cross-reactivity study of MDX-1106-fitc with normal human tissues ((b) (4) Study IM1258)
❖ Cross-reactivity study of MDX-1106-fitc with normal Cynomolgus monkey tissues ((b) (4) Study: IM1259)
❖ An Investigative Repeat-Dose Toxicity and Efficacy Study of MDX-010, 4C5 and 5H1 in Combination with HBsAg, DNP-Ficoll and SKMel Immunostimulants Following Three Monthly Administrations (b) (4) Study SUV00006)
❖ Investigative Study of the Effect of Ovalbumin Challenge in PD-1 Knockout and Wild-Type C57/BL6 Mice ((b) (4)-20120124)
❖ Anatomic pathology report: analysis of PD-2 and PD-L1 knockout mice (Study PD-1 and PD-L1 KO)

3.2 Studies Not Reviewed

❖ Ipilimumab: Exploratory In Vitro Activation and Cell-Surface Binding Using Mouse, Rat, Rabbit, Monkey and Human Tissues, Memo Report (930021444)
❖ Immunoglobulin G Subtype Mediated Effector Function In Vitro (b) (4)-1106-320)
❖ SEB Activation of Human PBMC with Nivolumab and Ipilimumab, Individually or in Combination (b) (4)-1106-323)
❖ Human Anti CTLA-4 Monoclonal Antibody Cell Line Development (MDX-010-008-R)
❖ Physicochemical Characterization of MDX-010 (MDX-010-011-R)
❖ MDX-010-Mediated Effector Function In Vitro (MDX-1106-010-006-R)
❖ Effect of Ipilimumab and MDX-1106 on T Cell Activation during an Allogeneic Mixed Lymphocyte Reaction (MLR) (MDX-1106-010-001-R)
❖ Effect of Combined MDX-1106 and Ipilimumab Treatment on Ex Vivo Cytokine Release in Human Peripheral Blood Cells (MDX-1106-010-008-R)
❖ PD-1 and CTLA-4 Blockade in the Murine MC38 Colon Adenocarcinoma Model (MDX-1106-010-002-R)
❖ PD-1 and CTLA-4 Blockade in the Murine CT26 Colon Adenocarcinoma Model (MDX-1106-010-003-R)
❖ PD-1 and CTLA-4 Blockade in the Murine SA1/N Fibrosarcoma Model (MDX-1106-010-004-R)
❖ Tumor Response to PD-1 and CTLA-4 Blockade in Murine B16-F10 Melanoma and J558 Models (MDX-1106-010-005-R)
❖ MDX-1408 and BMS-936558 Four-week intermittent-dose (qw) intravenous Exploratory combination pharmacodynamic and Toxicity study in monkeys (BMS Study DS10061)
❖ BMS-986016 and BMS-936558: Four-week intravenous combination toxicity study in monkeys with a 6-week recovery (BMS Study DN12123)

- A 4-Week Combination Toxicity Study of MDX-010 and MDX-1106 Administered by Intravenous Injection to Cynomolgus Monkeys, with a 1-Month Recovery Period (b) (4) Study SUV00106)

3.3 Previous Reviews Referenced

- Review of IND 100,052 by Melanie Hartsough, PhD, dated 24 July 2006

4 Pharmacology

4.1 Primary Pharmacology

MDX-1106-025-R: In Vitro Characterization of a Fully Human Anti-PD-1 Monoclonal Antibody

This study was performed to determine the binding affinity and specificity of MDX-1106 to PD-1. The ability of MDX-1106 to block PD-1 ligand binding and promote antibody-dependent cell-mediated or complement-dependent cytotoxicity was also assessed.

The affinity of MDX-1106 to human and cynomolgus monkey PD-1 was determined using surface plasmon resonance. Recombinant PD-1-Ig fusion protein was coated on a CM5 chip at 10 µg/mL and the antibody was passed over the antigen coated chip at concentrations ranging from 16.7 to 333 nM in order to obtain the binding kinetics. Background and non-specific binding signals were subtracted by flowing human- IgG_1 isotype and buffer alone on the antigen surface as controls. The affinity of MDX-1106 to human and cynomolgus monkey PD-1 was 3.06 and 3.92 nM, respectively.

The ability of MDX-1106 to bind human PD-1 was also assessed using enzyme-linked immunosorbent assay (ELISA). Serial dilutions of MDX-1106 (from 0.001 to 2 µg/mL) were tested for binding to immobilized PD-1-Ig fusion protein in a 96-well microplate. Bound antibody was detected using an HRP-conjugated secondary antibody specific to the human kappa chain. The addition of ABTS substrate produced optical densities proportional to bound antibody. As shown in Figure 1, the EC_{50} of MDX-1106 binding to human PD-1-Ig fusion protein was 0.39 nM.

Figure 1: Binding of MDX-1106 to PD-1-Ig Fusion Protein by ELISA

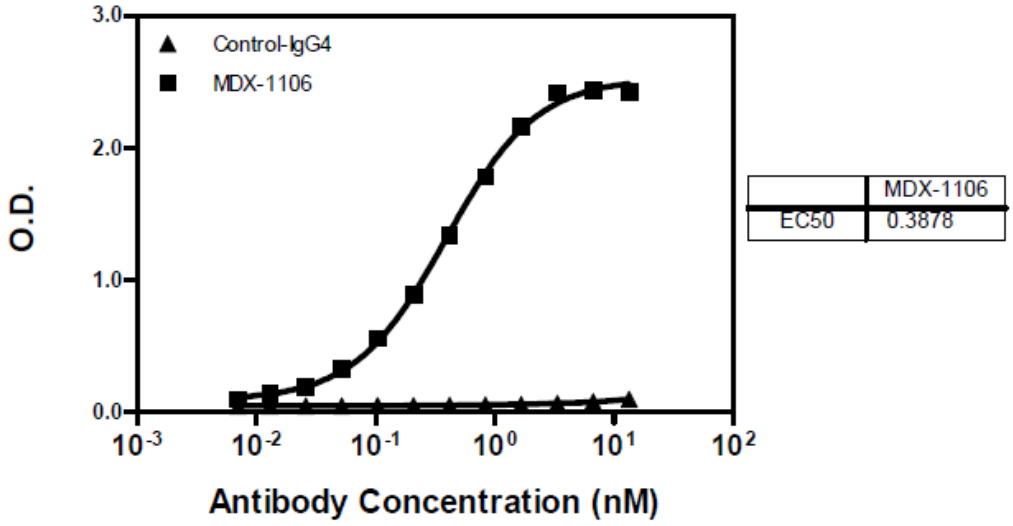

(Figure excerpted from Applicant's BLA)

The binding of MDX-1106 to other related members of the CD28 family was examined by standard ELISA. MDX-1106 (5C4-g4) was tested at a concentration of 1 µg/mL in the assay. As displayed in Figure 2, MDX-1106 bound to PD-1 but not to related molecules such as CD28, cytotoxic T-lymphocyte antigen 4 (CTLA-4), inducible T-cell costimulator (ICOS), or B and T lymphocyte attenuator (BTLA).

Figure 2: Binding of MDX-1106 to PD-1-Ig Fusion Protein by ELISA

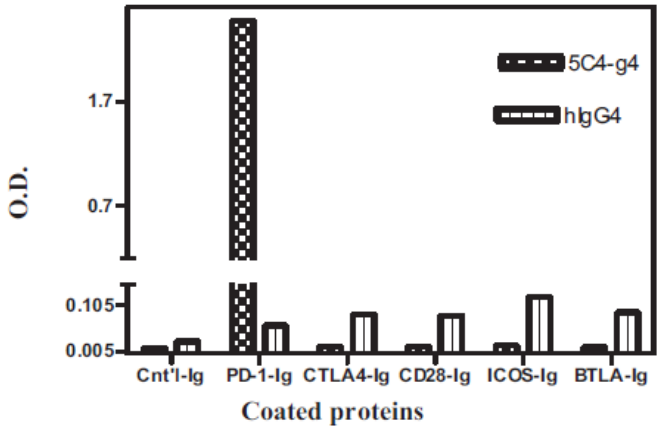

(Figure excerpted from Applicant's BLA)

Fluorescence-activated cell sorting (FACS) analysis confirmed that MDX-1106 bound to PD-1 transfected CHO cells (EC_{50} = 1.7 nM; Figure 3) and activated human CD4+ T cells (EC_{50} = 0.64 nM; Figure 4) expressing cell surface PD-1. Serial dilutions of antibody (from 0.003 to 10 µg/mL) were tested for binding to PD-1 molecules expressed on the cell surface of PD-1 transfected CHO cells and human CD4+ T cells activated by plate-bound anti-CD3 antibody. Human CD4+ T cells were prepared from PBMCs using the Dynal® CD4 T cell preparation kit. Bound antibody was detected using an FITC-

conjugated secondary antibody specific to the human kappa chain and analyzed using a flow cytometer.

Figure 3: Binding of MDX-1106 to CHO/PD-1 Cells

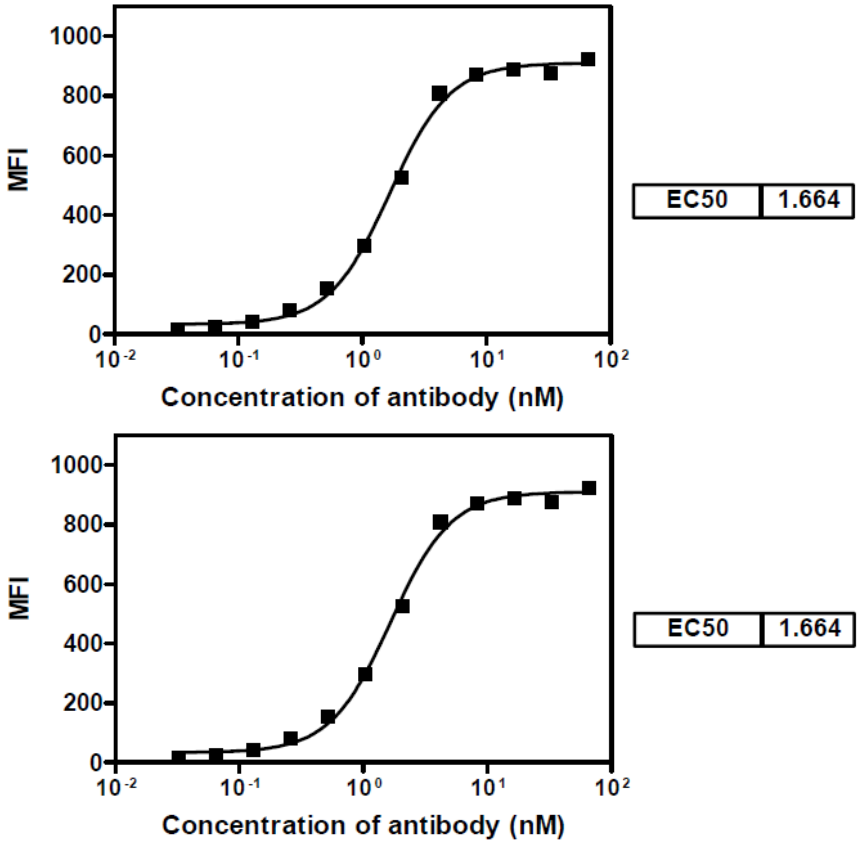

(Figure excerpted from Applicant's BLA)

Figure 4: Binding of MDX-1106 to Activated Human T Cells

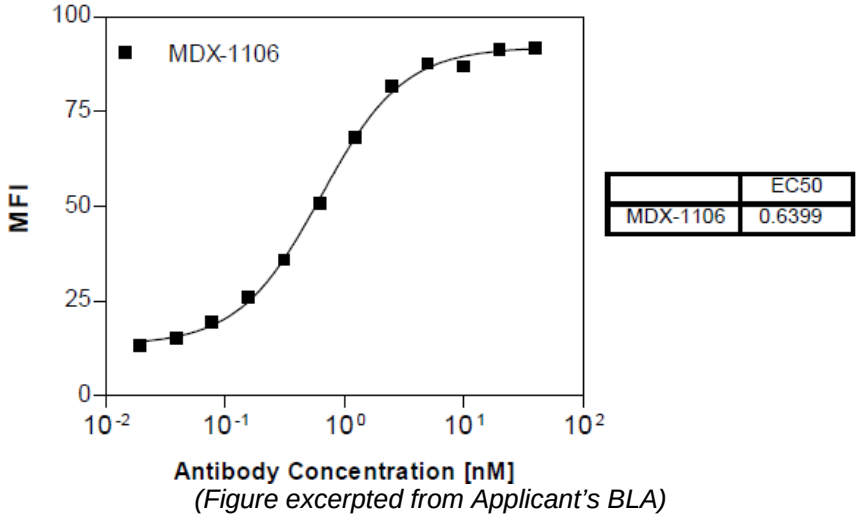

(Figure excerpted from Applicant's BLA)

FACS analysis also showed that MDX-1106 bound to cynomolgus monkey PD-1 (Figure 5), but not to rat (Figure 6) or rabbit PD-1 (Figure 7). Monkey and rat splenocytes were prepared mechanically by mashing of spleen. Rabbit PBMCs were prepared using a Ficoll gradient. MDX-1106 at 5 µg/mL was incubated with anti-CD3 and anti-IgG/IgM antibody-treated cynomolgus splenocytes to test cross-reactivity of MDX-1106 to monkey PD-1. Bound antibody was detected using an FITC conjugated secondary antibody, specific to the human gamma chain, and analyzed using a flow cytometer. Rat splenocytes and rabbit PBMCs were treated by anti-TCRαβ and anti-CD28 antibodies or by PMA and ionomycin, respectively. Binding of MDX-1106 to rat or rabbit PD-1 was detected by PE-conjugated anti-human IgG secondary antibody and analyzed using a flow cytometer.

Figure 5: Cross-Reactivity of MDX-1106 to Activated Cynomolgus Splenocytes

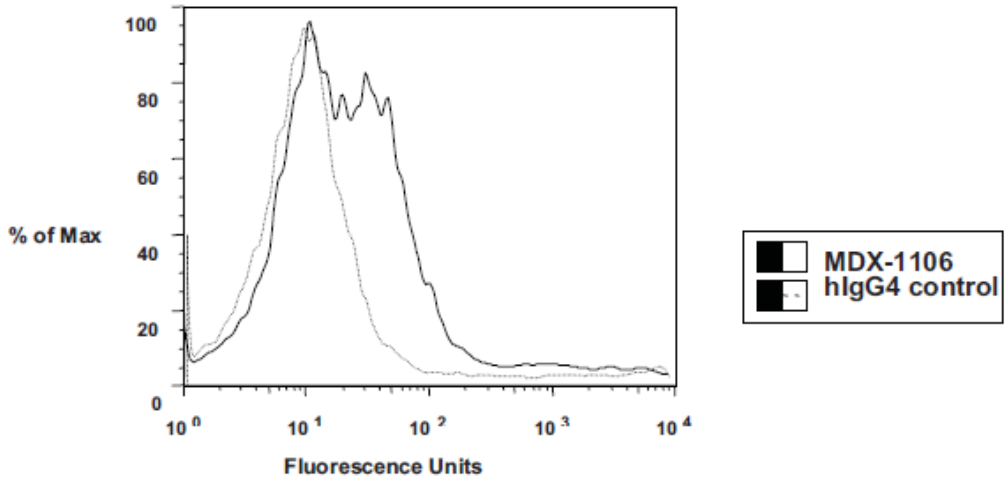

(Figure excerpted from Applicant's BLA)

Figure 6: Absence of MDX-1106 Reactivity to Activated Rat Splenocyte PD-1

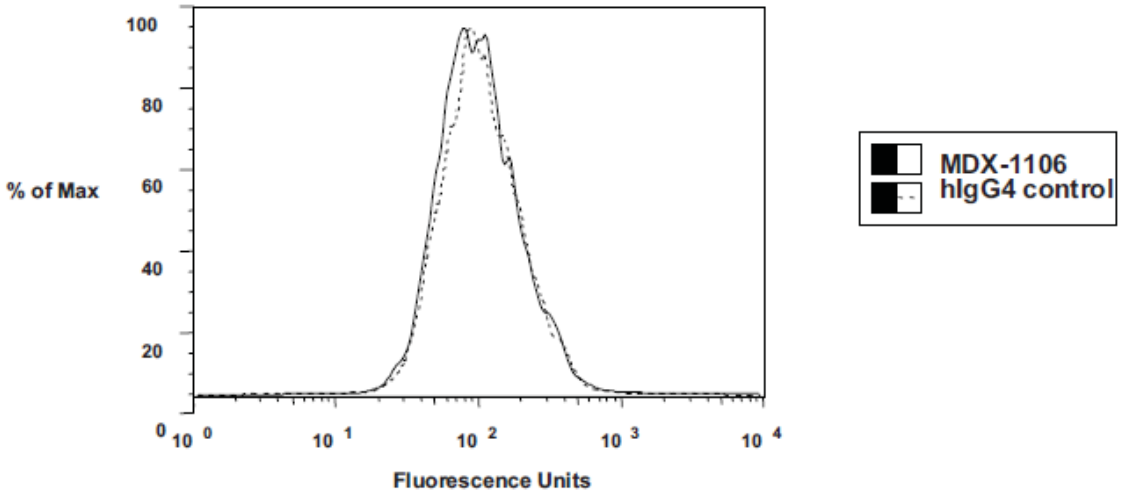

(Figure excerpted from Applicant's BLA)

Figure 7: Absence of Reactivity of MDX-1106 to Activated Rabbit PBMCs

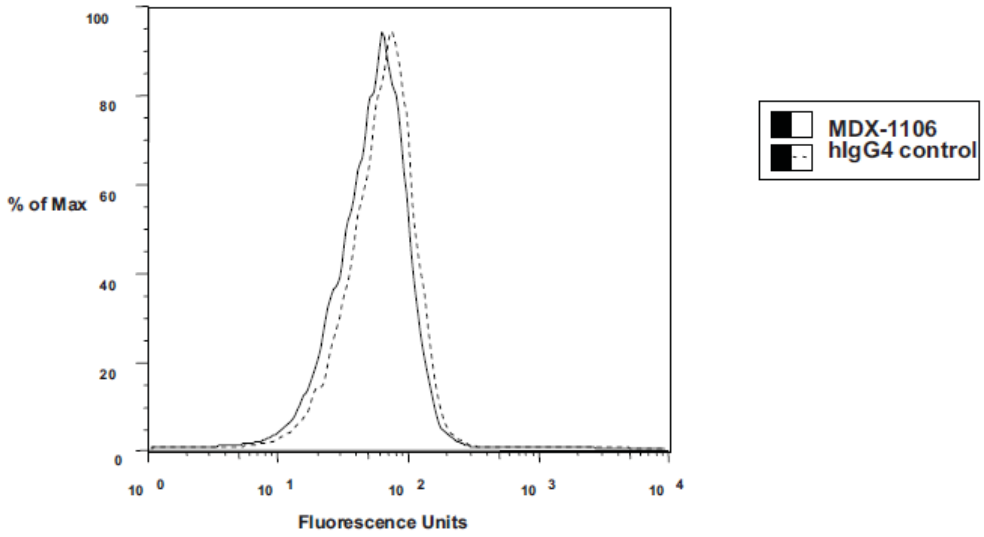

(Figure excerpted from Applicant's BLA)

Furthermore, FACS analysis showed that MDX-1106 blocked PD-L1 (EC_{50} = 1 nM; Figure 8) and PD-L2 (EC_{50} = 1 nM; Figure 9) ligand binding to human PD-1. Serial dilutions of MDX-1106 (from 0.005 to 10 µg/mL) were incubated with transfected CHO cells expressing human PD-1. Biotin-conjugated recombinant human PD-L1-Fc or PD-L2-Fc fusion protein was then added. Binding of the ligand to PD-1 on the CHO cell surface was detected by PE-conjugated streptavidin and analyzed using a flow cytometer.

Figure 8: Blocking of PD-L1 Binding to CHO/hPD-1 Cells

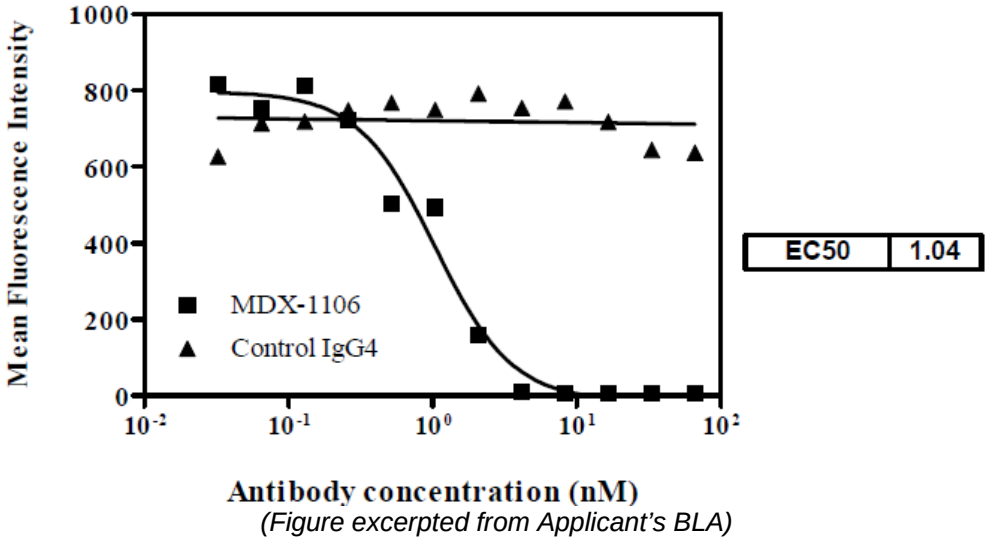

(Figure excerpted from Applicant's BLA)

Figure 9: Blocking of PD-L2 Binding to CHO/hPD-1 Cells

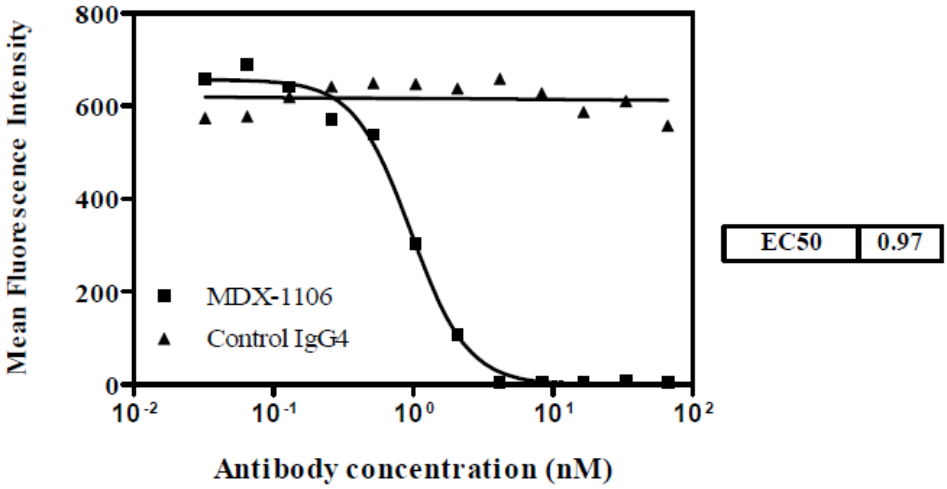

(Figure excerpted from Applicant's BLA)

The ability of MDX-1106 to promote antibody-dependent cell-mediated cytotoxicity (ADCC) was assessed using the DELFIA® cell cytotoxicity kit. Briefly, activated human CD4+ T cells were labeled with 2.5 µl of Delfia® BATDA reagent per 1 million cells for 20 minutes at 37°C. After washing four times with assay medium, cells were spun down and adjusted to 1×10^5 cells/ml. Labeled activated CD4+ T cells (100 µl) were added to a V-bottom 96-well plate, followed by the addition of 50 µl human PBMC in an effector to target (E/T) cell ratio of 50:1. Antibody (0.009 to 20 µg/mL of MDX-1106 or control anti-MHC-I) was then added to each well. After incubation for 1 hour at 37°C, the plate was spun down. Supernatant (20 µl/well) was transferred into a flat bottom 96-well plate, following by the addition of 180 µl/well europium-solution. The plate was read using a microplate reader. As demonstrated in Figure 10, while the positive control antibody (anti-HLA-ABC antibody) elicited ADCC activity against activated CD4 T cells, MDX-1106 did not mediate ADCC against these cells.

Figure 10: ADCC of MDX-1106 on Activated Human CD4 T Cells

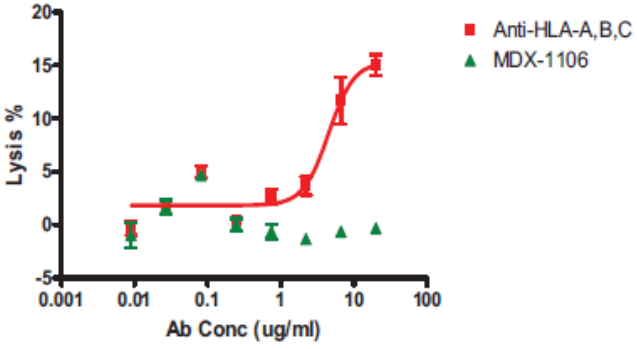

(Figure excerpted from Applicant's BLA)

Using a cell viability assay, the ability of MDX-1106 to promote complement-dependent cytotoxicity (CDC) was evaluated. Target-activated CD4+ (PD-1 expressing) T cells were suspended at 1 × 10^6 cells/mL in CDC buffer (RPMI + 0.1% BSA + 20 mM Hepes + 1% Pen/Strep) and dispensed at 50 µL/well in flat bottomed 96-well cell culture plates. Human complement (diluted 1:3) was then dispensed at 50 µL per well. Five-fold serial dilutions of MDX-1106, human IgG_4 isotype control, mouse anti-MHC Class I positive control, and mouse- IgG_1 isotype control were prepared, resulting in Ab concentrations from 640 pg/mL to 50 µg/mL. Antibodies and controls were dispensed in duplicated cell/complement mixtures and incubated at 37°C for 2 hours. To measure cytotoxicity, alamar blue was added at 50 µL/well and plates were incubated an additional 21 hours at 37°C. Plates were read on a fluorescent microplate reader to determine viable cells (cell count proportional to fluorescence units). As demonstrated in Figure 11, while the positive control antibody (anti-HLA-ABC antibody) exhibited CDC activity against activated CD4 T cells, MDX-1106 was unable to mediate CDC.

Figure 11: CDC of MDX-1106 against Activated Human CD4 T Cells

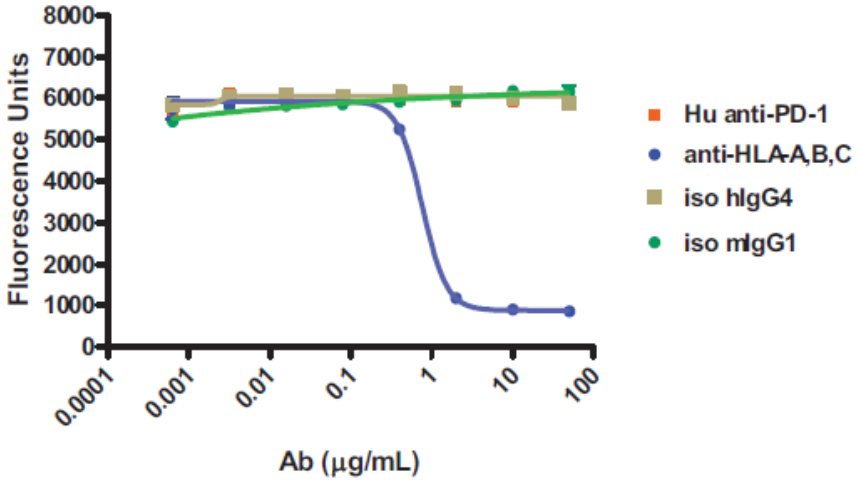

(Figure excerpted from Applicant's BLA)

(b) (4)-1106-321: PD-1 Epitope Sequence Analysis by Mass Spectrometry

The amino acid sequences recognized by nivolumab were evaluated by identification of PD-1 peptides generated by protease digestion and immunoprecipitation by nivolumab. Three peptides were identified, 1a (62-69), 1b (70-86), and 2 (118-136), as underlined below.

^{1}MQIPQAPWPVVWAVLQLGWRPGWFLDSPDRPWNPPTFSPALLVVTEGDNA^{50}
^{51}TFTCSFSNTSESFVLNWYRMSPSNQTDKLAAFPEDRSQPGQDCRFRVTQL^{100}
^{101}PNGRDFHMSVVRARRNDSGTYLCGAISLAPKAQIKESLRAELRVTERRAE^{150}

Peptides 1a and 1b are adjacent to one another in the linear sequence of PD-1. Peptide 1a was found to have the strongest affinity to nivolumab. The binding of nivolumab to antigen is likely dependent upon glycosylation of PD-1 since nivolumab bound only to glycosylated human PD-1 expressed in a mammalian cell line and did not bind to nonglycosylated human PD-1 expressed in *E. coli* (data not shown). Although the residues that comprise the nivolumab epitope are discontinuous, they are all located on the face of PD-1 that interacts with PD-L1. This finding is consistent with the ability of nivolumab to block interaction between PD-1 and its ligands. According to the Applicant, the cynomolgus amino acid sequence is highly homologous to human PD-1 and within peptides 1a, 1b, and 2, only one amino acid is different (data not shown).

MDX-1106-026-R: Effect of MDX-1106 on CD4+ T Cells during an Allogeneic Mixed Lymphocyte Reaction (MLR)

The purpose of this study was to determine whether MDX-1106 activates human CD4+ T lymphocytes (T) in the context of an allogeneic mixed lymphocyte reaction (MLR) as measured by cytokine release and T-cell proliferation.

Whole blood samples were obtained from four human donors (P33216, P33359, PCA060309D, and GR01738). Following purification of CD4+ T cells from 2 of the donors (P33216 and PCA060309D) and monocytes from the other 2 donors (P33359, GR01738), samples were incubated for 1 week in the presence of exogenous granulocyte macrophage-colony stimulating factor (rhGM-CSF) and interleukin-4 (rhIL-4) to promote dendritic cell (DC) differentiation. All cells were cryopreserved prior to use in the assays.

For the allogeneic T + DC MLR, in vitro-differentiated human DC were mixed with purified CD4+ allogeneic T cells at a ratio of 10:1 (T:DC). MDX-1106 and control antibodies (hIgG4 Iso) were prepared in culture medium in serial log dilutions from 50 µg/mL to 0.5 ng/mL and added to samples at the start of incubation. Culture supernatants were harvested on Day 5 for enzyme-linked immunosorbent assay (ELISA) analysis of interferon γ (IFN-γ) secretion. On Day 6, cultures were pulsed with 1 µCi tritiated thymidine per well during the final 18 hours of incubation. At the end of the incubation period, T cell proliferation was measured by calculating tritium incorporation with a scintillation counter. T cell proliferation and cytokine release was monitored for all samples in the absence of added antibodies.

PD-1inhibition by MDX-1106 resulted in enhanced T-cell activation in an allogeneic MLR as measured by increased IFN-γ secretion and T-cell proliferation, relative to cultures containing control antibody This effect was dose-dependent and reproducible over replicate assays (represented in Figure 12) and between multiple DC and T-cell donor pairs (Figure 12 and Figure 13).

Figure 12: Assay 1014-102105 Dose-Based Range of Response (T-Cell Donor P33216 + DC Donor P33359)

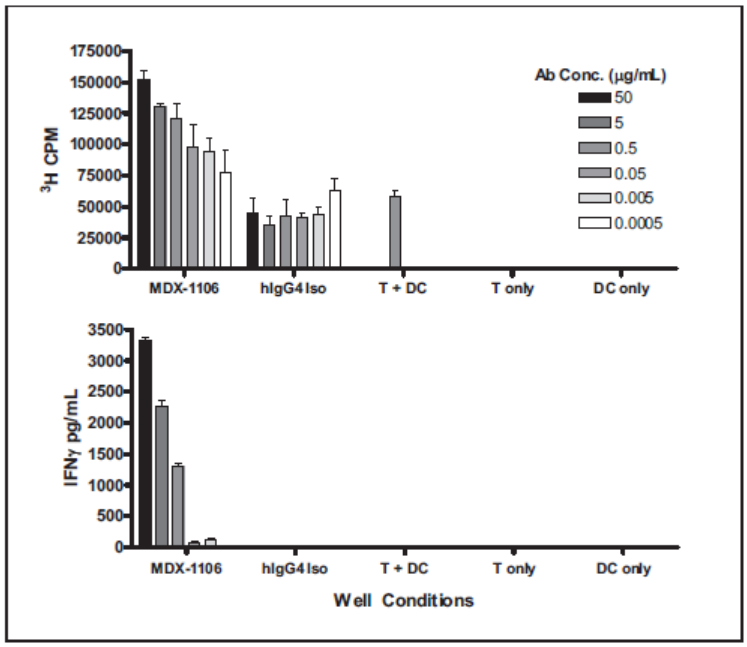

(Figure excerpted from Applicant's BLA)

Figure 13: Assay 0324-033006 Dose-Based Range of Response (T-Cell Donor PCA060309D + DC Donor GR01738)

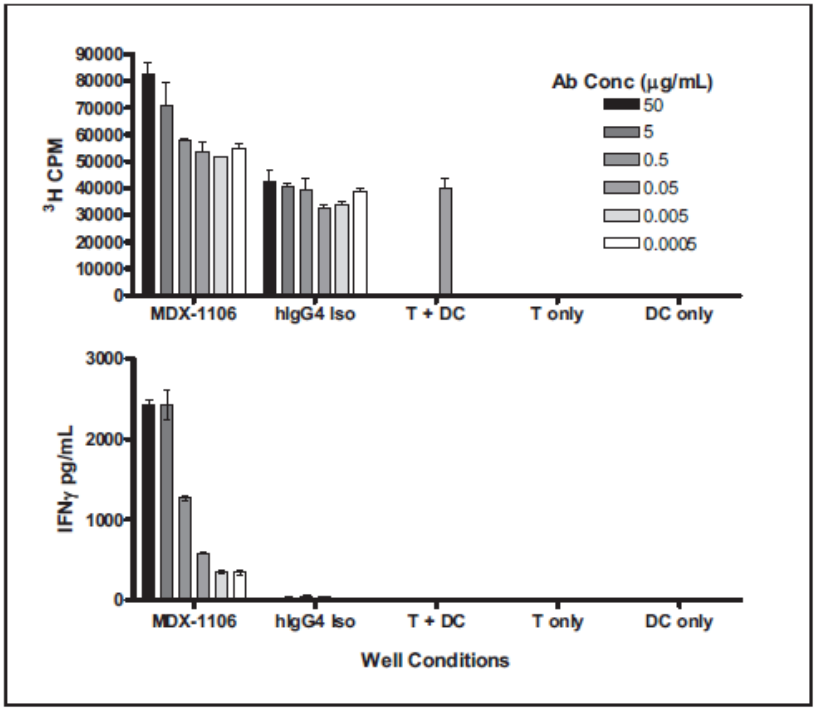

(Figure excerpted from Applicant's BLA)

MDX-1106-042-R: Effect of MDX-1106 on Recall Antigen-Activated T-Cell Secretion of Interferon-Gamma In Vitro

Cytomegalovirus (CMV) lysate can stimulate antigen-specific, memory T cell-mediated IFN-γ production by human peripheral blood mononuclear cells (PBMCs) isolated from donors previously infected by CMV. Thus, a series of in vitro assays were conducted to characterize the effect of MDX-1106 on CMV lysate-stimulated IFN-γ production by CMV-responsive human PBMC.

A series of 8 assays was conducted. Frozen PBMCs from 2 donors (Donors 2 and 3) were pre-screened for a CMV recall response using a lysate derived from CMV-infected cells. For assays 1-7 on Day 0, PBMC were cultured in Iscove's complete media supplemented with 10% heat-inactivated FCS (IF10) at $1x10^6$ cells/ml in 96-well microplates and stimulated with 0.5 µg/ml of CMV lysate. Serial-diluted 1D12 (IgG_4 isotype control), M1H4 (mouse anti-human-PD-1), and MDX-1106 were then introduced into the wells. On Day 4, supernatants were removed and antigen-induced IFN-γ response was evaluated by IFN-γ-specific enzyme-linked immunosorbent assay (ELISA).

As displayed in Figure 16, and representative of results from assays 1-7, MDX-1106 (up to 30 µg/mL) enhanced IFN-γ secretion in a dose-dependent manner following 4 days of CMV lysate-stimulated PBMC incubation. Across all seven assays (assay 8 was CMV lysate alone), the MDX-1106 EC_{50} values ranged from 0.001 to 0.018 µg/mL (data not shown).

Figure 14: Effect of MDX-1106 on IFN-γ in CMV-Restimulated PBMCs

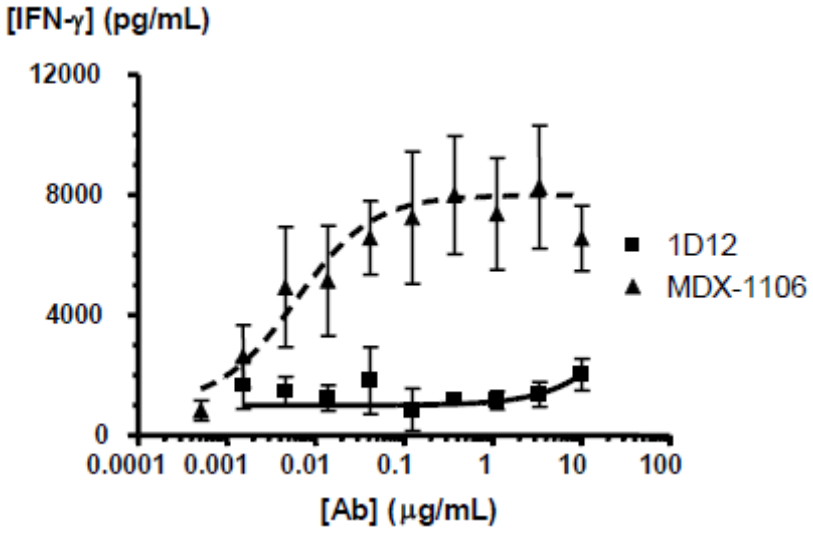

(Figure excerpted from Applicant's BLA)

For Assay 8, PBMC were cultured with serial dilutions of CMV lysate in the presence or absence of a 40 ng/ml fixed concentration of MDX-1106. As demonstrated in Figure 17,

150 pg/ml to 3 µg/ml of CMV lysate stimulated IFN-γ secretion. The addition of 40 ng/ml of MDX-1106 enhanced IFN-γ secretion over the entire range of lysate concentrations assayed and enhanced the maximum IFN-γ secretion from 5793 pg/ml for lysate alone to 13321 pg/ml for lysate with MDX-1106.

Figure 15: Assay 8 CMV Lysate Titration

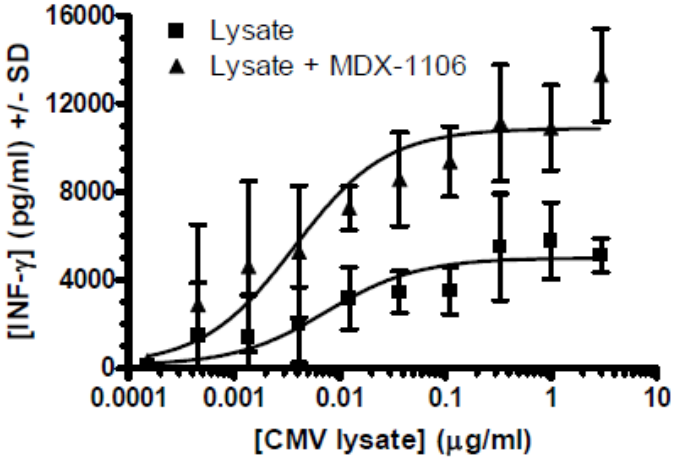

(Figure excerpted from Applicant's BLA)

MDX-1106-228-R: Effect of PD-1 Antibody on the Function of Hepatitis C Virus (HCV)-specific Human CD8+ T cells

Studies have shown that programmed death-1 (PD-1) receptor expression remains high on CD8+ T lymphocytes during chronic virus infections, such as Hepatitis C Virus (HCV), and that this high level of expression correlates with T cell exhaustion. Therefore, the purpose of this study was to determine if MDX-1106 can reverse T cell exhaustion by enhancing the function of HCV-specific CD8+ T cells isolated from an individual with chronic HCV infection.

To perform an intracellular cytokine stain (ICS) assay, peripheral blood mononuclear cells (PBMC) were isolated from a human donor with a chronic HCV infection and plated into 96-well flat-bottom plates at $2x10^5$ cells per well, in triplicate. HCV-4H peptide was added at a final concentration of 10 µg/ml and MDX-1106 or h IgG_4 isotype control antibody was added at a final concentration of 20 µg/ml. Following 6 days of incubation at 37°C, the activated PBMC were harvested, re-stimulated with 5 µg/ml of HCV peptide in the presence of GolgiPlug™ reagent (1:1000 dilution) to retain any cytokine produced inside the cells, and incubated at 37°C for 15 hours. Following incubation, the PBMC were resuspended in 0.05 ml PBS containing 10% human AB serum and 50 µg of purified human IgG to block Fc receptor interference. PBMC were stained with anti-CD8 antibody at 4°C for 20 minutes and stained with anti-IFN-γ and anti-TNF-α antibodies for 30 minutes at 4°C. The PBMC were then analyzed by flow cytometry.

As shown in Figure 18 and Table 2, following re-stimulation with HCV-4H peptide, a higher frequency of CD8+ T cells produced IFN-γ (2.4-fold increase) and TNF-α (2.7-fold increase) when cultured with MDX-1106 compared to the isotype control antibody. The majority of these T cells produced both IFN-γ and TNF-α simultaneously. Furthermore, the amount of cytokine produced on an individual cell level was enhanced in the presence of MDX-1106, which is reflected by a higher mean fluorescence intensity of IFN-γ and TNF-α staining (Table 2). The enhancing effect of PD-1 blockade on T cell function required T cell receptor stimulation since treatment with MDX-1106 alone had no effect.

Figure 16: PD-1 Blockade with MDX-1106 Enhances IFN-γ and TNF-α Production by HCV-Specific CD8+ T cells in an ICS Assay

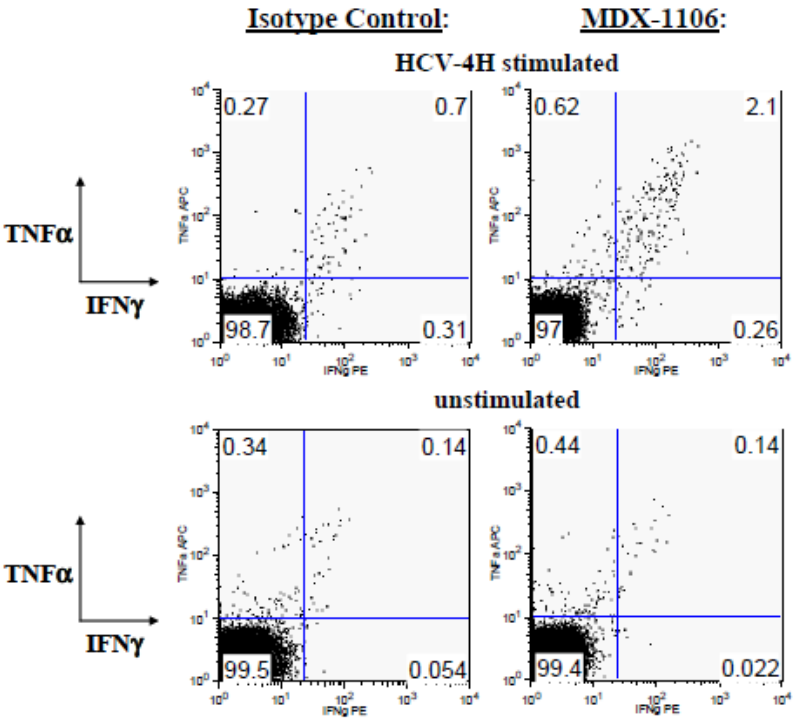

(Figure excerpted from Applicant's BLA)

Table 2: PD-1 Blockade with MDX-1106 Enhances IFN-γ and TNF-α Production by HCV-Specific CD8+ T cells in an ICS Assay

		% IFNγ+ (of CD8+)	IFNγ GMFI	% TNFα+ (of CD8+)	TNFα GMFI	% IFNγ+ TNFα+ (of CD8+)
MDX-1106 (BMS 936558)[a]	HCV-4H	2.4	82.4	2.7	75.5	2.1
MDX-1106 (BMS 936558)	No peptide	0.2	46.3	0.6	33.2	0.1
hIgG4 isotype	HCV-4H	1.0	57.4	1.0	40.1	0.7
hIgG4 isotype	No peptide	0.2	39.4	0.5	34.0	0.1

[a] Treatments shown above indicate the primary stimulation protocol. All samples were re-stimulated with HCV-4H peptide for cytokine analysis regardless of primary stimulation protocol.

(Table excerpted from Applicant's BLA)

The following published literature was submitted by the Applicant: Wong RM, Scotland RR, Lau RL, et al. Programmed death 1 blockade enhances expansion and functional capacity of human melanoma antigen-specific CTLs. Int Immunol 2007;19:1223-34.

In this study, the authors examined the effects of MDX-1106 on the in vitro expansion and function of human vaccine-induced CD8+ T cells (CTL) specific for the melanoma-associated antigens glycoprotein 100 (gp100) and melanoma antigen recognized by T cells (MART)-1. Peripheral blood mononuclear cells (PBMCs) were isolated from HIV-seronegative stage 3/4 resected melanoma patients who were vaccinated with gp100 and/or MART-1 peptide analogs. Monocyte-derived dendritic cells (DC) were cultured, pulsed with gp100-2M, MART-27L, or control HIV peptide for a minimum of 2 hours, and harvested. According to the authors, because PD-1-mediated interactions may occur naturally between different T cell subsets, bulk CD3+ T cells were used as responders for peptide stimulation. CD3+ cells purified from PBMCs were washed, re-suspended in AIM V 5% HS, anti-PD-1 antibody or matching IgG_4 isotype control, and then added to peptide-pulsed DC. All cultures were incubated for 11 days at 37°C. Exogenous cytokines were not added at any point. Aliquots of fresh PBMCs and peptide-stimulated CD3+ effector cells were stained with gp100-2M or MART-27L tetramer.

As illustrated in Figure 19, MHC peptide tetramer labeling showed that PD-1 blockade with MDX-1106 (αPD-1) during peptide stimulation increased the frequencies of gp100- and MART-1-specific CTL (left column), compared to IgG_4 control-treated cells (center column). Cells stimulated with a control HIV peptide in the presence of MDX-1106 did not demonstrate increases in CTLs specific for gp100 and MART-1 (right column). Labeling with a pan MHC class I-negative control tetramer was 0.0% for all conditions (data not shown).

Figure 17: Increase in Tumor Antigen-Specific T Cells from Melanoma Patients Following Peptide Restimulation *in Vitro* in the Presence of Nivolumab

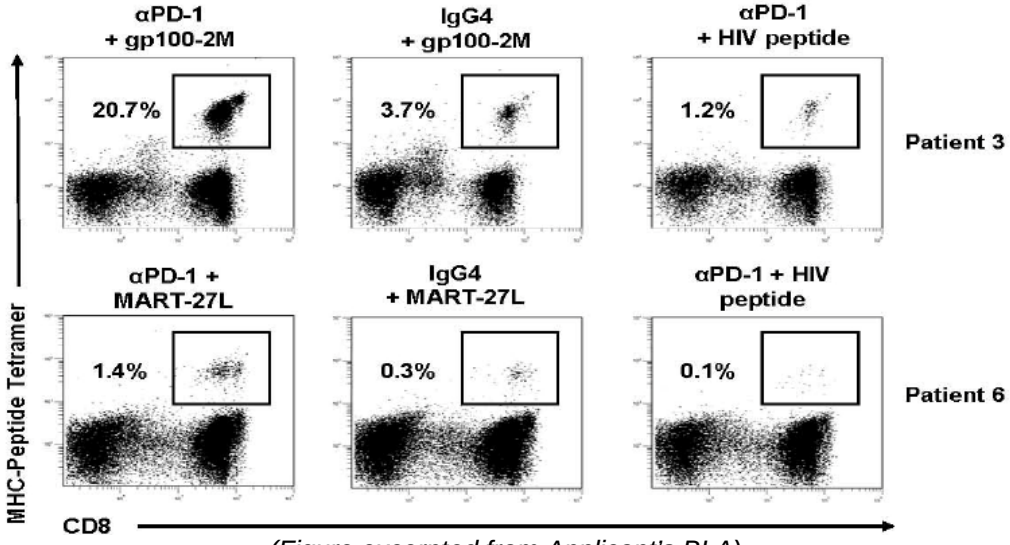

(Figure excerpted from Applicant's BLA)

MDX-1106-201-R: Effect of MDX-1106 on Ex Vivo Cytokine Expression in Human Peripheral Blood Cells

To determine if MDX-1106 affects cytokine expression in human peripheral blood cells, fresh whole human blood samples from nine healthy subjects were incubated with MDX-1106 or control antibodies for 4 or 6 hours, and 24 hours. The positive control was an anti-human-CD3 antibody and the negative control was an hIgG4 isotype antibody. Cytokines expressed in incubated samples were measured using beads coated with antibodies for six cytokines (IFN-γ, TNF-α, IL-2, IL-4, IL-6, and IL-10). Cytokine expression was also measured in all samples in the absence of added antibodies.

Incubation of MDX-1106 resulted in no significant effect on the release of IFN-γ, TNF-α, IL-2, IL-4, IL-6, and IL-10 in human blood cell samples (Table 2). The anti-CD3 positive control induced cytokine release in each of the same donors. Based on these data, up to 100 µg/mL of MDX-1106 does not cause cytokine release when incubated with human peripheral blood cells for up to 24 hours.

Table 3: Cytokine Release in Donors 1–6 Samples

		Cytokine Concentration (pg/ml)					
		IFN-γ	TNF-α	IL-10	IL-6	IL-4	IL-2
Human Blood Donor 1 at 4 hours							
Positive Control	10 µg/ml anti-CD3 Ab	>5000.0	1233.9	24.7	88.7	27.0	81.4
	100 µg/ml anti-CD3 Ab	>5000.0	1118.3	31.5	135.8	29.7	126.0
Negative Control	10 µg/ml hIgG4	3.9	3.1	3.0	12.1	1.1	2.4
	100 µg/ml hIgG4	10.2	3.7	3.1	12.1	1.9	1.9
	No antibody treatment	BDL	2.3	2.3	12.8	BDL	1.7
Test Article	10 µg/ml MDX-1106-IgG4	3.1	2.9	2.8	13.2	BDL	1.0
	100 µg/ml MDX-1106-IgG4	3.0	3.0	3.0	13.4	BDL	1.5
Human Blood Donor 1 at 24 hours							
Positive Control	10 µg/ml anti-CD3 Ab	>5000.0	608.3	105.2	3896.6	71.7	349.2
	100 µg/ml anti-CD3 Ab	>5000.0	1619.7	144.5	>5000.0	85.2	774.5
Negative Control	10 µg/ml hIgG4	6.9	1.5	3.2	10.1	1.8	0.8
	100 µg/ml hIgG4	29.1	3.1	4.6	13.4	4.3	3.8
	No antibody treatment	11.5	1.9	3.2	13.1	2.7	2.6
Test Article	10 µg/ml MDX-1106-IgG4	2.5	1.7	3.0	10.5	2.1	0.7
	100 µg/ml MDX-1106-IgG4	BDL	1.6	3.2	10.9	2.1	BDL
Human Blood Donor 2 at 4 hours							
Positive Control	10 µg/ml anti-CD3 Ab	>5000.0	1132.4	13.3	56.4	37.4	45.0
	100 µg/ml anti-CD3 Ab	>5000.0	1076.3	17.1	89.1	48.3	60.8
Negative Control	10 µg/ml hIgG4	19.5	2.2	2.6	5.3	1.8	2.5
	100 µg/ml hIgG4	12.0	3.7	3.2	6.5	4.0	3.2
	No antibody treatment	6.0	2.1	2.2	4.5	0.8	2.3
Test Article	10 µg/ml MDX-1106-IgG4	12.6	2.5	2.3	5.1	0.6	2.1
	100 µg/ml MDX-1106-IgG4	12.2	3.0	2.9	6.5	2.4	2.8
Human Blood Donor 2 at 24 hours							
Positive Control	10 µg/ml anti-CD3 Ab	>5000.0	520.1	185.8	1492.8	77.6	148.1
	100 µg/ml anti-CD3 Ab	>5000.0	837.7	251.5	2413.4	107.4	236.7
Negative Control	10 µg/ml hIgG4	10.2	1.9	2.8	83.5	2.1	0.6
	100 µg/ml hIgG4	12.6	1.6	2.4	6.0	2.5	1.8
	No antibody treatment	5.7	1.5	2.1	3.6	2.1	1.2
Test Article	10 µg/ml MDX-1106-IgG4	4.2	1.4	2.3	4.4	2.1	2.1
	100 µg/ml MDX-1106-IgG4	13.1	1.7	2.4	3.5	2.9	1.9

BDL = Below Detection Limit

		Cytokine Concentration (pg/ml)					
		IFN-γ	TNF-α	IL-10	IL-6	IL-4	IL-2
Human Blood Donor 3 at 4 hours							
Positive Control	10 µg/ml anti-CD3 Ab	1148.1	193.6	34.9	54.9	10.3	45.6
	100 µg/ml anti-CD3 Ab	1429.0	296.4	56.4	100.6	14.1	71.6
Negative Control	10 µg/ml hIgG4	11.1	1.9	2.8	3.8	2.6	3.0
	100 µg/ml hIgG4	14.5	2.4	2.9	4.8	2.5	3.1
	No antibody treatment	49.0	4.0	5.6	5.7	8.2	6.1
Test Article	10 µg/ml MDX-1106-IgG4	6.0	0.9	2.5	4.2	BDL	2.4
	100 µg/ml MDX-1106-IgG4	6.4	0.9	2.0	3.7	1.0	1.2
Positive Control	10 µg/ml anti-CD3 Ab	3202.2	161.4	728.8	966.1	31.5	247.0
	100 µg/ml anti-CD3 Ab	>5000.0	226.0	939.3	2141.3	52.3	635.5
Negative Control	10 µg/ml hIgG4	BDL	1.5	2.2	2.2	1.5	0.9
	100 µg/ml hIgG4	BDL	0.5	1.8	2.0	1.8	BDL
	No antibody treatment	11.8	1.1	2.7	2.4	2.8	1.5
Test Article	10 µg/ml MDX-1106-IgG4	BDL	0.7	2.3	2.2	2.0	0.7
	100 µg/ml MDX-1106-IgG4	BDL	1.4	2.3	2.0	0.9	0.7
Human Blood Donor 4 at 24 hours							
Positive Control	10 µg/ml anti-CD3 Ab	578.0	305.5	311.0	1813.5	102.1	766.5
	100 µg/ml anti-CD3 Ab	970.1	470.5	445.0	2809.0	142.0	1501.0
Negative Control	10 µg/ml hIgG4	4.7	2.0	4.5	10.6	3.2	2.6
	100 µg/ml hIgG4	15.6	1.4	4.7	12.1	3.8	1.7
	No antibody treatment	BDL	2.5	3.5	8.8	3.8	8.3
Test Article	10 µg/ml MDX-1106-IgG4	13.5	3.3	6.3	59.4	4.6	1.8
	100 µg/ml MDX-1106-IgG4	14.5	2.0	3.2	11.3	3.3	4.8

BDL = Below Detection Limit

		Cytokine Concentration (pg/ml)					
		IFN-γ	TNF-α	IL-10	IL-6	IL-4	IL-2
Human Blood Donor 5 at 4 hours							
Positive Control	10 µg/ml anti-CD3 Ab	4532.5	771.5	38.3	78.3	39.4	135.0
	100 µg/ml anti-CD3 Ab	>5000.0	1188.8	58.9	166.6	47.5	281.0
Negative Control	10 µg/ml hIgG4	16.4	2.7	3.1	5.5	2.8	2.3
	100 µg/ml hIgG4	7.1	2.2	3.0	4.5	2.9	1.2
	No antibody treatment	7.1	1.7	2.1	4.1	2.8	2.4
Test Article	10 µg/ml MDX-1106-IgG4	15.4	3.6	2.8	5.5	3.4	4.7
	100 µg/ml MDX-1106-IgG4	12.7	3.1	2.2	5.5	2.6	2.0
Human Blood Donor 5 at 24 hours							
Positive Control	10 µg/ml anti-CD3 Ab	>5000.0	566.2	191.5	3473.0	165.0	1352.6
	100 µg/ml anti-CD3 Ab	>5000.0	685.0	333.0	4703.0	204.5	2194.6
Negative Control	10 µg/ml hIgG4	22.9	1.6	3.9	5.6	3.2	4.6
	100 µg/ml hIgG4	15.0	1.2	4.0	8.7	2.7	1.6
	No antibody treatment	10.8	8.2	12.5	7.2	2.9	1.4
Test Article	10 µg/ml MDX-1106-IgG4	18.1	2.3	3.3	4.5	3.3	3.6
	100 µg/ml MDX-1106-IgG4	21.2	1.8	3.6	5.4	3.6	3.2

Human Blood Donor 6 at 4 hours							
Positive Control	10 µg/ml anti-CD3 Ab	>5000.0	1553.5	22.5	76.3	41.8	187.1
	100 µg/ml anti-CD3 Ab	>5000.0	1444.5	26.9	157.7	44.6	257.6
Negative Control	10 µg/ml hIgG4	10.2	3.8	2.5	5.6	2.9	3.1
	100 µg/ml hIgG4	14.5	3.6	2.5	4.7	3.4	4.6
	No antibody treatment	7.7	2.6	1.2	3.9	2.9	BDL
Test Article	10 µg/ml MDX-1106-IgG4	7.2	3.6	2.1	6.0	3.3	3.5
	100 µg/ml MDX-1106-IgG4	15.0	3.8	2.8	5.3	2.6	3.4
Human Blood Donor 6 at 24 hours							
Positive Control	10 µg/ml anti-CD3 Ab	>5000.0	928.5	212.2	868.5	136.9	503.8
	100 µg/ml anti-CD3 Ab	>5000.0	875.9	335.1	1717.2	186.5	841.7
Negative Control	10 µg/ml hIgG4	13.4	2.5	3.6	5.3	3.3	5.0
	100 µg/ml hIgG4	15.0	1.8	2.6	4.2	3.5	4.7
	No antibody treatment	BDL	1.0	2.8	3.6	3.9	4.6
Test Article	10 µg/ml MDX-1106-IgG4	9.2	2.1	2.7	5.7	3.0	2.4
	100 µg/ml MDX-1106-IgG4	12.5	2.2	2.8	4.4	3.2	3.1

(Table excerpted from Applicant's BLA)

MDX-1106-028-R: Binding and Blocking Characteristics of Chimeric Anti-Mouse-PD-1 Antibody, 4H2

Nivolumab does not recognize mouse PD-1. Therefore, to assess the efficacy of PD-1 blockade on the growth of transplantable tumors in mice, a surrogate anti-mouse PD-1 antibody was derived. Rats were immunized with mouse PD-1-Fc fusion protein, followed by fusion and screening of clones for reactivity to PD-1. Clone 4H2 was selected for development to its affinity for mouse PD-1. After the V region sequences of 4H2 were determined, the VL and VH sequences were grafted onto the murine kappa and IgG_1 Fc region. The chimeric antibody was then expressed from a transfected CHO cell line. Binding was determined using a fluorescently labelled secondary antibody to mouse IgG and reported as mean fluorescent intensity (MFI). As demonstrated in the following figures, the 4H2 anti-mouse PD-1 antibody binds to cells expressing murine PD-1 (EC_{50} = 2.9 nM, Figure 20) and blocks the binding of mouse PD-L1 (EC_{50} = 3.6 nM, Figure 21) and PD-L2 (EC_{50} = 4.9 nM, Figure 22) to mouse PD-1.

Figure 18: Binding of 4H2 to CHO/mPD-1 Cells

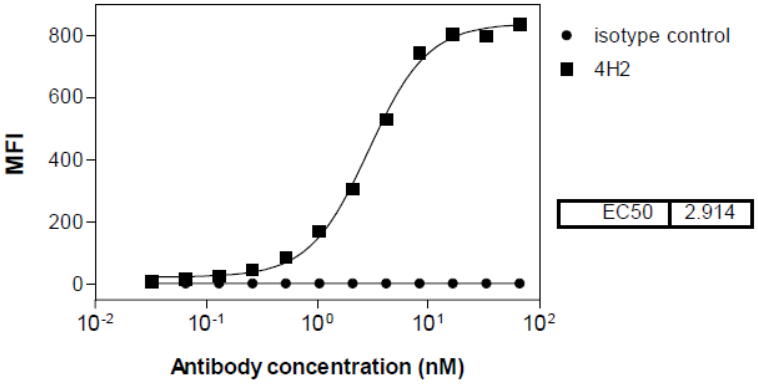

(Figure excerpted from Applicant's BLA)

Figure 19: Blocking of mPD-L1 Binding to CHO/mPD-1 Cells by 4H2

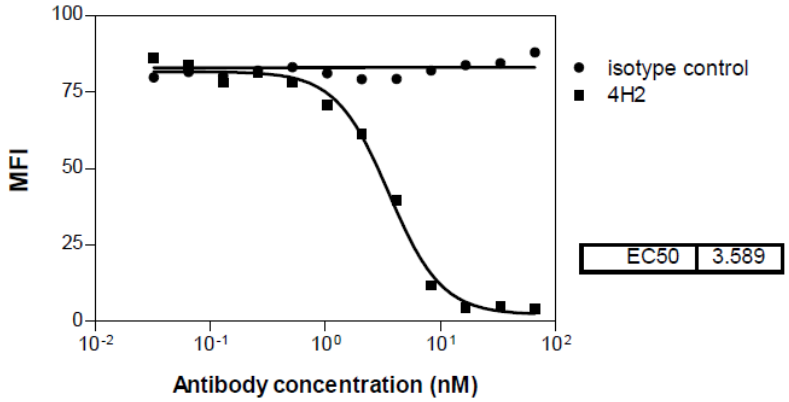

(Figure excerpted from Applicant's BLA)

Figure 20: Blocking of mPD-L2 Binding to CHO/mPD-1 Cells by 4H2

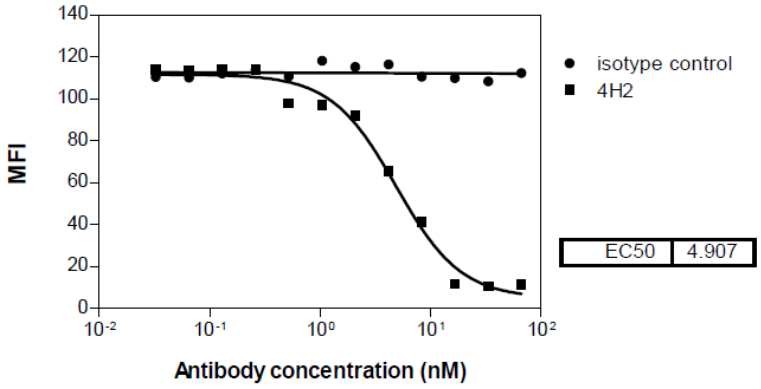

(Figure excerpted from Applicant's BLA)

MDX 1106-034-R: Effects of Anti-PD-1 Monoclonal Antibody in a J558 Myeloma Model

To assess the efficacy of murine anti-PD1 antibody (4H2) in vivo, a therapeutic/staged syngeneic tumor model was derived by subcutaneously injecting 1.5×10^6 J558 mouse myeloma cells into the right flank of BALB/c mice. When tumors reached a mean tumor volume of 130 mm^3, mice were randomized into 3 groups of 8 mice each. On Days 10, 13, and 17, each animal was injected intraperitoneally with 10 mg/kg of 4H2, mouse IgG_1 control antibody (m- IgG_1), or PBS (vehicle control). Tumor growth measurements were obtained twice weekly for approximately four weeks. Mice were euthanized if the tumor volume exceeded 1500 mm^3, tumors became ulcerated, or if they lost 15% of their body weight.

Tumor volume measurements in mice following administration of PBS, m- IgG_1, or 4H2 are shown in Tables 4-6, respectively. A comparison of mean and median tumor volumes across the three treatment groups suggested similar rates of tumor growth with

the exception of one instance of delayed tumor growth and two instances of tumor regression in 4H2-treated animals. The latter two animals remained tumor-free through study termination at Day 38. Interestingly, one of the mice that showed complete tumor regression had a tumor volume of 514 mm^3 on Day 14 which regressed to 58 mm^3 and 0 mm^3 on Days 17 and 21, respectively.

Table 4: J558 Tumor Volume in PBS Vehicle Control Treated Mice

Mouse	mm^3 4/20/2006 Day 10	mm^3 4/24/2006 Day 14	mm^3 4/27/2006 Day 17	mm^3 5/1/2006 Day 21	mm^3 5/4/2006 Day 24	mm^3 5/8/2006 Day 28	mm^3 5/15/2006 Day 35	mm^3 5/18/2006 Day 38
105949	10.37	35.73	798.31	2028.31				
105970	76.86	1080.69	1504.49					
105969	83.07	740.88	1680.00					
105968	92.46	134.40	1547.91					
105956	129.38	1048.05	3691.15					
105964	173.16	1319.72	2797.41					
105958	171.22	1157.87	3537.36					
105979	306.31	1158.95	4105.02					
Mean	130.35	834.54	2457.71	N/A	N/A	N/A	N/A	N/A
SD	88.96	491.13	1231.19	N/A	N/A	N/A	N/A	N/A
Median	110.92	1064.37	2238.70	N/A	N/A	N/A	N/A	N/A

Shading indicates animal died or was euthanized

(Table excerpted from Applicant's BLA)

Table 5: J558 Tumor Volume in m- IgG_1 Control Antibody Treated Mice

Mouse	mm^3 4/20/2006 Day 10	mm^3 4/24/2006 Day 14	mm^3 4/27/2006 Day 17	mm^3 5/1/2006 Day 21	mm^3 5/4/2006 Day 24	mm^3 5/8/2006 Day 28	mm^3 5/15/2006 Day 35	mm^3 5/18/2006 Day 38
105963	26.52	99.65	560.84	2251.5				
105943	63.72	439.45	2235.86					
105983	77.35	895.05	2219.78					
105974	120.89	1176.78	2190.51					
105981	124.51	941.18	2707.23					
105939	164.95	813.24	2403.16					
105973	169.65	983.83	2298.90					
105946	295.80	1155.51	3128.40					
Mean	130.42	813.09	2218.08	N/A	N/A	N/A	N/A	N/A
SD	83.04	368.47	742.22	N/A	N/A	N/A	N/A	N/A
Median	122.70	918.12	2267.38	N/A	N/A	N/A	N/A	N/A

Shading indicates animal died or was euthanized

(Table excerpted from Applicant's BLA)

Table 6: J558 Tumor Volume in 4H2 Treated Mice

Mouse	mm^3 4/20/2006 Day 10	mm^3 4/24/2006 Day 14	mm^3 4/27/2006 Day 17	mm^3 5/1/2006 Day 21	mm^3 5/4/2006 Day 24	mm^3 5/8/2006 Day 28	mm^3 5/15/2006 Day 35	mm^3 5/18/2006 Day 38
105965	33.71	49.50	351.28	1256.90	903.81	2244.68		
105955	55.00	741.31	1609.61					
105948	89.76	457.60	2280.00					
105975	97.02	0.00	0.00	0.00	0.00	0.00	0.00	0.00
105961	135.00	1605.74	1605.74					
105978	159.43	881.28	2232.00					
105986	180.60	1528.92	1528.92					
105987	291.78	514.71	58.07	0.00	0.00	0.00	0.00	0.00
Mean	130.41	722.38	N/A	N/A	N/A	N/A	N/A	N/A
SD	82.01	602.88	N/A	N/A	N/A	N/A	N/A	N/A
Median	116.01	628.01	1567.33	N/A	N/A	N/A	N/A	N/A

Shading indicates animal died or was euthanized

(Table excerpted from Applicant's BLA)

MDX 1106-023-R: Effect of Anti-PD-1 Monoclonal Antibody Administration on Unstaged MC38 Tumor Growth Rates in Mice

Murine anti-PD-1 antibody (4H2) was evaluated in vivo using a prophylactic/unstaged syngeneic tumor model derived by subcutaneously injecting 2×10^6 MC38 cells into the right flank of C57BL/6 mice. On the same day, each animal (n=10/group) was injected intraperitoneally with approximately 10 mg/kg of 4H2 or IgG_1 control antibody. Dosing was repeated on Days 3, 6, and 10. Flanks were checked for the presence and size of tumors every three days until death or euthanasia at tumor endpoint (tumor size ≥4000 mm^3). The response to 4H2 was measured by tumor growth inhibition (TGI; reference mm^3 – test article mm^3/reference $mm^3 \times 100$).

Tumor volume measurements in mice following administration of IgG_1 control antibody or 4H2 are presented in Tables 7 and 8, respectively. In the 4H2-treated group, three mice had tumors that completely regressed by Day 27. These mice remained tumor-free throughout the remainder of the observation period. The remaining six mice had a mean tumor volume of 850 mm^3 on Day 21 compared to the control mean tumor volume of 2955 mm^3. Overall, the mean TGI in the 4H2-treated group was 83% on Day 21.

Table 7: MC38 Tumor Volume in IgG_1 Control Antibody Treated Mice

Mouse	Sex	Birthdate	mm^3	mm^3	mm^3	mm^3	mm^3	mm^3	mm^3	mm^3	mm^3	mm^3
			Day 6	Day 10	Day 13	Day 17	Day 21	Day 27	Day 29	Day 32	Day 49	Day 61
			06/16/2005	06/20/2005	06/23/2005	06/27/2005	06/30/2005	07/6/2005	07/8/2005	07/11/2005	07/28/2005	08/09/2005
IgG1 Group (Control)												
84951	M	03/08/2005	55.55	344.52	519.55	1037.34	2414.00	4901.94				
84993	F	03/27/2005	95.40	161.98	345.06	537.26	1013.00	2136.90	3248.00	4043.52		
85232	F	04/03/2005	145.82	416.47	1090.17	2000.70	3116.00					
85245	F	04/04/2005	57.46	201.96	833.52	1367.10	2472.00	7464.10				
86052	M	04/08/2005	110.11	409.61	1136.34	1739.22	4258.00					
86063	M	04/12/2005	141.75	493.92	1419.34	3120.75	6343.00					
86066	F	04/12/2005	19.78	83.35	360.40	674.48	1175.00	2862.21	4359.60			
86072	F	04/12/2005	59.29	137.70	545.75	813.10	1184.00	2116.40				
86083	M	04/17/2005	16.72	695.52	1314.05	2424.86	4313.00					
87260	M	04/30/2005	0.00	255.78	1271.66	1104.90	3261.00					
Mean			**70.19**	**320.08**	**883.58**	**1481.97**	**2954.90**					
SD			48.88	179.30	392.79	790.88	1604.44					
Median			**58.38**	**287.93**	**858.55**	**1236.00**	**2713.45**					

* ulcerated tumor
Shading indicates animal died or was euthanized.

(Table excerpted from Applicant's BLA)

Table 8: MC38 Tumor Volume in 4H2 Treated Mice

Mouse	Sex	Birthdate	mm^3	mm^3	mm^3	mm^3	mm^3	mm^3	mm^3	mm^3	mm^3	mm^3
			Day 6	Day 10	Day 13	Day 17	Day 21	Day 27	Day 29	Day 32	Day 49	Day 61
			06/16/2005	06/20/2005	06/23/2005	06/27/2005	06/30/2005	07/6/2005	07/8/2005	07/11/2005	07/28/2005	08/09/2005
4H2 Group (Anti-PD-1 mAb)												
84955	M	03/09/2005	119.70	196.79	91.20	5.20	0.00	0.00	0.00	0.00	0.00	0.00
85239	F	04/03/2005	75.90	53.30	9.90	0.00	0.00	0.00	0.00	0.00	0.00	0.00
86055	F	04/08/2005	44.55	73.43	112.32	345.70	526.00	1166.02	*1327.10			
86060	M	04/11/2005	56.43	703.56	746.96	997.56	1346.00	2836.28	4084.10			
86070	F	04/12/2005	33.02	179.74	6.24	10.23	12.58	56.10	94.75	164.24	620.74	2794.58
86081	M	04/17/2005	126.98	328.86	241.08	254.32	524.20	1588.36	3020.20			
86750	M	04/23/2005	113.85	129.32	58.05	6.00	5.00	0.00	0.00	0.00	0.00	0.00
86760	M	04/26/2005	70.60	115.85	98.49	459.10	1149.00	3518.07				
87264	M	04/30/2005	171.60	267.53	300.69	1005.31	600.00	3250.37	3391.22			
87266	M	04/30/2005	86.39	100.46	127.89	367.16	956.00	2562.49	3720.02			
Mean			**89.90**	**214.88**	**179.28**	**345.06**	**511.88**	**1497.77**				
SD			40.63	182.34	208.70	366.75	483.46	1378.59				
Median			**81.15**	**179.74**	**112.32**	**345.38**	**524.20**	**1438.18**	**1327.10**			

* ulcerated tumor
Shading indicates animal died or was euthanized.

(Table excerpted from Applicant's BLA)

MDX 1106-200-R: Effects of Varying Anti-PD-1 Doses on Staged MC38 Tumors in Mice

To determine the response of MC38 colon carcinoma cells to escalating doses of murine anti-PD-1 antibody (4H2) in vivo, a therapeutic/staged syngeneic tumor model was derived by subcutaneously injecting 2×10^6 MC38 cells into the right flank of C57BL/6 mice. Six days after implantation of MC38 cells, 5 groups of 10 animals each were randomized by tumor size and injected intraperitoneally (IP) with one of the following;

Group 1: 10 mg/kg mouse- IgG_1 (m-IgG_1) + 10 mg/kg rat-IgG_1 (r-IgG_1) (control)
Group 2: 10 mg/kg 4H2 + 10 mg/kg rat-IgG_1 (r-IgG_1)
Group 3: 3 mg/kg 4H2
Group 4: 10 mg/kg 4H2
Group 5: 30 mg/kg 4H2

Dosing was repeated on Days 10 and 13. Flanks were checked for the presence and size of tumors every three days until death or euthanasia at tumor endpoint (tumor size ≥4000 mm^3). The response to 4H2 was measured by tumor growth inhibition (TGI; reference mm^3 – test article mm^3/reference mm^3 × 100).

All but one control mouse reached the maximum tumor size endpoint and died or was euthanized within 27 days post tumor implantation. As summarized in Table 9, administration of 3, 10, or 30 mg/kg of 4H2 resulted in TGI and tumor regression. TGI was greatest in the 30 mg/kg treatment group.

Table 9: Tumor Volume over Time in a Staged MC38 Model

	Day 6	Day 13		Day 20		Day 59
Treatment	Mean Tumor Volume (mm^3)	Mean Tumor Volume (mm^3)	Mean % TGI	Median Tumor Volume (mm^3)	Median % TGI	% Mice Tumor-Free
m-IgG1-10 mg/kg + r-IgG1-10 mg/kg	93.56	580.6	N/A	1566.0	N/A	0
4H2-10 mg/kg + r-IgG1-10 mg/kg	96.67	204.4	65	190.3	88	0
4H2-3 mg/kg	85.13	205.0	65	632.0	60	20
4H2-10 mg/kg	84.22	229.7	60	505.0	68	10
4H2-30 mg/kg	83.64	150.3	74	70.0	96	10

(Table excerpted from Applicant's BLA)

MDX 1106-006-R: Dose-Response Effects of Anti-PD-1 Monoclonal Antibody on Unstaged SA1/N Tumor Growth Rate and Immune Response at Tumor Re-Challenge

The efficacy of escalating doses of murine anti-PD-1 antibody (4H2) was assessed in vivo using a prophylactic/unstaged syngeneic tumor model derived by subcutaneously injecting 2 × 10^6 SA1/N murine fibrosarcoma cells into the right flank of A/J mice. In Part 1 of the study, 7 groups of 10 mice each were injected intraperitoneally on Days 1, 4, 7, 10, 14, 17, and 20 with 0.3, 1, 3, 10, or 30 mg/kg of 4H2, 30 mg/kg of mouse IgG_1 control antibody (m- IgG_1), or PBS (vehicle control). Tumor growth measurements were obtained twice weekly for approximately seven weeks. The response to 4H2 was measured by tumor growth inhibition (TGI; reference mm^3 – test article mm^3/reference

mm^3 × 100). Mice were euthanized if the tumor volume exceeded 1500 mm^3, tumors became ulcerated, or if they lost 15% of their body weight.

Fifteen days after the initial implantation, median tumor volume values showed tumor growth inhibition in mice dosed with 4H2 (Table 10). By study termination (Day 50), there were 1/10, 2/10, 2/10, and 4/10 tumor free mice in the 0.3, 1, 3, and 30 mg/kg 4H2 dose groups, respectively. All mice in the PBS or m- IgG_1 groups reached the maximum tumor size endpoint and died or were euthanized.

Table 10: Tumor Volume on Day 15 in an Unstaged SA1/N Model

Treatment group	Tumor Volume at Day 15 Post Implantation				Day 50
	Mean (mm^3)	TGI (%)	Median (mm^3)	TGI (%)	Tumor-free
PBS	1443		1213		0
IgG1 30mg/kg	2160		2192		0
4H2 0.3 mg/kg	1743	19	1583	28	1
4H2 1 mg/kg	1666	23	1775	19	2
4H2 3 mg/kg	N/A	N/A	886	60	2
4H2 10 mg/kg	987	54	1097	50	0
4H2 30 mg/kg	1349	38	808	63	4

Note: In the 4H2 3mg/kg treatment group, less than 100% of the study animals were alive and therefore the mean and TGI% were not calculated.

(Table excerpted from Applicant's BLA)

In Part 2 of the study, the nine tumor free 4H2-treated A/J mice were re-challenged by subcutaneously injecting 2 × 10^6 SA1/N cells into the right flank approximately one month post-4H2 dosing. The goal was to evaluate if mice previously challenged with SA1/N cells and successfully treated with 4H2 would remain refractory to tumor growth following a second challenge to SA1/N cells. Nine naïve A/J mice were also implanted with SA1/N cells subcutaneously into the right flank to serve as a control group. Tumor growth measurements were obtained twice weekly up to Day 62.

The results showed that 100% of naive mice implanted with SA1/N cells developed tumors. In contrast, the nine mice previously treated with 4H2 and re-challenged did not develop tumors during 62 days of observation (data not shown).

MDX 1106-022-R: Dose-Response Effects of Anti-PD-1 Monoclonal Antibody in a Therapeutic SA1/N Tumor Model

To assess the activity of escalating doses of murine anti-PD-1 antibody (4H2) in vivo, a therapeutic/staged syngeneic tumor model was derived by subcutaneously injecting 2 × 10^6 SA1/N murine fibrosarcoma cells into the right flank of A/J mice. When tumors reached a mean tumor volume of 87 mm^3, mice were randomized into 7 groups of 10 mice each and intraperitoneally injected with 0.3, 1, 3, 10, or 30 mg/kg of 4H2, 30 mg/kg of mouse IgG_1 control antibody (m- IgG_1), and PBS (vehicle control). Dosing was

repeated on Days 6, 9, 12, and 15. Tumor growth measurements were obtained twice weekly for approximately seven weeks. The response to 4H2 was measured by tumor growth inhibition (TGI; reference mm^3 – test article mm^3/reference mm^3 × 100). Mice were euthanized if the tumor volume exceeded 1500 mm^3, tumors became ulcerated, or if they lost 15% of their body weight.

Nineteen days after initial implantation, median tumor volume values showed TGI in mice dosed with 4H2 (Table 11). By study termination (Day 36), there were 1/10, 2/10, 2/10, and 1/10 tumor free mice in the 1, 3, 10, and 30mg/kg 4H2 dose groups, respectively. All mice in the PBS or m- IgG_1 groups reached the maximum tumor size endpoint and died or were euthanized.

Table 11: Tumor Volume on Day 19 in a Staged SA1/N Model

	Day 19				Day 36
	Mean (mm^3)	TGI (%)	Median (mm^3)	TGI (%)	Tumor Free Mice
PBS Control	1063	N/A	807	N/A	0
IgG1 Control	1026	N/A	958	N/A	0
Anti-PD-1, 0.3 mg/kg	755	26	693	28	0
Anti-PD-1, 1 mg/kg	869	15	703	27	1
Anti-PD-1, 3 mg/kg	514	50	581	39	2
Anti-PD-1, 10 mg/kg	417	59	423	56	2
Anti-PD-1, 30 mg/kg	479	53	407	58	1

(Table excerpted from Applicant's BLA)

In Part 2 of the study, the six tumor free 4H2-treated A/J mice were re-challenged by subcutaneously injecting 2 × 10^6 SA1/N cells into the right flank approximately one month post-4H2 dosing. The goal was to evaluate if mice previously challenged with SA1/N cells and successfully treated with 4H2 would remain refractory to tumor growth following a second challenge to SA1/N cells. Ten naïve A/J mice were also implanted with SA1/N cells subcutaneously into the right flank to serve as a control group. Tumor growth measurements were obtained twice weekly up to Day 42.

The results showed that 100% of naive mice implanted with SA1/N cells developed tumors by Day 7 and reached the maximum tumor size endpoint and died or were euthanized by Day 21. The six mice previously treated with 4H2 and re-challenged developed small tumors that regressed by Day 10. Four of these mice remained tumor free up to study termination on Day 42 (data not shown).

Effects of Anti-PD-1 Monoclonal Antibody in a Renal Cell Carcinoma (MDX 1106-036-R), 4T1 Breast Carcinoma (MDX 1106-035-R), T26 Colon Carcinoma (MDX 1106-021-R), and B16F10 Melanoma Model (MDX 1106-020-R)

These four studies were conducted to assess the in vivo efficacy of murine anti-PD-1 antibody (4H2) in syngeneic mouse tumor models derived from renal cell carcinoma (Renca), 4T1 breast carcinoma, CT26 colon carcinoma, or B16F10 melanoma cells. In all four models, tumors were refractory to 4H2 treatment (data not shown). In the

Renca and 4T1 models, prophylactic administration of 4H2 to mice implanted with unstaged tumor cells did not impact tumor growth and growth rates were nearly identical between the 4H2-treated and control groups. In the B16F10 and CT26 models, staged tumors grew very aggressively and 4H2 failed to significantly reduce the growth rate of established tumors.

5 Pharmacokinetics/ADME/Toxicokinetics

5.1 PK/ADME

A single-dose PK study of nivolumab was conducted in the cynomolgus monkey at doses of 1 and 10 mg/kg. Nine experimentally-naive monkeys (3/Sex at 1 mg/kg and 3M at 10 mg/kg) received one IV bolus injection on Study Day 1 and were monitored for clinical signs, changes in body weight and food consumption for 28 days. Clinical pathology sampling for tolerability was performed on Study Days 7 and 28, and PK sampling was performed at 0.25, 0.5, 1, 2, 4, 8, and 24 hours post-dose on Day 1, then daily on Days 3, 7, 10, 14, 21, 24 and 28. Immunogenicity was assessed on Study Day 28.

Clinical signs included watery and/or mucoid feces, and alopecia/bruising/abrasions on skin; the relationship of these findings to treatment and/or procedural activities was unclear as there were no control animals in this study. Hematology and clinical chemistry results were unremarkable.

As illustrated in Applicant-Table 12 and Applicant-Figure 23, peak (C_{max}) and overall (AUC_{last}) exposures were linear over the 10-fold dose range evaluated. Half-life estimates were highly variable, but were consistent with most monoclonal antibodies (~ 1 week). The variability in estimated half-life was likely due to the onset of anti-drug antibody (ADA) formation during the terminal elimination phase, as 78% of animals were ADA-positive by Day 28 (Applicant-Table 13). Exposure was maintained in all animals through at least 384 hours (16 days post-dose).

Table 12: Mean PK parameter estimates in the monkey following administration of a single IV dose

Parameter (Units)	1 mg/kg (Group 1)				10 mg/kg (Group 2)	
	Males		Females		Males	
	Mean[a]	SD	Mean[a]	SD	Mean[a]	SD
C_{max} (µg/mL)	34.3	2.20	30.6	1.71	346	21.6
t_{max} (h)	0.5	NA	0	NA	0	NA
t_{last} (h)	384	NA	384	NA	648	NA
AUC_{last} (µg·h/mL)	4010	645	3570	573	47100	12400
AUC (µg·h/mL)	4470	423	4050	616	64200	27400
$t_{1/2}$ (h)	124	20.3	139	12.7	261	226

NA: Not applicable.
a: Median for t_{max} and t_{last}; n=3.

Figure 21: Mean concentration-time profile of nivolumab following administration of a single IV dose in the monkey

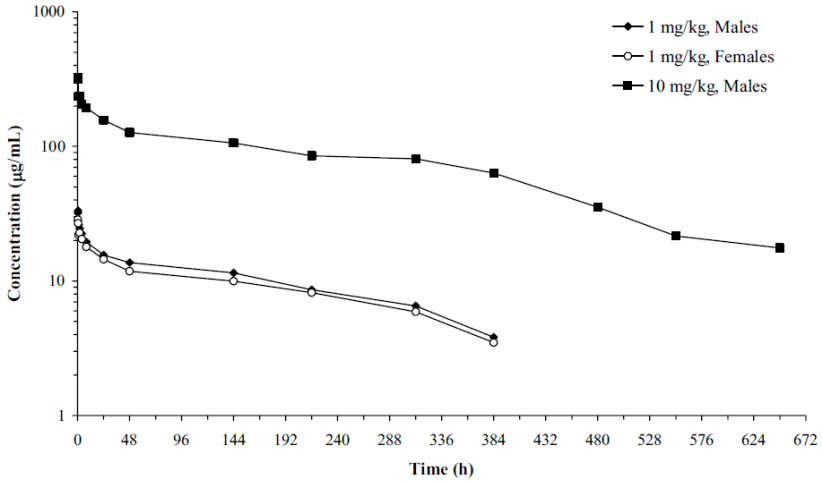

Table 13: ADA response following administration of a single IV dose of nivolumab in the monkey

Table 2: Study SUV00027 Antibody Response Results			
Group, Test Article, Dose Level	**animal**	**Day 28**	**Titration of Day 28 Positive Results***
Group 1 MDX-1106 1mg/kg	1001-MF11202M	Positive	1:1600
	1002-MF4338M	Positive	1:200
	1003-MF1294M	Negative	N/A
	1501-MF22323F	Positive	1:200
	1502-MF4060F	Positive	1:3200
	1503-MF16336F	Positive	1:800
Group 2 MDX-1106 10mg/kg	2001-MF12134M	Positive	1:3200
	2002-MF3241M	Positive	1:200
	2003-MF22286M	Negative	N/A

*Titration of Day 28 Positive Result is defined as the lowest dilution factor of the positive Day 28 sample at which the Mean OD value is ≤1.25 times the Mean OD value of the pre dose sample at the same dilution.

N/A = not applicable

6 General Toxicology

6.2 Repeat-Dose Toxicity

Study title: A 30-Day Toxicity Study of MDX-1106 Administered by Once Weekly Intravenous Injection to Cynomolgus Monkeys, Followed by an Approximate 4-Week Recovery Period

Study no.:	SUV00025
Study report location:	4.2.3.1
Conducting laboratory and location:	(b) (4)
Date of study initiation:	14 December 2005 (1st dose)
GLP compliance:	Yes
QA statement:	Yes
Drug, lot #, and % purity:	Drug:MDX-1106 Batch: 1106-05-01FC-Tox Purity:100% monomer (HPLC-GPC); 95-97% (Stability potency metric: binding by ELISA)

Key Study Findings

- There were no preterm deaths.
- A diffuse pattern of inflammatory infiltration was observed in organs and tissues, but no target organ toxicity was identified by clinical pathology or histological analysis when nivolumab was administered by weekly IV injection to cynomolgus monkeys at doses of 1, 10, or 50 mg/kg/dose for 1 month.

Methods

Doses:	0, 1, 10, 50 mg/kg
Frequency of dosing:	Weekly (Days 1, 8, 15, 22 and 29)
Route of administration:	IV bolus
Dose volume:	10.7 mL/kg
Formulation/Vehicle:	Sterile saline for injection – the formulation of the test article (an aqueous solution) was not provided in the report
Species/Strain:	*Macaca fascicularis* (Chinese origin)
Number/Sex/Group:	5/Sex (3/Sex in main, 2/Sex in recovery, all groups)
Age:	Male: 2.8 to 5.4 years Female: 2.2 - 5.3
Weight:	Male: 2.6 - 3.8 kg Female: 2.0 - 3.1 kg
Satellite groups:	None
Unique study design:	❖ Immunophenotyping ❖ Receptor occupancy ❖ Hormone Levels
Deviation from study protocol:	Reported deviations were unlikely to have affected overall study interpretation (missed/delayed measurements/sample collections, etc.).

Except for histopathology, immunophenotyping, and toxicokinetic tabulations, the following summary references Dr. Hartsough's review of this study under IND 100,052.

Observations and Results

Mortality

All animals survived to scheduled termination.

Clinical Signs

Unremarkable

Body Weights

There were no treatment-related effects of nivolumab administration on mean body weights.

Figure 22: Male body weights in the 1-month repeat-dose study

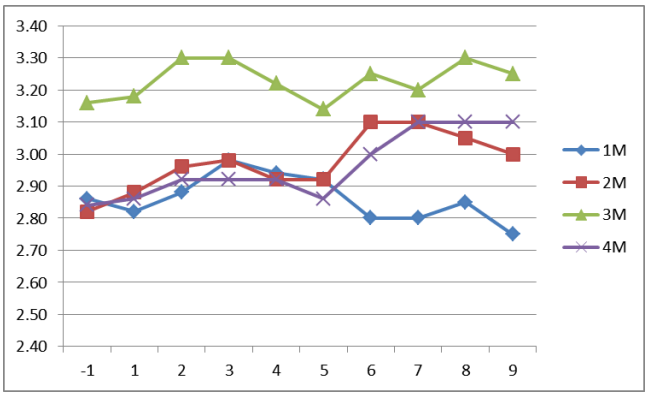

Figure 23: Female body weights in the 1-month repeat-dose study

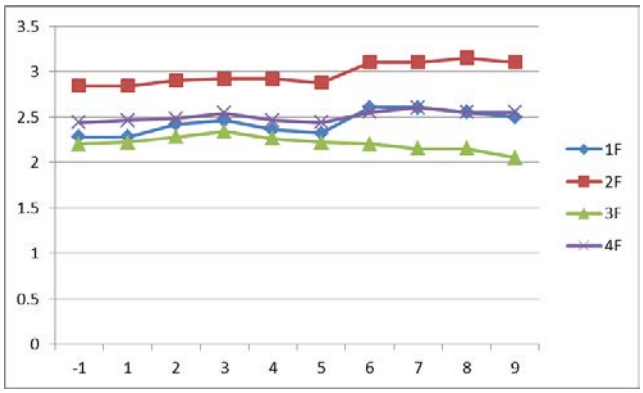

Feed Consumption

Unremarkable

Ophthalmoscopy

Unremarkable

ECG

Unremarkable

Hematology

Unremarkable. Fluctuations in hematology parameters were considered incidental, transient, or related to procedural activities (e.g. serial phlebotomy). There was no evidence of a dose-relationship in the magnitude and/or direction of changes, and there were no patterns of change in clusters of hematology parameters that were indicative of an effect of treatment.

Clinical Chemistry

Unremarkable. In general, fluctuations in serum chemistry values were within the range of pre-study values or within the range commonly observed in this age and strain of animal, and were not considered treatment-related. There were no dose-related changes in individual chemistry parameters, and no patterns of change suggestive of target organ toxicity.

Urinalysis

Unremarkable

Gross Pathology

Unremarkable

Organ Weights

Unremarkable

Histopathology

Adequate Battery
Yes
Peer Review
No
Histological Findings

Table 14: Histological findings of potential or equivocal relationship to treatment

Sex	Male				Female			
Group (mg/kg/Day)	0	1	10	50	0	1	10	50
Organ, Histopathological Description								
Adrenal, depletion, secretory: zona fasciculata: diffuse	1R							
--hemorrhage, focal			1R					
Brain, infiltrate, mononuclear cell: choroid plexus, focal			1					
--infiltrate, mononuclear cell: choroid plexus, multifocal			1+2R		1R	1	1+1R	1R
--infiltrate, mononuclear cell: meninges, diffuse				1				
--infiltrate, mononuclear cell: meninges, focal		1			1R	1R		2
--infiltrate, mononuclear cell: meninges, multifocal		2R	2R	1+1R			2+1R	1
--infiltrate, mononuclear cell: parenchyma, perivascular, focal	1		1	1R		1R	1R	
--infiltrate, mononulear cell,: parenchyma, perivascular, multifocal	1+1R		1	1+1R			1R	1+1R
--mineralization: meninges, multifocal								
--malacia, focal						1		

Sex	Male				Female			
Group (mg/kg/Day)	0	1	10	50	0	1	10	50
Organ, Histopathological Description								
Cecum, trematode parasite (gastrodiscoides): lumen						1		
--nematode parasite (trichuris)			1					
--inflammation, chronic: diffuse								1
Colon, hemorrhage: focal	1						1R	1
--hemorrhage: multifocal		1+1R						
--inflammation, chronic: diffuse								1
Duodenum, hemorrhage: focal	1R						2	
Epididymis, polyp		1			--	--	--	--
Esophagus, infiltrate, mononuclear cell, focal				1R				
Eyes, infiltrate, mononuclear cell: ciliary body: focal	1R			1+2R			1R	1
--infiltrate, mononuclear cell: ciliary body: multifocal			1R			1		
Heart, hemorrhage: diffuse								1
--hemorrhage, multifocal		1						
--hemosiderin, multifocal							1R	
--infiltrate, mononuclear cell, myocardium, multifocal	2R	2R	2R	2R		1R	1R	2R
Injection site, fibrosis, focal	1		1	1			1	2
--edema, dffuse					1			
--hemorrhage, diffuse							1	
--hemorrhage, multifocal					1			
--infiltration, mononuclear cell, focal		1R						
--pigment, brown: dermis, diffuse			1					
--inflammation, acute, diffuse							1	
--inflammation, acute, focal			1		1			
--inflammation, choronic, diffuse			1R			1		
--inflammation, chronic, focal			1R				1	
--thrombus, focal								1
--regeneration, myofiber, multifocal			1					
Kidney, cyst, glomerulus, focal						1		
--mineralization, papilla, focal		1		1			1R	
--mineralization, papilla, multifocal				1+1R			1	
--mineralization, cortex, focal			1R					
--infiltrate, mononuclear cell		1				1		
--infiltrate, mononuclear cell, interstitium, multifocal	2+2R	1+1R	3+2R	2+2R	2+2R	1+1R	3+2R	3+1R
--regeneration, tubular epithelium, multifocal			1R	1+1R	1		1R	
--glomerular sclerosis: focal	1R		1R				1	
--congestion, glomerular tuft: multifocal				1				
--dilatation, tubules, multifocal					1			
--cast, protein, multifocal				2	1			
--cast, cellular, multifocal				1R				

Sex	Male				Female			
Group (mg/kg/Day)	0	1	10	50	0	1	10	50
Organ, Histopathological Description								
--vacuolation, cytoplasm, tubular epithelium, cortex, multifocal								1
Liver, infiltrate, mononuclear cell, periportal, multifocal		1		2	1	1		
--infiltrate, mononuclear cell, paremchuma, multifocal		2			1	2		1
--lipidosis, centrilobular, multifocal								1
--infiltrate, eosinophil, periportal, multifocal						1		
LN, Mandibular, hyperplasia, lymphoid		1	1		2	3		
--extramedullary hematopoiesis						1		
LN, Mesenteric, hyperplasia, lymphoid	1	1	1			2	1	
--infiltrate, eosinophil	1		1		1	1	1	
Lungs, hemosiderin, multifocal				1				
--fibrosis, pleura, diffuse						1		
--inflammation, chronic, alveolar wall, focal		1		1				1
--inflammation, chronic, alveolar wall, multifocal							1	
--alveolar macrophages increased, multifocal				1				
Optic nerve, infiltrate, mononuclear cell, perivascular, focal				1R				
Pancreas, infiltrate, mononuclear cell; focal		1						
--ectopic tissue, spleen	1	1+1R	1+1R	1R	1			1R
--infiltrate, mononuclear cell, islet, focal		1R						
--infiltrate, mononuclear cell; multifocal				1				
--polyp, mesentery, focal							1	
Parathyroid, infiltrate, mononuclear cell, multifocal					1R		1	
--infiltrate, mononuclear cell, focal						1R		
Pituitary, cyst	1R			1	1R		2R	
--infiltrate, nononuclear cell, focal		1R	1R	1R				
Prostate, infiltrate, mononucleara cell, multifocal	2+2R	2+2R	3+2R	2+2R	--	--	--	--
Rectum, inflammation, chronic diffuse						1		1
--infiltrate, mononuclear cell, multifocal	2+1R	3+1R	2+2R	3+2R	1+2R	3+1R	3+2R	2+2R
--mineralization, duct, multifocal	1							
Seminal Vesicles, mineralization, lumen, multifocal			1+1R		--	--	--	--
--infiltrate, monunuclear cell, multifocal			1R					
Skin, granuloma, focal		1						
--infiltrate, mononuclear cell, multifocal			1R					
Spinal Cord, thoracic, infiltrate, mononuclear cell, meninges, focal				1				

Sex	Male				Female			
Group (mg/kg/Day)	0	1	10	50	0	1	10	50
Organ, Histopathological Description								
Spleen, hyperplasia, lymphoid	1R				1R		3+1R	
--hyplasia, nodular, focal			1R					
--hyperplasia, nodular, white pulp, focal							1R	
--hyperplasia, nodular, white pulp, multifocal	1R							
Stomach, hemorrhage, diffuse			1					
--amyloid deposition, lamina propria, multifocal			1R					
--bacteria, lumen						1		
--hemorrhage, focal		1R						
--inflammation, acute, focal					1			
--inflammation, acute multifocal		1	1		1		1+1R	
Stomach, non-glandular,								
Testes, fibrosis, interstitium, diffuse			1		--	--	--	--
--fibrosis, interstitium, multifocal	1R	2	1+1R		--	--	--	--
Thymus, involution	2	1		1	1+2R	1+1R		2+1R
--cyst	1	3	1+1R	1+1R	1+1R	1+1R	1+1R	2+1R
--hemorrhage, focal		1R		1+1R			2R	1R
--hemorrhage, multifocal			2R	1+1R	1R			
Thyroid, infiltrate, mononuclear cell, focal	1R		1		1R			1
--infiltrate, mononuclear cell, multifocal		2	1	1		1		
--ectopic thymus	1	1R			1R			1R
--degeneration, basophilic follicle, focal		1		1				
Tongue, infiltrate, mononuclear cell, focal				1				
Trachea, inflammation, cytoplasm, epithelium, diffuse			1R					
Urinary bladder, vacuolation, cytoplasm, epithlium diffuse			1R					

R = Recovery cohort animal

Special Evaluation

Thyroid hormones (TSH, T3 and T4) were measured predose and on Day 28. There were no treatment-related effects noted.

Toxicokinetics

TK sampling was performed predose, and at 0.25, 0.5, 1, 2, 4, 8, 24, and 72 hours post-dose on Days 1 and 22, and predose and at 1 hour on Days 8, 15 and 29, and prior to necropsy of recovery cohort animals on Day 56. The LLOQ for this assay was 1 µg/mL. Plasma levels of nivolumab were assessed using an ELISA-based antigen-capture method (where the antigen employed was an Fc-PD-1 chimera). Following incubation in Fc-PD-1 coated plates, nivolumab was detected with a mouse-anti-human IgG_4 secondary antibody conjugated to AlkPhos. As indicated in Figure 26, exposures were

essentially proportional with dose and exposures were maintained throughout the study in mid- and high-dose cohorts.

Figure 24: Nivolumab concentration-time profiles (M+F) obtained in the 1-month monkey study

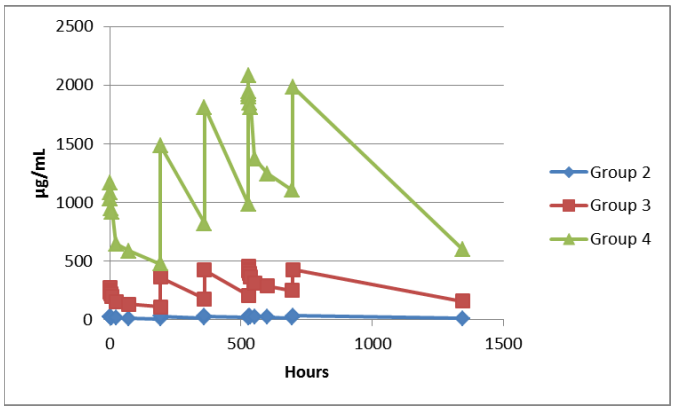

A bridging ELISA was used to detect anti-nivolumab mAbs. Samples were incubated in nivolumab-coated plates. Anti-nivolumab antibodies were detected via addition of a biotinylated nivolumab mAb + a streptavidin-AlkPhos-conjugated detection system. The Applicant did not indicate how the cutpoint for this assay was determined.

As illustrated in Table 15, ADA was detected in approximately half of the low dose animals, and in only one mid- and high-dose animal per group (combined M+F). While it is theoretically possible to induce tolerance by administering high levels of antigen, it is more likely that inverse relationship between dose and ADA frequency reflects a failure of assay sensitivity. As the assay relies on competitive binding between administered drug and labeled drug, high levels of circulating drug may fully saturate the anti-product antibody, leaving an insufficient quantity of free binding sites for the system to detect a response. The Applicant does not comment on drug tolerance in their validation report for this assay.

Table 15: Anti-drug antibody formation in the 4-week monkey study

Group	Animal	Day	Result
	2001	30	Negative
	2002	30	**Positive**
	2003	30	Negative
	2004	57	Negative
	2005	57	Negative
	2501	30	Negative
	2502	57	**Positive**
	2503	57	**Positive**
	2504	30	**Positive**
Group 2	2505	30	Negative

Group	Animal	Day	Result
	3001	30	Negative
	3002	30	Negative
	3003	30	**Positive**
	3004	57	Negative
	3005	57	Negative
	3501	30	Negative
	3502	57	Negative
	3503	57	Negative
	3504	30	Negative
Group 3	3505	30	Negative
	4001	30	Negative
	4002	30	Negative
	4003	30	Negative
	4004	57	**Positive**
	4005	57	Negative
	4501	30	Negative
	4502	57	Negative
	4503	57	Negative
	4504	30	Negative
Group 4	4505	30	Negative

Receptor occupancy

Receptor occupancy was evaluated prior to the recovery necropsy (Week 8) by staining with either biotin-conjugated nivolumab or a biotinylated anti-PD-1 antibody (26D5) that binds to another epitope on the PD-1 molecule. As illustrated in Applicant-Table 16, the majority of animals had appreciable receptor occupancy even after a 4-week washout, a substantial proportion of CD3+ cells in all dose groups exhibited reduced binding of biotin-nivolumab (biotin-MDX1106), indicating stearic hindrance by either receptor downregulation or drug-residence. There was little difference between groups (including controls) in the extent of 26D5 binding, which suggests that receptor down-regulation did not account for the majority of the reduction noted with the biotinylated therapeutic antibody. A number of animals were ADA-positive by the end of the study, and in those animals, binding of biotin-MDX-1106 was comparable to previously untreated controls, which also correlated with reduced and/or ablated plasma drug levels.

Table 16: Receptor occupancy in monkeys 4-weeks after cessation of dosing

MDX-1106 Dose (mg/kg)	Monkey ID	% Cells Stained with hIgG4-Biotin in CD3 T-cell Gate	% Cells Stained with 26D5-Biotin in CD3 T-cell Gate	% Cells Stained with MDX-1106-Biotin in CD3 T-cell Gate	PD-1 Receptors Occupied by MDX-1106	Serum Level of MDX-1106 (µg/ml)	Anti-MDX-1106 Response
0	1004	1.83	13.7	42.4	No	N/A	N/A
(saline)	1005	2.72	13.6	58.2	No	N/A	N/A
	1502	3.33	13	28.5	No	N/A	N/A
	1503	2.56	7.13	46.9	No	N/A	N/A
1	2004	2.12	8.48	2.58	Yes	12.6	–
	2005	2.33	9.73	2.14	Yes	11.9	–
	2502	3.18	14.2	38.4	No	BDL	+
	2503	1.11	11.7	37.6	No	BDL	+
10	3004	2.41	7.73	2.6	Yes	120.4	–
	3005	2.42	5.4	1.34	Yes	191.1	–
	3502	4.02	16.2	3.09	Yes	150.8	–
	3503	2.26	11.8	2.91	Yes	174.8	–
50	4004	2.32	17.6	65.1	No	BDL	+
	4005	2.43	7.62	2.41	Yes	641.4	–
	4502	4.07	14	3.13	Yes	654.5	–
	4503	2.14	14.4	1.76	Yes	506.0	–

N/A: not-applicable
BDL: below detection limit ((b) (4)

Flow Cytometry

There were no treatment-related changes in peripheral blood B (CD20+) or T (CD3+) cells, and no changes in T cell subsets (CD3+CD4+ or CD3+CD8+), NK cells (CD3-CD16+), or monocyte (CD3-CD14+) subsets. Changes from baseline were noted for many of the populations evaluated; however, as similar changes were also noted in controls, they are not considered treatment-related.

Dosing Solution Analysis

Materials were dosed as supplied and were not subsequently formulated prior to administration. Dose solutions were characterized by their labeling and the certificates of analysis that accompanied the materials. The manufacturer's stability data support the stability of the test article under the storage conditions used in the conduct of this study.

Study title: A 3-month intravenous toxicity study of MDX-1106 with a 28-day recovery period in cynomolgus monkeys

Study no.:	(b) (4)-552003
Study report location:	4.2.3.2
Conducting laboratory and location:	(b) (4)
Date of study initiation:	25 July 2006 (first dose)
GLP compliance:	Yes

QA statement:	Yes
Drug, lot #, and % purity:	Drug (MDX-1106) Lot: M48A-06-02FC Purity: 100% (HPLC-GPC), 93% (Antigen binding ELISA)

Methods

Doses:	0, 10, and 50 mg/kg
Frequency of dosing:	2X/Week
Route of administration:	IV bolus injection
Dose volume:	1-3 mL/kg
Formulation/Vehicle:	0.9% sodium chloride for injection, USP
Species/Strain:	*Macaca fascicularis* (Vietnamese origin)
Number/Sex/Group:	4/Sex (Main Study) 2/Sex (Recovery Cohort – all groups)
Age:	2-3 years
Weight:	Males: 1808-2557 grams Females: 1765-2394 grams
Satellite groups:	None
Unique study design:	Hormone measurements; immunophenotyping
Deviation from study protocol:	Reported deviations were unlikely to have affected overall study interpretation.

Note that the day of first dose administration is designated as Study Day 0.

Key Study Findings

- There were no preterm deaths.
- A diffuse pattern of inflammatory infiltration was observed in organs and tissues, but no target organ toxicity was identified by clinical pathology or histological analysis.
- T3 and TSH levels were decreased in high dose females; however, there was no histological evidence of thyroid disturbance and levels of T4 were unaffected .
- There was no effect on the other hormones evaluated; however, post-dose hormone levels were often observed to be more highly variable than those measured pre-dose.

Observations and Results

Mortality

There were no preterm deaths

Clinical Signs

Diarrhea/mucoid, red or soft feces was observed in treated males and females. In addition, emesis was observed in 1 treated male and 1 treated female. The frequency of diarrhea/red or mucoid feces was lower during the post-dose period suggesting possible reversibility. It should be noted that animals were pair-housed during non-dosing days; therefore these data are difficult to interpret, as it is not clear whether the

pair assignments were by dose-group or across dose groups (the applicable SOPs were not provided in the report).

Body Weights

There was an apparent decrease in mean body weight gain in treated males during the dosing phase (Figure 27). The apparent drop in body weights in all males and in control females was due to selection bias at the end of the dosing phase, such that animals designated as recovery cohort animals were lighter than those designated for the main study necropsy. The effect on overall body weight in males is unclear, but may in part result from the effects on the GI tract (diarrhea). Some incidences of inappetence and emesis were observed; however, they were sporadic and unlikely explain the differences in weight gain observed during the course of the study.

Figure 25: Male body weights in the 13-week repeat-dose study

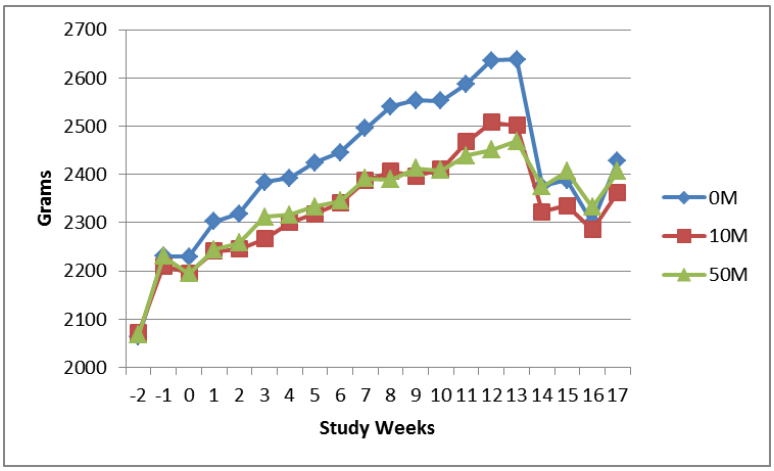

There were no effects of nivolumab treatment on female body weights (Figure 28). The apparent decrease in mean body weight of control females during Week 14 was the result of selection bias; the animals that were selected for the recovery cohort were lighter than the animals that were selected for termination at the end of the dosing interval.

Figure 26: Female body weights in the 13-week repeat-dose study

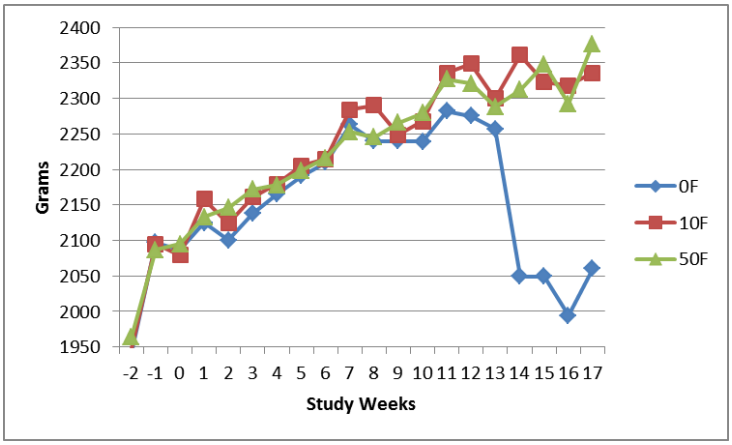

Feed Consumption

The report states that the data were collected qualitatively; however, the data were not contained in the report. Individual incidences of inappetence were recorded in the clinical observations; however, the observations were distributed across all groups (including control) and animals were pair-housed on non-dosing days, therefore individual feed consumption data are difficult to report and interpret.

Ophthalmoscopy

Unremarkable

ECG

One high-dose female (#2257) exhibited ventricular premature contractions (PVCs) on the first dosing occasion. Another high-dose female (#2258) exhibited PVCs at the end of the treatment interval. Although PVCs can be considered a normal variant in this species, an effect of nivolumab on cardiac rhythm cannot be excluded as both incidences were reported in high-dose animals.

There were no effects of nivolumab treatment on ECG interval durations (mean and/or individual), as values were generally within the range of baseline or concurrent control measurements. There was also no effect of nivolumab treatment on oxygen saturation. A transient decrease in body temperature was observed in high dose males on Study Day 0 (first dosing interval). This was not observed at subsequent timepoints. No change in body temperature was observed in females.

Hematology

Unremarkable

Clinical Chemistry

Unremarkable

Urinalysis

Unremarkable

Gross Pathology

Unremarkable

Organ Weights

Unremarkable

Histopathology

Adequate Battery
Yes
Peer Review
No

Histological Findings:

Histological findings of diffuse mononuclear infiltration were consistent with the known mechanism of action of nivolumab. As PD-1 is involved in the downregulation of the immune responses in local tissues, an increased frequency of resident inflammatory cells is an expected finding with drugs that inhibit this pathway. There were no clear observations of autoimmune disease in these animals. As illustrated in Table 17, histological findings in individual animals did not correlate with individual clinical pathology changes.

Group (mg/kg/Day)	0	10	50	0	10	50
Sex	Male			Female		
Organ, Histopathological Description						
Adrenal, cortex: infiltrate, mononuclear			1			
--adhesion (present)	1R					
Adrenal, medulla: mineralization		1				
Brain, pigment, brown		1				
--degeneration, grey matter		1				
Cecum: parasites, trematodes		1		1		
--dilatation, glandular		1				
Colon: congestion			1			
--pigment			1			
Duodenum: infiltrate, mononuclear	1		1			
Epididymis, immature	3+2R	4+2R	4+2R	--	--	--
Eyes: atrophy, retinal	1R	1R	1R			1
Gallbladder: infiltrate, mononuclear	2					
Heart: infiltrate, mononuclear**	1R	2+1R	2+1R	2	2	3+2R
Ileum: hemorrhage		1				

Group (mg/kg/Day)	0	10	50	0	10	50
Sex	Male			Female		
Organ, Histopathological Description						
Injection site: hemorrhage	1	1	2	1	3	2
--inflammation, chronic active	3	3	2			
--inflammation, acute			1		1	
--pustule, intraepithelial				1	1	
Kidney: infiltrate, mononuclear**	1	4+2R	1+2R	2+1R	3	3
--mineralization		1				
Liver: vacuolation, hepatocellular			1			1R
--congestion			1			
--infiltrate, mononuclear			1			2+1R
LN, Mandibular: hyperplasia, lymphoid	1					
LN, Mesenteric: depletion, lymphoid			1			
Lungs: infiltrate, mononuclear			1			
--inflammation, chronic		1	1+1R		1R	3
--pigment, brown						1
--inflammation, granulomatous	1R					
Marrow, Femur: hypercellular**	2R	1	2+1R	1		1
Marrow, Sternum: hypercellular			1			1
Nasal Level I: inflammation, acute	1R			1		
--hyperkeratosis						1
Nasal Level III: inflammation, acute		1				
Nasal Level IV: inflammation, acute		1				
Nerve, Sciatic: degeneration, axonal		1	1			
Ovaries: Mineralization	--	--	--	1+1R	1R	1+1R
--cyst	--	--	--	1		
Pancreas: infiltrate, mononuclear**		1	1	1		
Prostate: immature	2+2R	4+2R	4+2R	--	--	--
--infiltrate, mononuclear	1R	1		--	--	--
Rectum: infiltrate, mononuclear						1
Salivary Gland, mandibular: infiltrate, mononuclear**	2	3+1R	3+1R	2	1+1R	3
Seminal Vesicles: immature**	1R	2R	2R			
Skeletal Muscle: infiltrate, mononuclear	1	1			1	1R
Spleen: depletion, lymphoid			1			
--eosinophilic proteinaceous deposits					1	1
Stomach: infiltrate, mononuclear	3+1R	4+1R	4+1R	4+2R	4+1R	3+1R
Testes: immature	3+2R	4+2R	4+2R	--	--	
Thymus: macrophages, tingible body	1	1	1	1		
--atrophy**	1	2	1			
Thyroid glands: hypertrophy, follicular cell			1	1		
--infiltrate, mononuclear			1			
--cyst, follicular (present)		1R				
Urinary bladder: infiltrate, mononuclear		2	1			
--ectopic tissue (present)					1	
Uterus: pigment, brown				1R		

** = increasing severity with dose; R = denotes recovery cohort animals

Table 17: Asessment of the correlation between individual histological changes and clinical pathology endpoints

Group	Animal	Histopathological Change	ALP/ALT/AST/GGT	UN/CREA
0 M	2229	Kidneys: infiltrate, mononuclear (Grade 1)	529/65/45/54.3	22.0/0.4
10M	2228	Kidneys: infiltrate, mononuclear (Grade 1) Liver: infiltrate, mononuclear (Grade 1)	880/90/92/116.3	27.1/0.7
10M	2231	Kidneys: infiltrate, mononuclear (Grade 1)	397/53/92/41.0	27.1/0.4
		Kidneys: mineralization (Grade 2)		
10 M	2242	Kidneys: infiltrate, mononuclear (Grade 1)	943/65/72/108.3	25.8/0.5
10 M	2245	Kidneys: infiltrate, mononuclear (Grade 1)	596/108/90/84.0	24.4/0.4
50 M	2239	Liver: vacuolation, hepatocellular (Grade 1) Liver: congestion (Grade 2)	672/50/59/56.2	22.6/0.5
50 M	2243	Kidneys: infiltrate, mononuclear (Grade 1) Liver: infiltrate, mononuclear (Grade 1)	470/81/54/62.6	22.9/0.5
0F	2256	Kidneys: infiltrate, mononuclear (Grade 2)	481/69/52/72.6	23.5/0.4
0F	2265	Kidneys: infiltrate, mononuclear (Grade 1)	568/49/48/67.3	20.4/0.4
10 F	2251	Kidneys: infiltrate, mononuclear (Grade 2)	397/41/107/56.7	23.5/0.4
10 F	2262	Kidneys: infiltrate, mononuclear (Grade 1)	423/48/50/50.5	31.9/0.4
10 F	2263	Kidneys: infiltrate, mononuclear (Grade 1)	495/58/69/35.6	25.5/0.6
50 F	2258	Kidneys: infiltrate, mononuclear (Grade 2)	262/52/68/39.7	25.3/0.5
50 F	2260	Kidneys: infiltrate, mononuclear (Grade 2) Liver: infiltrate, mononuclear (Grade 1)	619/61/52/60.1	23.7/0.5
50 F	2261	Kidneys: infiltrate, mononuclear (Grade 3) with tubular degeneration in the areas of infiltrate Liver: infiltrate, mononuclear (Grade 1)	425/40/55/73.4	23.9/0.4
10 M (R)	2240	Kidneys: infiltrate, mononuclear (Grade 1)	460/55/34/41.3	19.2/0.4
10 M (R)	2241	Kidneys: infiltrate, mononuclear (Grade 1)	813/47/37/113	18.9/0.5
50 M (R)	2237	Kidneys: infiltrate, mononuclear (Grade 1)	1006/72/50/64.2	16.1/0.5
0 F (R)	2249	Kidneys: infiltrate, mononuclear (Grade 2)	516/51/42/75.4	15.6/0.5
50 F (R)	2235	Kidneys: infiltrate, mononuclear (Grade 2)	687/157/174/62.9	20.9/0.4
50 F (R)	2250	Liver: infiltrate, mononuclear (Grade 1)	500/53/66/68.4	19.6/0.5
50 F (R)	2254	Liver: vacuolation, hepatocellular (Grade 2)	557/47/57/106.2	19.8/0.6

Week 13 Control Range (Male)	Week 13 Control Range (Female)	Recovery Control Range (Male)	Recovery Control Range (Female)
ALP: 572-1307	ALP: 399-604	ALP: 656-755	ALP: 516-716
ALT: 49-154	ALT: 49-66	ALT: 38-72	ALT: 51-52
AST: 44-154	AST: 48-84	AST: 28-58	AST: 42-47
GGT: 54-104	GGT: 59-75	GGT: 51-81	GGT: 57.8-75.4
UN: 21.4-30.8	UN: 20.4-23.8	UN: 21.6-24.5	UN: 15.6-18.8
CREA: 0.4-0.6	CREA: 0.3-0.5	CREA: 0.3-0.5	CREA: 0.5

Toxicokinetics

TK sampling was collected predose and at 1, 4, 8, and 24 hours post-dose on Days 0 (first dose), 21, 89, and 90. During non-TK weeks, blood samples were collected only pre-dose and at 1 hour post-dose. During recovery, samples were collected weekly.

Mean concentration-time profiles (M+F) for 10 and 50 mg/kg animals are given in Figure 29, and the toxicokinetic parameters are summarized in Applicant-Table 18.

Table 18: Toxicokinetic summary from the 3-month monkey study

Parameter	Week	MDX-1106	
		10 mg/kg twice a week	50 mg/kg twice a week
Cmax[a] (µg/mL)	13	801	3,610
AUC(0-168h) (µg•h/mL)	13	117,000	531,000

[a] Cmax values were estimates of time 0 (ie, initiation of dosing).

Applicant Table 19 summarizes the immunogenicity results obtained in this study. The methods employed in the TK and ADA sample analyses rely on the same methods used to support the 1-month study. As described in the TK discussion of the 1-month monkey study, the ADA method appears to be inadequately sensitive due to poor drug tolerance. It is likely that the number of ADA-positive animals reflected in Applicant-Table 19 underestimates the true number of ADA-positive animals in the study as a result of competition for binding by high residual drug levels.

The Applicant did not perform incurred sample reanalysis in either of the two bioanalytical studies that support the toxicological assessment of nivolumab.

Table 19: Immunogenicity results from the 13-week monkey study

Group, Test Article, Dose Level	animal	Week 4	Week 8	Week 13	Week 17
Group 2 MDX-1106 10mg/kg	2228	Negative	Negative	Negative	NA
	2231	Negative	Negative	Negative	NA
	2240	Negative	Negative	Negative	Negative
	2241	Negative	Negative	Negative	Negative
	2242	Negative	Negative	Negative	NA
	2245	*Positive*	*Positive*	*Positive*	NA
	2247	Negative	Negative	Negative	NA
	2251	Negative	Negative	Negative	NA
	2252	Negative	Negative	Negative	Negative
	2257	Negative	Negative	Negative	Negative
	2262	Negative	Negative	Negative	NA
	2263	Negative	Negative	Negative	NA
Group 3 MDX-1106 50mg/kg	2232	Negative	Negative	Negative	NA
	2233	Negative	Negative	Negative	NA
	2235	Negative	Negative	Negative	Negative
	2237	Negative	Negative	Negative	Negative
	2239	Negative	Negative	Negative	NA
	2243	Negative	Negative	Negative	NA
	2250	Negative	Negative	Negative	Negative
	2254	Negative	Negative	Negative	Negative
	2258	Negative	Negative	Negative	NA
	2259	Negative	Negative	Negative	NA
	2260	Negative	Negative	Negative	NA
	2261	Negative	Negative	Negative	NA

NA = not applicable

Figure 27: Nivolumab concentration-time profiles (M+F) obtained in the 13-week monkey study

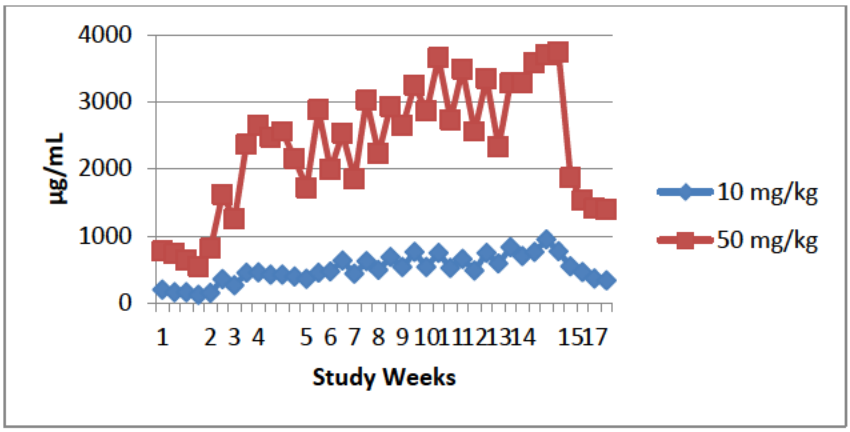

Dosing Solution Analysis

Materials were administered as supplied and were not reformulated; accordingly, the materials were characterized by their labeling and the accompanying certificates of analysis. The Study Director states that data documenting the purity and stability of the test article was on file with the Applicant, but the report did not contain the data.

Special Evaluation

Immunophenotyping was performed prior to each scheduled termination using lymphocytes isolated from peripheral blood, spleen and lymph nodes. Table 20 lists the populations characterized in this study.

Table 20: Lymphocyte populations analyzed

Marker	Population
CD3	T cells
CD14	Monocytes
CD11cHi	Dendritic cells
CD20	B cells
CD3+CD45RA-	Memory T cells
CD3+CD25+	Regulatory T cells
CD4+CD28+CD95- and CD8+CD28+CD95-	Naïve T cells
CD4+CD28+CD95+ and CD8+CD28+CD95+	Central memory T cells
CD4+CD28-CD95+ and CD8+CD28-CD95+	Effector memory T cells

As illustrated in Figure 30 and Figure 31, there was an increase in CD4+ and CD8+ effector memory T cells in mid and/or high dose animals relative to concurrent controls at the end of the dosing interval. In addition, there were more CD8+ central memory T cells in mid- and/or high-dose animals (Figure 32). These findings are expected due to the mechanism of action, since PD-1 inhibition prevents the dampening of the immune

response and therefore permits proliferation and differentiation of T cells for a longer period of time than would occur in the presence of an intact PD-1 pathway.

Figure 28: EM CD28-CD95+ Lymphocytes as %CD4+ lymphocytes in peripheral blood, spleen and lymph nodes (Weeks 13 and/or 17)

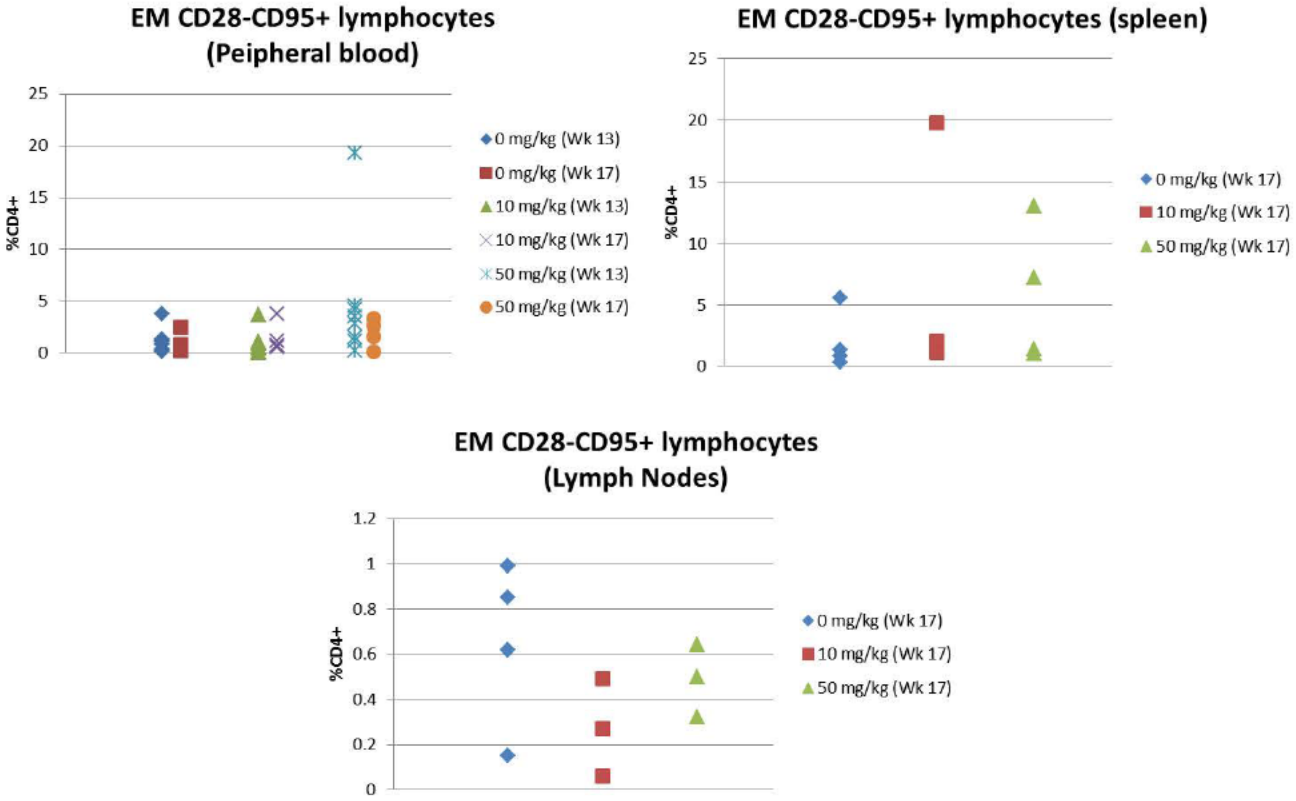

Figure 29: CD28-CD95+ Lymphocytes as %CD8+ lymphocytes in peripheral blood, spleen and lymph nodes (Weeks 13 and/or 17)

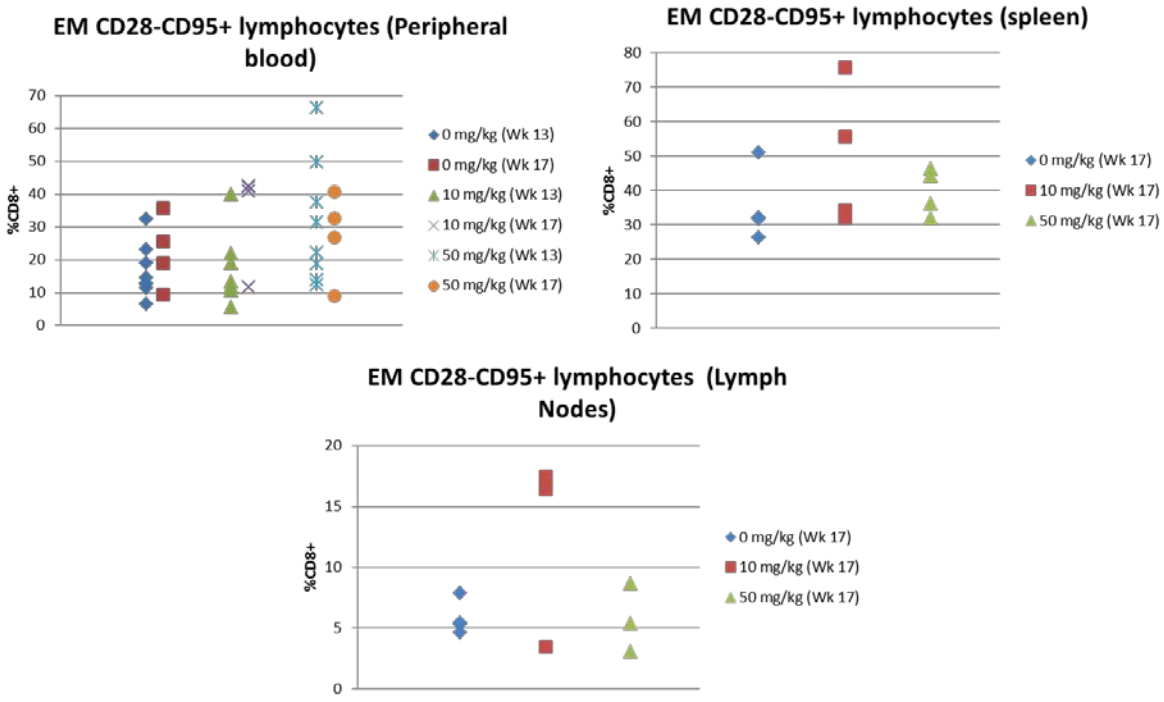

Figure 30: CM CD28+CD95+ Lymphocytes as %CD8+ lymphocytes in peripheral blood, spleen and lymph nodes (Weeks 13 and/or 17)

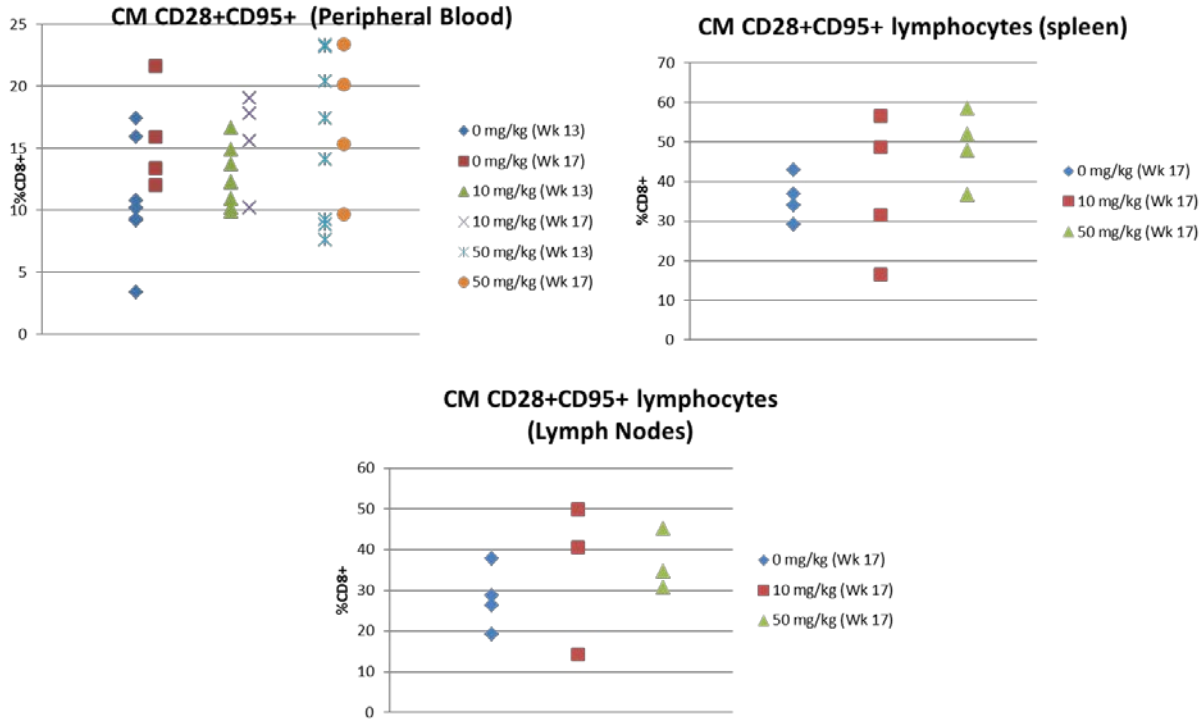

7 Genetic Toxicology

Genetic toxicology studies were not conducted with nivolumab, since, as a monoclonal antibody, it is not expected to interact directly with DNA or other chromosomal material. This is in keeping with the principles of the ICH S6 guideline for the Preclinical Safety Evaluation of Biotechnology-Derived Pharmaceuticals.

8 Carcinogenicity

Carcinogenicity studies were not conducted with nivolumab, which is consistent with its use in patients with advanced malignancies (*see* the ICH S9 Guideline for the Nonclinical Evaluation of Anticancer Pharmaceuticals). If nivolumab is developed for use in other indications, an assessment of its carcinogenic potential may be warranted; however rodent bioassays are likely inappropriate, as nivolumab does not appear to be active in rodents.

9 Reproductive and Developmental Toxicology

9.3 Prenatal and Postnatal Development

Study title: BMS-936558: Intravenous Study of Pre- and Postnatal Development in Cynomolgus Monkeys with a 6-Month Postnatal Evaluation

Study no.:	20012606
Study report location:	4.2.3.5.3
Conducting laboratory and location:	(b) (4) United States
Date of study initiation:	19 March 2012
GLP compliance:	Yes
QA statement:	Yes
Drug, lot #, and % purity:	Drug: MDX-1106 **Lot: 2B71294** Purity (SE-HPLC): 99% Purity (Binding & potency activity by ELISA): 104% **Lot: 1L6087** Purity (SE-HPLC): 98% Purity (Binding activity by ELISA): 86%

Key Study Findings

- Administration of BMS936558 was associated with a dose-related increase in pregnancy loss, particularly during the third trimester. The rate of pregnancy loss

in this study exceeded the average historical control frequency, and the individual study incidence noted in historical controls, and is considered treatment-related.

- Aside from one umbilical thrombus noted in one 50 mg/kg female that aborted on GD47, no cause was ascribed to any of the first-trimester pregnancy losses, and all evaluable fetuses/stillbirths appeared normal.
- Three of the 4 infants lost in the 10 mg/kg dose group were delivered prematurely (GD 131, 135 and 143) and died within the first two weeks.
- There were no clear treatment-related gross or histopathological lesions in infants that died prior to scheduled termination; the cause of death was ascribed to prematurity and failure to thrive.
- Toxicokinetic exposure was maintained in most dams and high-dose infants through the end of the study (PPD 182±1)

Methods

Doses:	0, 10, 50 mg/kg An additional group (designated as Group 4 and consisting of 3 dams), was included in the study but none of the dams received test article or the vehicle control. Tissues were collected from Group 4 dams and fetuses as corresponding references to BMS-396558-treated animals, as needed.
Frequency of dosing:	Twice weekly
Dose volume:	The test article was formulated as a 10 mg/mL solution and administered as either a 1 or 5 mL/kg injection
Route of administration:	IV injection (0.1 mL/sec)
Formulation/Vehicle:	0.9% sodium chloride for injection
Species/Strain:	*Macaca fascicularis* (Chinese origin) Animals were confirmed SIV-negative (by serology and PCR) prior to study assignment, and were monitored for TB as required by facility SOP. Dams were 3.7-9.3 years of age at the time of dose-initiation, and weighed 2.5-5.1 kg
Number/Sex/Group:	16 pregnant dams/group

Satellite groups: None

Study design:

- Dams were dosed twice weekly beginning on GD20, 21 or 22 (depending on the day of pregnancy confirmation by ultrasound) and continued twice weekly until parturition or pregnancy loss.
- Pregnancy was monitored by ultrasonography every 2 weeks.
- Dams were allowed to deliver naturally and rear infants until postpartum day (PPD) 182±1.
- Dams were monitored for viability, clinical signs, food consumption, body weight, clinical pathology, TK, ADA, immunophenotyping, and formation of antinuclear antibodies.
- Infants underwent teratology and neurobehavioral assessments, and evaluation of clinical pathology, and toxicokinetic parameters.
- The development of the immune system was evaluated in infants at 6 months of age by assessing TDAR (against HBsAg and TT), lymphoid organ weights and histopathology.
- Dosing was discontinued when pregnancy loss was observed, and females were euthanized following sample collection for TK and immunogenicity evaluations.
- All Group 4 females (non-dosed) were euthanized following study termination; surviving Group 1-3 females were returned to the testing facility colony on PPD182±1.

Deviation from study protocol: Reported deviations do not appear to affect overall study interpretation.

Observations and Results

Table 21: Summary of pregnancy or infant losses

BMS-936558 Dose	0 mg/kg	10 mg/kg	50 mg/kg	Historical Control Incidences
1st Trimester Pregnancy Loss	2/16 (12.5%) 1502 (GD33) 1513 (GD47)	0	4/16 (25%) 3506 (GD31) 3502 (GD32) 3514 (GD33) 3507 (GD47)[a]	36/467 (7.7%)[e] [0 to 16.7%]
2nd Trimester Pregnancy Loss	0	0	0	3/201 (1.5%)[f] [0 to 11.1%]
3rd Trimester Pregnancy Loss	1/14 (7.1%) 1511 (GD121)	2/16 (12.5%) 2505 (GD124) 2503 (GD158)	4/12 (33.3%) 3509 (GD113) 3512 (GD127) 3515 (GD161) 3503 (GD167)	31/198 (15.7%)[f] [0 to 31.3%]
Infant Loss	2/13 (15.4%) 1501 (GD138/BD16) 1516 (GD153/BD32)[b]	4/14 (28.6%) 2508 (GD131/BD1) 2516 (GD135/BD1)[c] 2510 (GD143/BD13) 2511 (GD153/BD35)[d]	0	18/161 (11.2%)[f] [0 to 20.0%]

For pregnancy loss, GD = Gestation day when pregnancy loss was first noted.
For infant loss, GD/BD = Gestation length/Day of infant loss after birth.
For Historical Control Incidences, (%) = Overall incidence and [%] = Incidences for individual studies.
[a] Embryonic loss due to umbilical thrombus and considered unrelated to BMS-936558 treatment.
[b] Infant euthanized due to complications with pectus excavatum.
[c] Infant euthanized due to evidence of maternal mutilation.
[d] Infant died under ketamine sedation for blood collection; the death was considered unrelated to BMS-936558.
[e] Based on control data from 6 GLP embryo/fetal development studies (2006-2012; unaudited summary HCD data) and 12 GLP enhanced pre- and postnatal development studies (ePPND) (2008 to present) conducted at the Testing Facility.
[f] Based on control data from 12 ePPND studies conducted at the Testing Facility (2008 to present).

F_0 Dams

Survival: There were no preterm deaths of dams in this study.

Clinical signs:
- Abortion in 3 control females (Days 33-121), one 10 mg/kg female (Day 124) and six 50 mg/kg females (Days 31-127)
- Stillbirth in one 10 mg/kg female (Day 158) and two 50 mg/kg females (Days 161 and 167)

Body weight: Unremarkable

Feed consumption: Unremarkable

Clinical Pathology: Unremarkable; the few statistically significant changes lacked an apparent dose-relationship, and/or were transient.

Necropsy observation: Necropsies were performed for dams (in all dose groups) that aborted, whose infants were stillborn, and for all females in the high dose (50 mg/kg) dose level. There were no treatment-related gross observations in dams that were euthanized in this study.

Toxicokinetics: Exposure was maintained in all but one treated dam for the duration of the dosing phase (through GD Day 134)

Exposure was maintained through Postpartum Day 91 in all but one surviving 10 mg/kg dam evaluated, and in all surviving high dose dams evaluated. While a low level of exposure was observed on PPD 182 in 1/10 surviving dams in the 10 mg/kg dose group and 4/10 surviving dams in the 50 mg/kg dose level, a higher proportion of infants tested (8/11) in the 50 mg/kg dose group had demonstrable exposure on BD182. All but one infant tested had measurable exposure on BD91.

No drug was detected in control animals at any timepoint (note, however, that the LLOQ was 0.4 µg/mL).

Mean Maternal TK			
Parameter	GD	Dose Level (mg/kg)	
		10	50
C_{max} (µg/mL)	20-22 & 27-29	364	1950
	132-134 & 139-141	917[a]	3960[a]
$AUC_{(0-168h)}$ (µg*hr/mL)	20-22 & 27-29	33900	178000
	132-134 & 139-141	117000[a]	541000[a]
Trough	20-22b	203	997
	69-71[c,a]	531	2361
	125-127[d,a]	629	2810
	132-134[e,a]	556	2770

[a]Excludes dam 2509 (concentrations were BLQ)
[b]Collected predose on GD27-29
[c]Collected predose on GD 76-78
[d]Collected predose on GD132-134
[e]Collected predose on GD 139-141

Mean Maternal and Fetal TK

Dose	PPD	Maternal	Infant [a]	Ratio
10[b]	14	371	271	0.7
	91	24	17.5	0.7
	182	2.38[c]	BLQ	NA
50	14	1280	1120	0.9
	91	95	116	1.2
	182	6.86[d]	1.82	NA

[a] mean concentrations reflect M+F combined
[b]Excludes Dam 2509 and her infant for which levels were BLQ
[c] N = 1
[d] N = 3
LLOQ = 0.4 µg/mL
NA = not applicable because most samples were BLQ

Anti-Drug Antibody (ADA)

- ADA was detected in 22% of the dams (6/10 females in the 10 mg/kg dose group and 1/16 females in the 50 mg/kg dose group). The majority of these were not consistently positive over the sampling period, and in only one dam (2509), did the presence of ADA appear to affect drug exposure (by accelerated clearance).
- It is likely that the presence of circulating drug inhibited the detection of ADA; thus, the estimate of 22% may be an under-representation of the true rate of ADA formation.
- There was no correlation between ADA and pregnancy loss.

Dosing Solution Analysis: Dose solution analysis was not performed because the test article was administered as supplied (not formulated); thus, the test articles were characterized by their labeling and accompanying certificates of analysis.

Dose formulation stability was performed with samples collected on-study that were subsequently shipped back to the manufacturer for analysis. The analysis was performed under GMP conditions and the results met pre-specified acceptance criteria of ±10% for each timepoint; however, the method of the analysis (absorbance at 280 nm) was not stability-indicating because spectrophotometric absorbance does not

distinguish between intact and denatured proteins. Together, (1) the Applicant's concentration measurements (A280 of returned samples), (2) the drug product stability data that demonstrated acceptable potency (by ELISA) when stored at 25^{o} C for up to 6 months, and (3) the measured toxicokinetic exposures in treated animals and their infants, support the stability of the compound under the conditions of the study.

Lymphocyte phenotyping: Unremarkable

Antibody Isotypes There were no differences in the mean serum IgG, IgA or IgM levels at any timepoint evaluated (TD20-22, GD139-41, or PPD91).

ANA There were no anti-nuclear antibody responses in any dam at any timepoint evaluated (GDs 20-22, 139-141 or PPD91)

Other One 50 mg/kg dam (#3507) that aborted on GD47 was found to have a thrombus in the umbilical cord. Other embryos, placentas and umbilical cords were identifiable or evaluable from the remaining abortions.

F_1 Generation

Survival:

- Three Group 1 (control), two Group 2 (10 mg/kg) and eight group 3 (50 mg/kg) females aborted (≤GD 140) or had stillbirths (≥GD 140).
- The remaining offspring were born alive
- There were 15M and 14F evaluable offspring at the terminal timepoint; however, none of the infants in the high dose group survived to scheduled termination.
- The increased incidence of abortion/stillbirth exceeds that of concurrent and historical controls in both the 10 and 50 mg/kg dose groups and is therefore considered treatment-related.
- All infants survived to scheduled termination on BD182 except for 2 control and 4, 10 mg/kg infants that were found dead or were euthanized during the early neonatal period

(BD1-BD35; Applicant-Table 21). One of the 10 mg/kg infants died secondary to anesthesia; thus, its death is of uncertain relationship to treatment.

- The incidence of infant loss in the 10 mg/kg dose group exceeds historical and concurrent controls and is considered treatment-related.

Clinical signs: Preterminal clinical signs in infants that died prior to scheduled termination included weight loss, reduced feeding, and lethargy. These findings are consistent with failure to thrive secondary to extreme prematurity.

Body weight: There was a decrease in mean body weight of infants in the 10 mg/kg dose group at birth and at 6 months, and an episodic decrease in mean body weight gain of infants in the 10 mg/kg dose group over the 6-month postnatal period. Because the decreases in body weight and body weight gain in the 10 mg/kg dose group were not statistically significant over the entire postnatal period, and there were no effects on body weight observed in infants in the 50 mg/kg dose group, the effects are of equivocal relationship to treatment. The Applicant suggests that the apparent decreases in mean infant body weight and weight gain of the 10 mg/kg group may reflect the extreme prematurity of two infants (born GDs 131 and 135) and the fact that there were fewer male offspring in that group.

Feed consumption: Not measured

Morphometry and Visceral Examination: The following statistically significant observations were noted in 10 mg/kg infants:

- Reduced mean chest circumference relative to controls (7%)
- Reduced mean right and left femur length (7%)
- Reduced mean right and left foot length (7%)
- Skeletal examinations were unremarkable
- Infant heart (gross pathological) examinations were unremarkable
- Gross necropsy observations included multiple red foci in the colon of one 50 mg/kg male infant, which correlated with hemorrhage

	in the GALT, which is of potential relationship to treatment. One infant in the 10 mg/kg dose group was found with an ovarian cyst. Reductions were also observed in these parameters in infants of the 50 mg/kg dose group; however, the changes were not statistically significant. The Applicant suggests that the effects are attributable to differences in the mean gestational age of infants in the control (159.4 days) vs. the 10 mg/kg (152.6 days) dose groups.
Organ weights	Unremarkable.
Neurological assessment:	The Applicant performed neurobehavioral assessments on infants on BDs 7 and 14. The Applicant states that the results obtained in all treatment groups were within the range of expected variability for neonatal cynomolgus monkeys. Note that statistical analyses were not performed, and the Applicant does not provide historical control ranges for the parameters assessed.
Reproduction:	Not evaluated.
Clinical Pathology	Unremarkable; sporadic differences from control appeared to lack a dose-relationship and/or were transient.
TK/ADA	Only one infant had detectable ADA (#2096, the infant of dam#2509). ADA was detected on BD14 and was still detectable on BD182.
Lymphocyte Phenotyping	Unremarkable. A number of lymphocyte subsets (NK cells, T-helper and Cytotoxic T cells) were increased (some of reached statistical significance) in treated groups relative to concurrent controls; however, the pattern was neither clearly dose-related nor temporally consistent.
TDAR	Treatment with nivolumab did not prevent the ability of infant monkeys to mount a T-cell dependent antibody response to either hepatitis B surface antigen (HBsAg, administered on Days 42 and 126) or tetanus toxoid (TT, administered on Day 126). There was no effect of nivolumab treatment on TDAR in this study as antibody responses in treated

infants were comparable to controls for both antigens evaluated, (Applicant-
Figure 35, and Applicant-Figure 36) although the mean response to the second antigen challenge (by HBsAg) was consistently higher in nivolumab treated groups.

Antibody Isotypes There were no differences in the mean serum IgG or IgM levels at any timepoint evaluated (BD35, BD91, or BD182). There was a decrease in mean serum IgA levels on BD35 in the 50 mg/kg dose level (Applicant-Figure 33).

ANA There were no anti-nuclear antibody responses in any infant at any timepoint evaluated (BDs 35, 91, or 182)

Figure 31: Distribution of IgA levels for infant cynomolgus monkeys

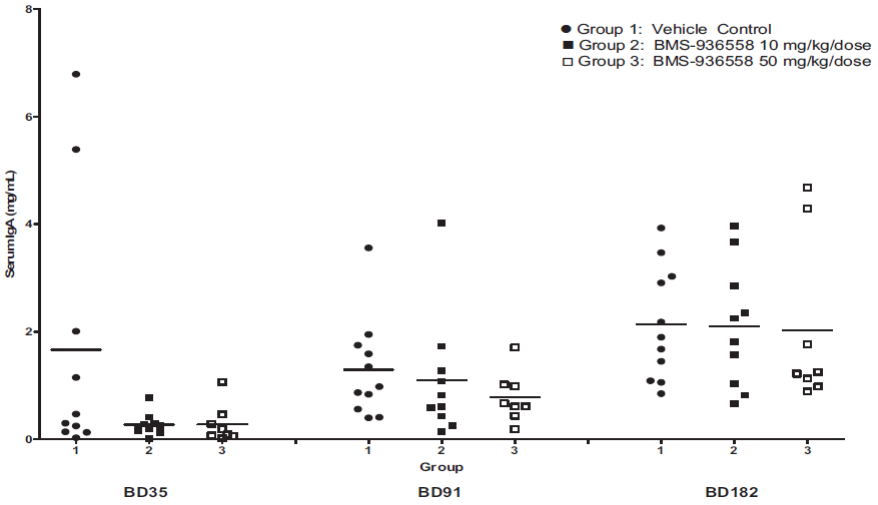

Figure 32: TDAR response to HBsAg in Infants (Challenge 1)

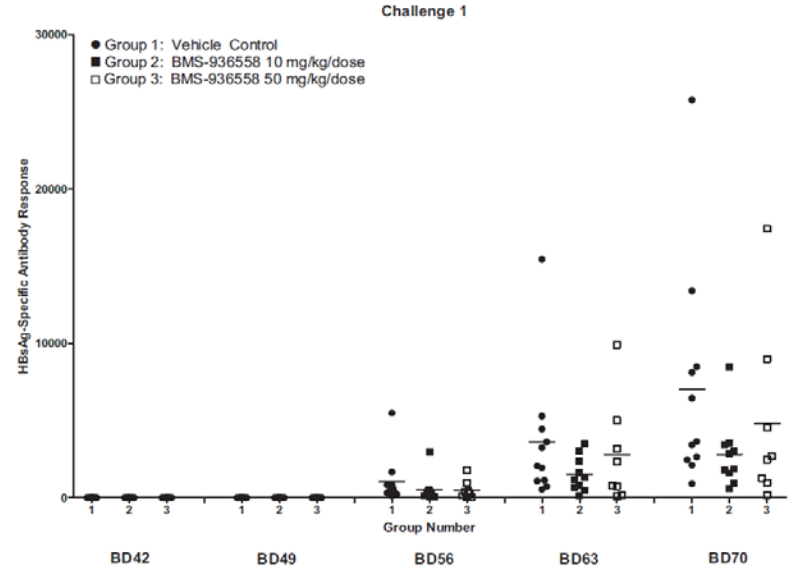

Horizontal line is the group mean

Figure 33: TDAR response to HBsAg in Infants (Challenge 2)

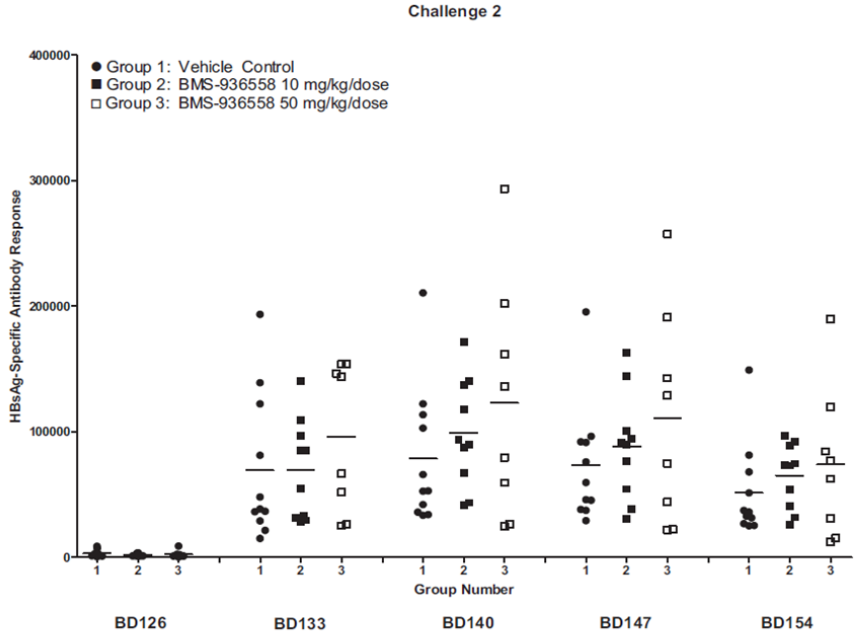

Horizontal line is the group mean

Figure 34: TDAR response to TT in Infants

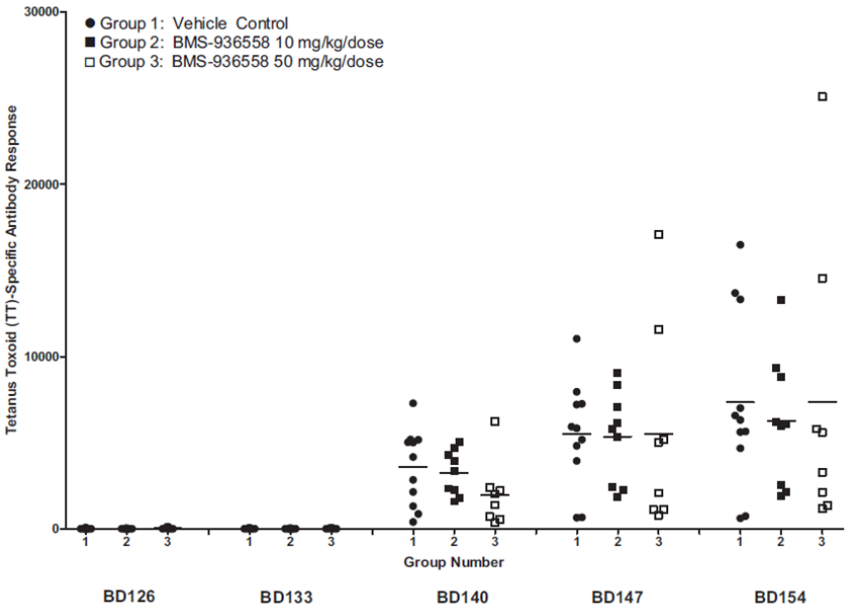

10 Special Toxicology Studies

10.1 Cross-Reactivity Study of MDX-1106-FITC with Normal Human Tissues (Study: IM1258)

The purpose of this study was to assess the pattern of nivolumab binding in cryosections of normal human tissues (cadaveric origin; N = 3/tissue). Tissues were incubated with FITC-labeled nivolumab at concentrations of 1 or 10 µg/mL. Tissue binding was detected with the aid of a peroxidase-conjugated secondary (anti-FITC) antibody incubated in the presence of the colorimetric substrate, diaminobenzidine (DAB).

Consistent with the known distribution of PD-1 on activated lymphocytes, a broad pattern of immunoreactivity was observed in lymphocyte populations of many tissues evaluated, particularly circulating blood, the breast, the GALT of the small intestine, kidney, liver, lung, lymph node, spleen, ovary, pancreas, peripheral nerve, prostate, thymus, tonsil, urinary bladder, and uterus. The staining pattern was restricted to the extracellular membrane, which is consistent with the known subcellular distribution of PD-1 in these cells. In addition, immunoreactivity was observed in the endocrine cells of the adenohypophysis; however, because the subcellular staining pattern was cytoplasmic in these tissues, the physiological relevance of this finding is unclear.

10.2 Cross-Reactivity Study of MDX-1106-FITC with Normal Cynomolgus Monkey Tissues (IM1259)

The purpose of this study was to assess the pattern of nivolumab binding in cryosections of normal tissues from cynomolgus monkeys (N = 2/tissue). Tissues were incubated with FITC-labeled nivolumab at concentrations of 1 or 10 µg/mL and binding was detected using a peroxidase-conjugated anti-FITC secondary antibody. The distribution of immunoreactivity was similar to that observed in humans; staining was generally restricted to the lymphocyte populations of tissues, and within that population was mostly detected on the cell membrane.

In the liver, spleen, uterus, and lung, cytoplasmic staining of mesothelial cells was observed. Cytoplasmic (granule) staining was also observed in the endocrine cells of the adenohyophysis. Because PD-1 is a membrane-associated receptor, the biological significance of the cytoplasmic staining pattern observed in these tissues is unclear.

10.3 Investigative Study of the Effect of Ovalbumin Challenge in PD-1 Knockout and Wild-Type C57/BL6 Mice

The purpose of this study was to assess the effect of PD-1 deficiency on the response to pulmonary ovalbumin challenge in mice. On Days 0 and 7, animals received intraperitoneal injections of ovalbumin (OVA) + alum, followed by administration of ovalbumin by pharyngeal aspiration (PA) on Days 14 and 28. The magnitude of the anti-OVA allergic response was evaluated at 4, 24, or 72 hours following the final PA exposure by quantifying cytokine protein levels in the lung and blood, the extent of cellular infiltration into the lung, the levels of circulating MUC-1 protein levels, and the levels of circulating OVA-specific IgG and IgE. In addition, histopathology of the lungs, heart, spleen, and lymph nodes was performed.

There were 5 preterm deaths, the majority of which occurred in OVA-treated PD-1 KO animals (Table 22).

Table 22: Summary of preterm mortality in the ovalbumin challenge assay

Group	Number of Deaths	Day(s) of Death
WT	1/18	12
PD-1 KO OVA	1/48	9
PD-1 KO OVA	3/48	2, 5 and 21

Relative to vehicle-control exposure, OVA-exposure increased the number of infiltrating immune cells in bronchoalveolar fluid (BALF) in both WT and PD-1 deficient animals; however, the magnitude of the effect was greater in PD-1 deficient animals (Applicant-Figure 37; asterisk = significantly different from vehicle; a = significantly different from WT). While the cellularity of BALF increased with OVA exposure in both WT and PD-1 deficient animals, the magnitude of the increase was greater in females relative to

males, suggesting that PD-1 deficiency may render females more sensitive to pulmonary sensitization (data not shown).

Figure 35: Influence of genotype on BALF cellularity following OVA challenge (M+F)

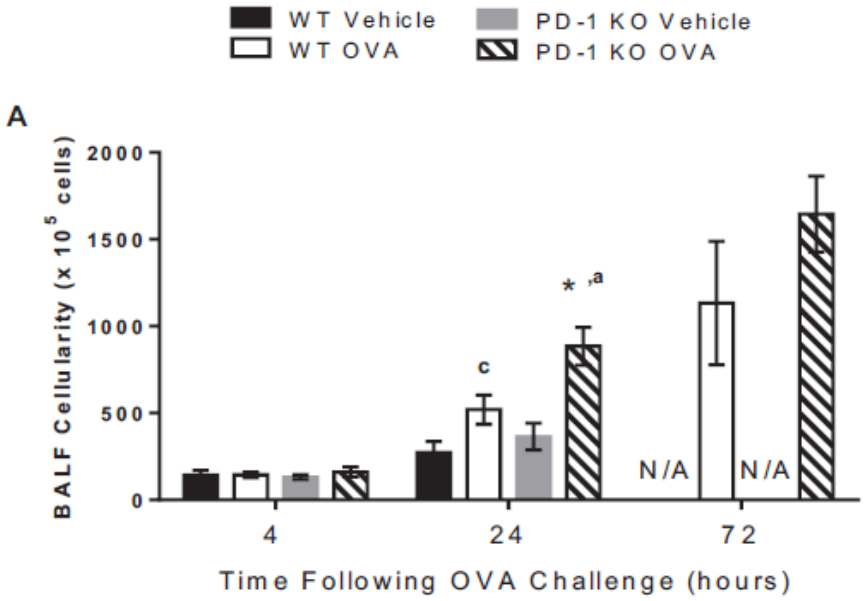

Further, while there was no significant difference between OVA-treated WT and PD-1 deficient animals in the number of infiltrating macrophages or eosinophils, there were more neutrophils and lymphocytes observed in the BALF of OVA-treated PD-1-deficient animals (Figure 38). By 72 hours post-exposure, there were no differences between OVA-exposed WT and PD-1 deficient animals in the lymphocyte subsets observed in BALF (data not shown).

Figure 36: Effect of genotype on cytology of infiltrating immune cells in the BALF at 24-hours post-OVA challenge (M+F)

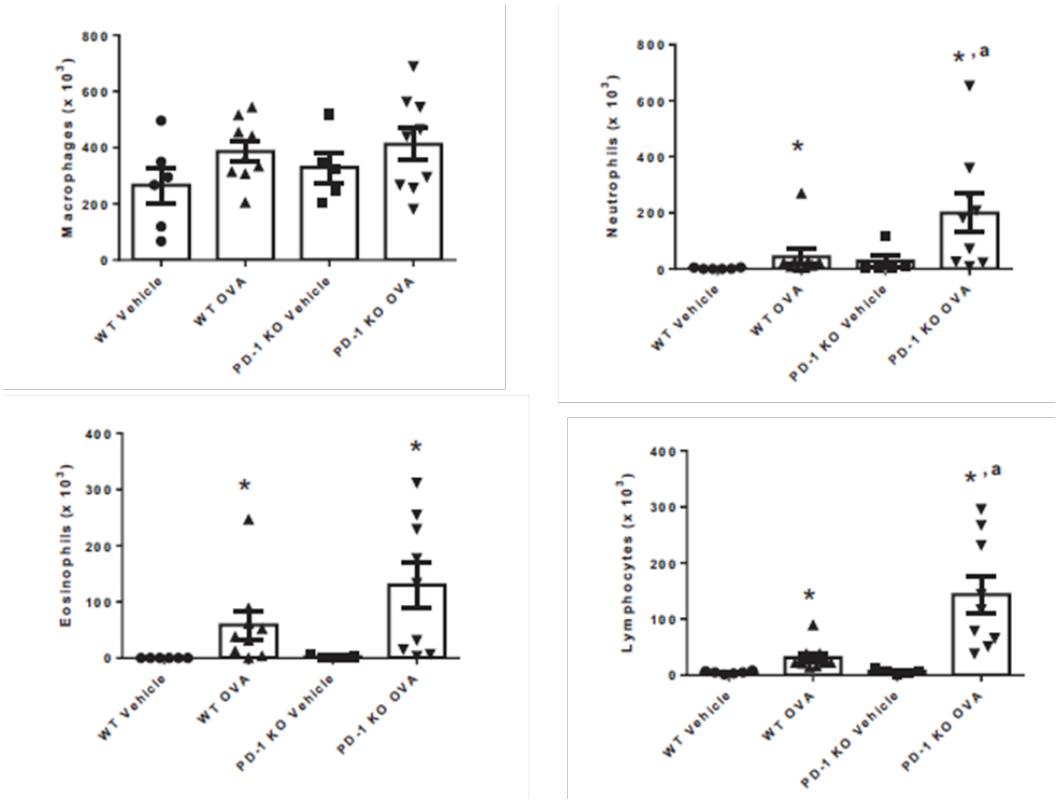

As illustrated in Applicant-Figure 39, levels of OVA-specific IgG_1 in serum (A), BALF (B) and lung homogenate (C) were increased in all OVA-treated groups relative to vehicle controls, but only levels in the BALF were significantly higher in PD-1 KOs than in WT animals (asterisk = significantly different from vehicle; a = significantly different from WT). There was no effect of genotype on the levels of anti-OVA IgE in lung homogenate (data not shown).

Figure 37: Influence of genotype and gender on levels of anti-OVA IgG_1 in serum, BALF and lung homogenate, respectively

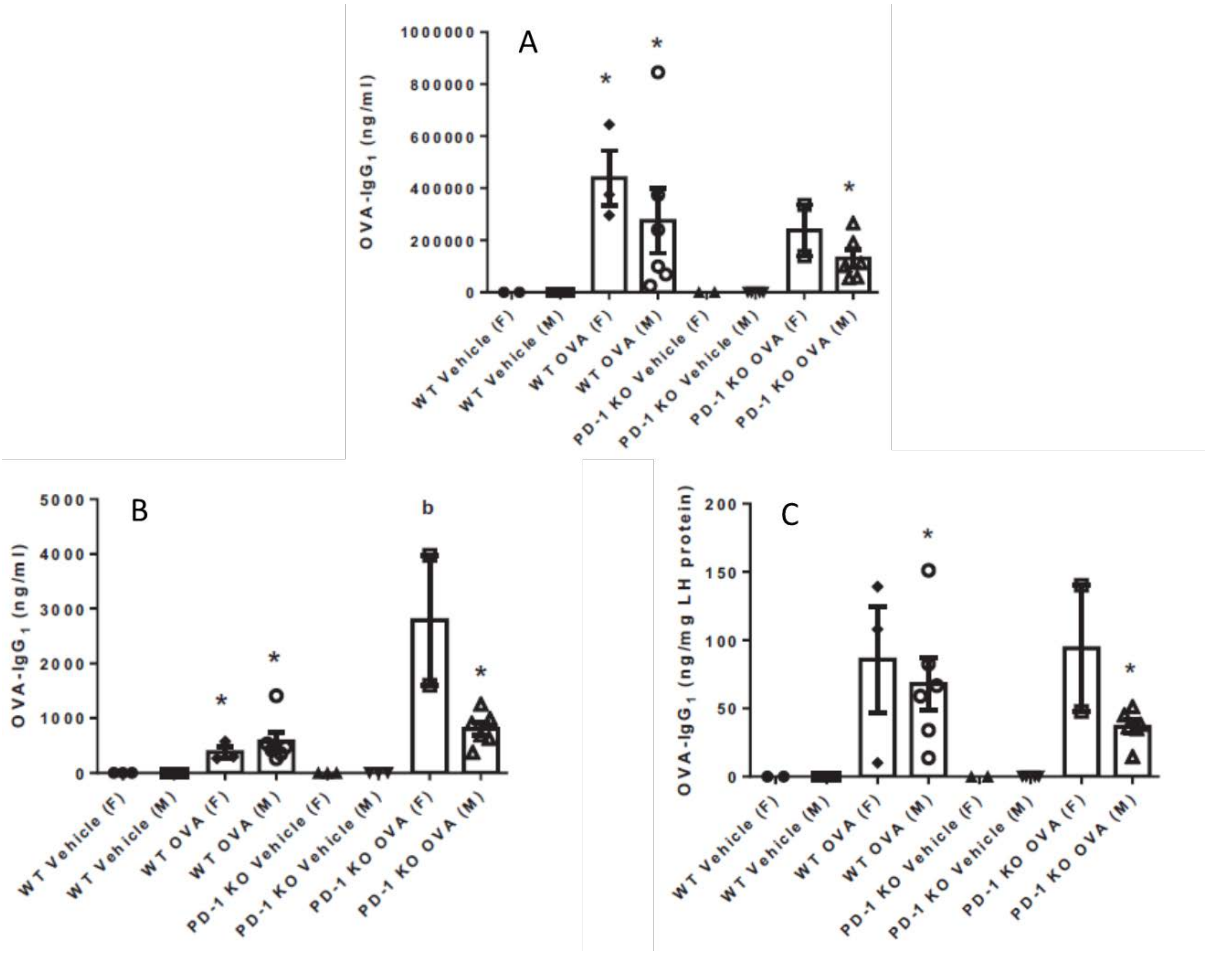

A number of pro-inflammatory chemokines and cytokines, including IFN-γ, IL-1a, Ccl2, Ccr1, and Ccl4, were preferentially upregulated (mRNA) in lung tissues from OVA-challenged PD-1 KO mice relative to OVA-challenged WT mice (Applicant-Table 23). These levels correlated with an observed increase in immune cells in the lungs (measured in BALF).

Of note, the anti-inflammatory cytokine, IL-10, was also preferentially upregulated in PD-1 KO mice relative to WT mice at early timepoints following OVA-challenge, suggesting that IL-10 may physiologically limit the magnitude of the inflammatory response in a PD-1 deficient environment.

There was no difference in the histological appearance of airways from OVA-challenged WT and -PD-1 KO animals (data not shown), despite the evidence of increased WBC airway transit in BALF samples from OVA-challenged PD-1 KO mice relative to -WT mice. Histological findings were comparable between the two genotypes, including findings of perivascular and peribronchiolar neutrophil or eosinophil accumulation, mucus accumulation, interstitial edema and vascular leukocytosis.

Table 23: Fold-change in cytokine mRNA expression in OVA-challenged PD-1 KO mice compared with OVA-challenged WT mice

	Hours Post OVA Challenge		
Transcript	**4 Hours**	**24 Hours**	**72 Hours**
TNFa	-1.18	1.69*	1.28
Il1a	-1.18	1.09	-1.42**
Il1b	-2.07	1.58*	-1.27
Il10	4.30**	3.71**	1.78
Cxcl1	-1.65	-1.12	-2.55*
Ccl2	-1.25	2.41**	-1.08
Ccr1	-1.23	1.87**	-1.40
Ccl4	1.77	3.13**	3.33*
Il12b1	1.78	1.86	1.73
Il12b2	-1.12	1.20	1.10
Il6	-2.39	1.45	-1.13
Il2	1.31	-1.24	-3.08
Il4	1.74	-1.17	-2.30**
Ifng	7.03**	4.49**	6.62**
Il17a	1.95	-1.09	-2.09
Csf3	-1.21	1.16	-1.93
Csf2	-1.55	1.07	-1.52

[a] Fold of fold change values in gene transcripts (Table 5.1.2.2-1) of OVA-treated PD-1 KO mice relative to OVA-treated WT mice.

*$p \leq 0.05$, **$p \leq 0.005$

The Applicant also evaluated cytokine protein levels in lung tissue. These data are summarized in Applicant-Table 24.

Table 24: Summary of cytokine protein levels in lung tissue of OVA-challenged mice

		Fold Change Relative to Respective Vehicle Control[b]		
Cytokine	Strain	4 hours	24 hours	72 hours[c]
IL-2	WT	1.67*	0.98	1.03
	PD-1 KO	1.96*	1.13*	1.08
KC	WT	6.42	1.50*	1.11
	PD-1 KO	3.40*	1.49*	0.99
MIP1-α	WT	1.14*	1.72*	1.29
	PD-1 KO	4.68*	5.75*	6.02*
RANTES	WT	0.86	2.29*	1.43
	PD-1 KO	2.73*	4.24*	5.59*
IL-6	WT	3.41	0.97	0.86
	PD-1 KO	1.37*	1.17*	0.89*
IL-12p40	WT	1.22	1.28	0.90
	PD-1 KO	2.37*	1.38*	1.86*
MCP-1	WT	1.74	1.09	0.78*
	PD-1 KO	2.04*	1.32*	0.96
MIP-1β	WT	1.24	1.00	0.73*
	PD-1 KO	1.94*	1.45*	1.61*
TNF-α	WT	1.04	0.89*	0.86*
	PD-1 KO	1.24*	1.06	1.00

[a] Cytokine data are included in this summary table if differences relative to respective controls (see below table note) were statistically significant at any time point in either test strain.

[b] WT vehicle-treated group data are respective control for WT OVA-challenged group data and PD-1 KO vehicle-treated group data are respective control for PD-1 KO OVA-challenged group data.

[c] Fold Change and p value calculations for 4 and 72 hours data were performed using respective vehicle control data at 24 hours.

*$p \leq 0.05$

Lastly, the Applicant evaluated the effect of PD-1 genotype on expression of the PD-1 ligands, PD-L1 and PD-L2, following challenge with OVA. As illustrated in Applicant-Table 25, expression of PD-1 ligands was increased in OVA-challenged PD-1 KOs relative to OVA-challenged WT animals.

Table 25: mRNA levels of PD-L1 (Left) and PD-L2 (Right) relative to Vehicle-treated WT animals

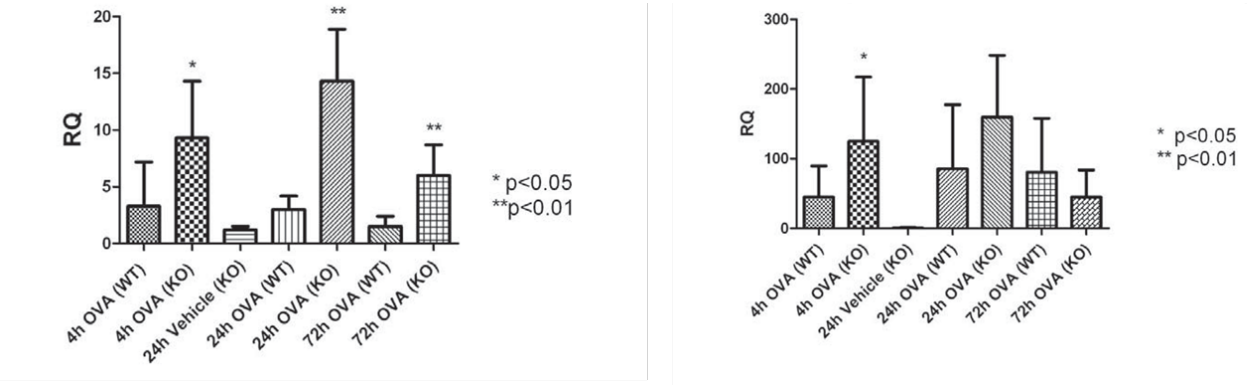

10.4 An Investigative Repeat-Dose Toxicity and Efficacy Study of MDX-010, 4C5 and 5H1 in Combination with HBsAg, DNP-Ficoll and SKMel Immunostimulants Following Three Monthly Administrations (SUV00006)

The purpose of this study was to characterize the toxicity of MDX-010 (ipilimumab; Group 2), 4C5 (nivolumab; Group 3), and 5H1 (an anti-CTLA4 antibody; Group 4) in cynomolgus monkeys (of Indonesian origin), on the humoral response to the following immunostimulant regimens:

- Intramuscular injections of hepatitis B surface antigen (HBsAg) on Days 1, 29 and 57
- Intradermal injections of 2,4-dinitryphehyl-Ficoll (DNP-Ficoll) on Days 1 and 29
- Subcutaneous injections of 10^6 SKMel cells on Days 1, 29 and 57

The Study was conducted in two phases. Phase 1 (Study Days 1-139) was designed to assess the effect of MDX-010, 4C5, or 5H1 on the humoral immune response to immunostimulants. Phase 2 (Study Days 140-154) was designed to assess the effect of MDX-010 and 5H1 on the reactivation of immune responses following re-stimulation with antigen on Day 140 (as measured by antibody titers to HBsAg and SKMel).

During Phase 1, test articles were administered following a once monthly administration schedule at doses of 10 mg/kg for 3 months. The test articles and immune-stimulants were administered concurrently, as described in Applicant-Table 26. During Phase 2, only immune stimulants were administered.

Table 26: Immunotoxicology study design (Phase 1)

Phase 1							
Group No.	No. of M/F	Dose Schedule	Test Article/ Immunostimulant	Dose Route	Dose Level	Dose Conc.	Dose Volume
1	3/3	Days 1, 29, 57	Saline	IV	0 mg/kg	0 mg/mL	2 mL/kg
			HBsAg	IM	10 µg	20 µg/mL	0.5 mL
			SKMel	SC	$5X10^6$ cells	---	0.5 mL
		Days 1 and 29	DNP-Ficoll	ID	100 µg	1 mg/mL	0.1 mL
2	3/3	Days 1, 29, 57	MDX-010	IV	10 mg/kg	5 mg/mL	2 mL/kg
			HBsAg	IM	10 µg	20 µg/mL	0.5 mL
			SKMel	SC	$5X10^6$ cells	---	0.5 mL
		Days 1 and 29	DNP-Ficoll	ID	100 µg	1 mg/mL	0.1 mL
3	3/3	Days 1, 29, 57	4C5	IV	10 mg/kg	5.76 mg/mL	1.7 mL/kg
			HBsAg	IM	10 µg	20 µg/mL	0.5 mL
			SKMel	SC	$5X10^6$ cells	---	0.5 mL
		Days 1 and 29	DNP-Ficoll	ID	100 µg	1 mg/mL	0.1 mL
4	3/3	Days 1, 29, 57	5H1	IV	10 mg/kg	5 mg/mL	2 mL/kg
			HBsAg	IM	10 µg	20 µg/mL	0.5 mL
			SKMel	SC	$5X10^6$ cells	---	0.5 mL
		Days 1 and 29	DNP-Ficoll	ID	100 µg	1 mg/mL	0.1 mL

No. = number; M = male; F = female; IV = intravenous; IM = intramuscular; SC = subcutaneous; ID = intradermal; Conc. = concentration; --- = not applicable

For Phase 1 of this study, 6 animals per group (3M and 3F) received test article treatments (Saline, MDX-010, 4C5 or 5H1) by intravenous injection on Days 1, 29 and 57, and were challenged with antigen (SKMel (subcutaneous), HBsAg (intramuscular), or DNP-Ficoll (intradermal)) on Days 1 and 29. Blood samples for humoral and cellular immune responses were collected through Day 100. Based on a weak or absent immune response to HBsAg, 5 Group 3 animals and 3 Group 4 animals were removed from study (i.e. these animals did not proceed onto Phase 2 of the study).

There was one preterm death. On Study Day 42, one Group 2 male that received MDX-010 was euthanized in moribund condition due to colitis.

On Day 140, and the remaining animals commenced Phase 2 of the study in which they were re-challenged with their assigned test article (either saline, MDX-010 or 5H1), and immunological assessments were performed through Day 154, prior to necropsy.

Table 27: Immunotoxicology study design (Phase 2)

Phase 2							
Group No.	No. of M/F	Dose Schedule	Test Article	Dose Route	Dose Level	Dose Conc.	Dose Volume
1	3/3	Day 140	Saline	IV	0 mg/kg	0 mg/mL	2 mL/kg
2	3/2[a]	Day 140	MDX-010	IV	10 mg/kg	5 mg/mL	2 mL/kg
3	2[b]/0	Day 140	Saline	IV	0 mg/kg	0 mg/mL	2 mL/kg
4	1/1	Day 140	5H1	IV	10 mg/kg	5 mg/mL	2 mL/kg

No. = number; M = male; F = female; IV = intravenous; Conc. = concentration
[a] One Group 2 female was euthanized during Phase 1.
[b] One Group 4 male in Phase 1 was moved to Group 3 in Phase 2.

Plasma exposures to MDX-010 and 5H1 were maintained through Day 71 in all surviving study animals. Exposure to 4C5 (nivolumab) was ablated in the majority of animals by Day 43.

Animals were tested for anti-drug antibody on Days 14, 43, and 71. Under the conditions of the assay, there were no ADA-positive animals in the MDX-010 group at any timepoint. In contrast, 4 of 6 animals that received 4C5 were ADA positive by Day 43; however, the format of the MDX-010 assay appears to be highly sensitive to the presence of residual drug and may not have been capable of detecting ADA levels that were not exposure-ablating; thus, the frequency of ADA-positivity in this study may have been underestimated.

Animals treated with MDX-010 and 5H1 mounted a robust antibody response following inoculation with SKMel during Phase 1 (Applicant-Figure 40, Left). Treatment with MDX-010 led to a robust antibody response against HBsAg; however, there was no effect of either 5H1 or 4C5 (Figure 40, Right) on the anti-HBsAg response. There was no response to DNP-Ficoll in any of the groups tested. The responses to SKMEL in animals treated with 4C5 increased more modestly than those of animals treated with CTLA4 antibodies.

Figure 38: Humoral immune response to SKMel (Left) or HBsAg (Right)

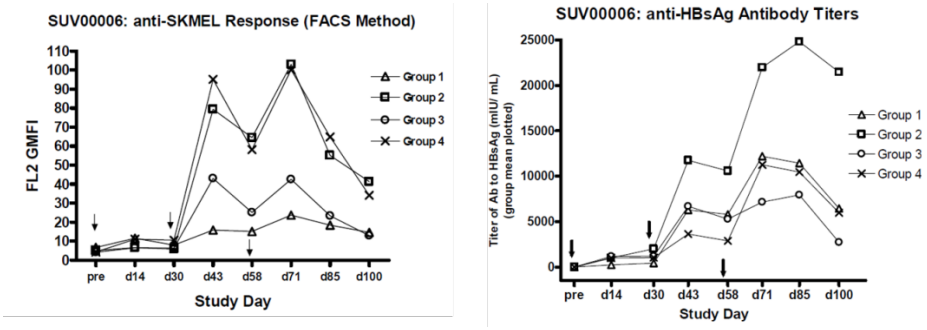

Treatment with MDX-010 and 5H1 had no effect on the following WBC subsets in peripheral blood: percentage of CD3+ T cells, CD20+ B cells, $CD11c^{hi}$ dendritic cells, CD14 monocytes, activated lymphocytes (using HLA-DR, DP, or DQ as activation

markers for CD3+CD4+ or CD3+CD8+ T cells, and CD25 as an activation marker of T and B cells).

Treatment with both MDX-010 and 5H1 induced small increases in memory CD4+ T cells (both central and effector memory subsets; Applicant-Figure 41). All three treatments decreased the proportion of naïve T CD4+T cells. There was no notable effect on Treg subsets (CD4+CD25+, including CTLA4+ cells), or on CD8+ subsets in peripheral blood. Treatment with all three antibodies increased CD4+ effector memory cells; however, nivolumab (4C5) treatment was the most potent in this endpoint.

Figure 39: Effect of MDX-010, 5H1 or 4C5 on CD4+ subsets in peripheral blood

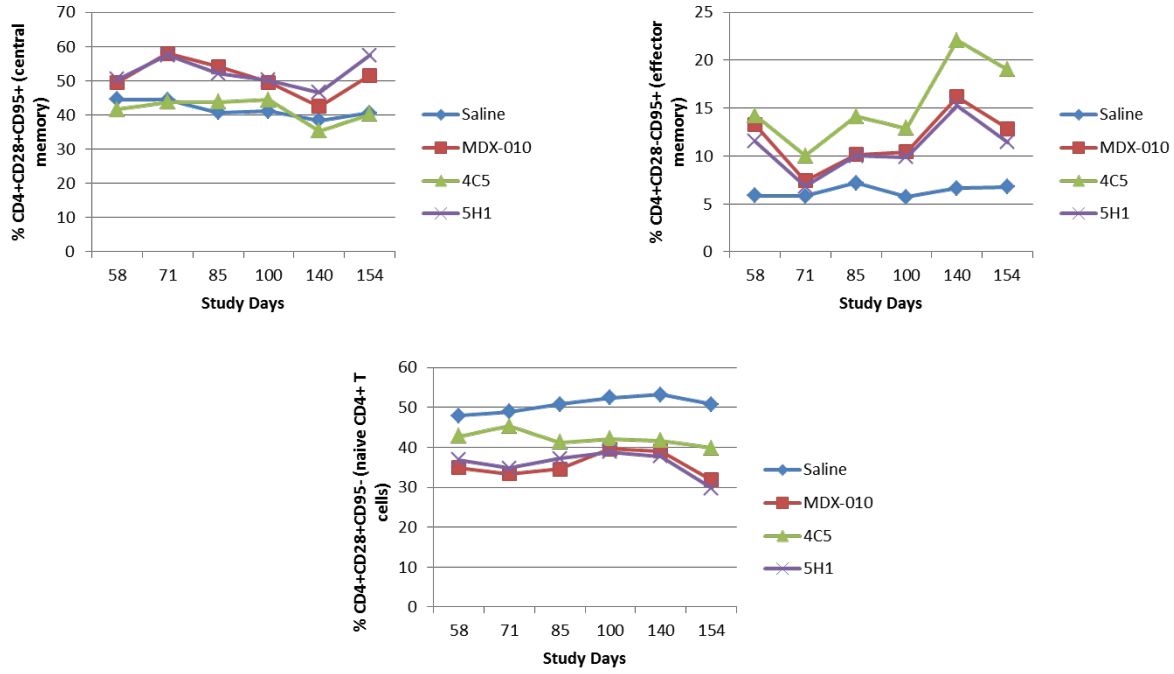

10.5 Anatomic Pathology Report: Analysis of PD-2 and PD-L1 Knockout Mice (Study #: PD-1 and PD-L1 KO)

The Applicant performed histopathological evaluations of 7 (4M/3F) PD-1 KO mice ranging from 65-82 weeks and 7 (4M/3F) PD-L1 KO mice, ranging from 52-65 weeks of age. Nine (5M/4F) WT mice, ranging from 38-42 weeks of age, were also evaluated. All mice were on a C57BL background. This analysis was limited to: ears, gross lesions, skin, salivary gland, intestine, spleen, pancreas, liver, mesenteric lymph nodes, kidneys, ribs and sternum, and lungs.

Histological observations that were apparently related to PD-1 pathway deficiency (by increased incidence and/or severity) are summarized in Table 28. Overall, there was an increased incidence and/or severity of inflammatory lesions of the liver, heart, kidney

and paw (skin/joint) in PD-1 pathway-deficient animals relative to WT animals. This is consistent with the body of published data on PD-1 deficient animals.

Table 28: Genotype-related histopathological evaluation of adult WT, PD-1 KO, and PD-L1 KO mice

Tissue, histopathological description (severity)	**WT**	**PD-1 KO**	**PD-L1 KO**
Liver, infiltrate, mixed inflammatory cell, parenchyma, focal/multifocal (minimal-mild**)	1M/2F	1M/0F	4M/0F
--mononuclear, perivascular, focal/multifocal (minimal-mild**)		4M/2F	1M/1F
--lymphoid hyperplasia, perivascular, multifocal/focal (mild)	0M/1F	0M/1F	0M/2F
Heart, infiltrate, mononuclear, atrium, focal			0M/1F
Kidney, chronic renal disease (minimal-moderate**)	5M/4F	4M/3F	4M/2F
--cysts, cortex and hydronephrosis, unilateral (moderate)		1/0	
Mesenteric lymph nodes, lymphoid hyperplasia (mild)	1M/0F	3M/2F	
--plasmacytosis, medullary cords (minimal-mild**)	1M/1F		0M/2F
Rear paws, infiltrate, mixed inflammatory cell, dermis/hypodermis (minimal)	0M/3F	3M/3F	1M/3F
--osteoarthritis, digit and/or tarsal-metatarsal (minimal)	2M/1F	3M/1F	2M/2F
--osteoarthritis, tarsal/metatarsal (mild)			2M/0F
--ulcerative poditis, subacute (mild)		1M/0F	

11 Integrated Summary and Safety Evaluation

Programmed cell death-1 (PD-1) is an inducible receptor belonging to the immunoglobulin superfamily that is expressed primarily on activated CD4+ and CD8+ T cells, NK cells, B cells and monocytes. The interaction of PD-1 with its ligands, programmed cell death–ligands 1 and 2 (PD-L1 and PD-L2), leads to down-regulation of T cell responses, including T cell proliferation and cytokine production and limits immune-destruction of tissues (*discussed in* Wang, et al., 2011). Expression of PD-1-ligands is broad and inducible. The PD-L2 ligand, expressed primarily on activated dendritic cells, macrophages and mast cells, is more restricted in its distribution than the PD-L1 ligand, which exhibits both a broad basal expression pattern and the potential for upregulation under conditions of immune stimulation. Activation of PD-1 inhibits CD28 signaling through the PI3K/AKT pathway (probably through recruitment of the SHP-2 and SHP-1 phosphatases to the immune synapse) thus blocking the upregulation of pro-inflammatory mediators (e.g., IL-2 and IFNγ) and survival signals (e.g. Bcl-xl; Figure 42).

Figure 40: Summary of the PD-1 signaling pathway in activated T cells

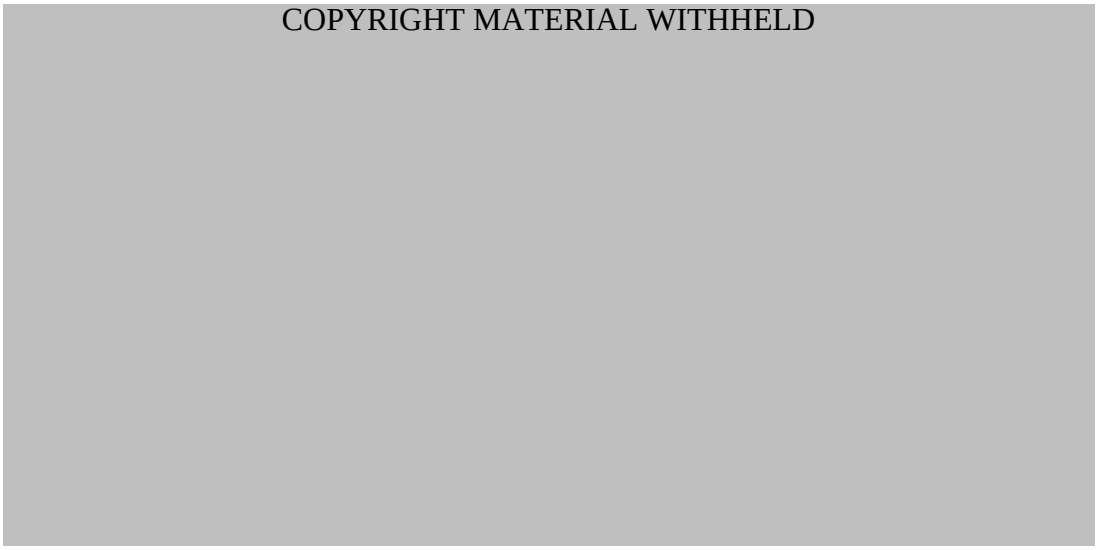

c.f. Keir, ME, *et al*., 2008. *Annu. Rev. Immunol*. 2008. 26:677–704

The interaction between PD-1 and its ligands, thus, plays a role in maintaining the balance between immune activation and tolerance (Figure 43). In addition to the inhibitory effects of ligand-engagement on the PD-1-expressing T cell, there is also evidence of bidirectional signaling between the activated T cell and the APC. Engagement of PD-Ls with PD-1 has been demonstrated to modulate the function of activated dendritic cells via increasing production of cytokines such as IL-10, associated with dampening the immune response.

Figure 41: PD-1 and PD-1 ligands in tolerance and inflammation

c.f. Sharpe, et al., 2007. Nature Immunology

Direct evidence for the role of PD-1 in maintaining self-tolerance derives from a large body of data generated in PD-1 knockout animals, and from studies of mouse and human autoimmunity. PD-1 is expressed in immune privileged sites such as the eye

and the placenta; accordingly, loss of PD-1 activity at these sites, either by application of a PD-1 inhibitor or by functional or genetic deletion, leads to ocular graft rejection and increased rates of spontaneous abortion, respectively (*reviewed in*: Fife & Bluestone, 2008). In mice, inactivation of PD-1 or its ligands leads to a number of autoimmune conditions, including systemic lupus erythematosus (SLE), dilated cardiomyopathy, diabetes, and experimental autoimmune encephalitis (EAE). Moreover, numerous single nucleotide polymorphisms (SNPs) have been identified in the human PD-1 gene that are associated with autoimmune disease (reviewed in Okazaki and Honjo, 2007).

Nivolumab is a fully human IgG_4 monoclonal antibody that binds to PD-1. Binding of the antibody to PD-1 inhibits the interaction between the receptor and its ligands. By blocking the interaction between PD-1 and its ligands, nivolumab blocks inhibitory signals that control T cell activation, thereby promoting T cell responses.

The binding affinity of nivolumab to PD-1 was evaluated using surface plasmon resonance. The affinity (Kd) of nivolumab to PD-1 expressed on human and cynomolgus monkey T cells was 3.06 nM and 3.92 nM, respectively. The ability of nivolumab to bind human PD-1 was also assessed using an enzyme-linked immunosorbent assay (ELISA). The results demonstrated saturable binding of nivolumab to human PD-1-Ig fusion protein, with an EC_{50} of 0.39 nM. To establish the specificity of binding of nivolumab to PD-1, binding to related members of the CD28 family was examined by ELISA. Nivolumab did not bind to CD28, inducible T-cell costimulator (ICOS), cytotoxic T-lymphocyte antigen 4 (CTLA-4), or B and T lymphocyte attenuator (BTLA). Flow cytometry analysis confirmed that nivolumab bound to activated human and cynomolgus monkey T cells, but not to activated rat or rabbit T cells. Flow cytometry analysis also showed that nivolumab blocked binding of PD-L1 and PD-L2 to human PD-1.

An antibody-dependent cell-mediated cytotoxicity (ADCC) assay using IL-2 activated PBMCs was performed to evaluate if nivolumab could induce ADCC of target cells. Among four donors, nivolumab did not mediate ADCC of activated human PD-1+ CD4+ T cells. Complement-dependent cytotoxicity (CDC) of nivolumab was also examined using activated human PD-1+ CD4+ T cells. The results showed that nivolumab did not mediate CDC on activated CD4+ T cells. In addition, nivolumab on its own did not directly induce cytokine release from fresh human blood samples.

The effects of nivolumab on the immune response were assessed in vitro utilizing a variety of assays. In a mixed lymphocyte reaction (MLR), CD4+ T cells recognized allogeneic monocyte-derived dendritic cells (DC) resulting in T cell proliferation and cytokine release. The addition of nivolumab to donor T cell-DC pairs resulted in a dose-dependent increase in T cell activation, as measured by IFN-γ secretion and T-cell proliferation. In another assay, the effect of nivolumab on an antigen-specific T cell recall response was investigated using human PBMCs isolated from donors previously infected with cytomegalovirus (CMV). Following re-stimulation with CMV, nivolumab significantly enhanced cytokine release in a dose-dependent manner.

High levels of PD-1 on T cells isolated from patients with chronic infections has been correlated with T cell exhaustion, a process associated with downregulation of the immune response and failure to clear infections. For example, in HIV-infection, T-cell anergy correlated with high PD-1 expression levels has been reported to lead to reduced viral clearance, and PD-1 blockade improved T cell anti-viral responses, though the effect was highly variable (Rosignoli et al., 2009). Similar reports of T-cell exhaustion have been observed in hepatitis C virus (HCV) infection models. To determine the ability of nivolumab to reverse T cell exhaustion, the Applicant measured cytokine release from HCV-specific CD8+ T cells isolated from an individual with chronic HCV infection. In the presence of nivolumab, re-stimulation of PBMCs from this donor with a HCV peptide increased the number of CD8+ T cells and cytokine production by those cells. The Applicant also submitted a published study in which the authors (Wong RM, et al., 2007) demonstrated increases in the frequency of tumor antigen-specific T cells in vitro from a melanoma patient vaccinated with melanoma peptides following restimulation with those peptides in the presence of nivolumab; stimulation of the same cells with an irrelevant peptide had no effect on melanoma specific T cell function even in the presence of PD-1 blockade. Although all these assays used cytokine release as a surrogate measure for increased T cell response, nivolumab did not induce cytokine release from human PBMCs in the absence of T cell stimulation.

Since nivolumab does not recognize mouse PD-1, a surrogate anti-mouse PD-1 antibody (4H2) was derived to assess the efficacy of PD-1 blockade on tumor growth in syngenic tumor models. 4H2 was shown to bind to cells expressing murine PD-1 (2.9 nM) and inhibit binding of murine PD-1 to PD-L1 (EC_{50} = 3.6 nM) and PD-L2 (EC_{50} = 4.9 nM). The administration of anti-mouse PD-1 antibody 4H2 resulted in delayed tumor progression in the MC38 colon carcinoma, Sa1N fibrosarcoma, and J558 myeloma models, with complete tumor regressions observed in some individual mice in these studies. In these models, the administration of 4H2 at the time of tumor implantation (prophylactic/unstaged) or after tumors were established (therapeutic/staged) delayed or prevented the outgrowth of tumors. In four other syngeneic tumor models derived from renal cell carcinoma, 4T1 breast carcinoma, CT26 colon carcinoma, and B16F10 melanoma, tumors were refractory to treatment with 4H2.

While nivolumab bound to PD-1 from humans and cynomolgus monkeys to a similar extent, it did not bind to PD-1 from rodents or rabbits; accordingly, the cynomolgus monkey was chosen as the toxicology model for this drug. Nivolumab did not possess effector activity, as demonstrated by lack of binding to C1q or CD64. There was no evidence of cytokine release, as assessed by measuring cytokine levels following culture of hPBMCs in nivolumab -immobilized (air-dried) plates. Finally, in murine xenograft models, nivolumab exhibited anti-tumor activity when administered alone and in combination with other chemotherapeutic agents.

Nivolumab was evaluated in two repeat dose studies in the cynomolgus monkey and was well-tolerated in the monkey. In both the 4- and the 13-week studies, a diffuse pattern of inflammatory infiltration was observed in organs and tissues, but no target organ toxicity was identified by clinical pathology or histological analysis when

nivolumab was administered by weekly or twice-weekly IV injection to cynomolgus monkeys at doses of 1, 10 or 50 mg/kg/week for 13 weeks. This is consistent with data from an abbreviated histopathological study of adult mice in which increased incidences and/or severities of spontaneous inflammatory lesions were noted in the liver, kidney, and paws (joints and skin) of PD-1 pathway deficient animals relative to WT animals. An apparent decrease in mean body weight gain of treated males was noted in the 13-week study; however, aside from an increase in the incidence of diarrhea and/or soft feces for which there were no correlating histological findings in the GI tract, there were no other correlating clinical signs sufficient to explain the effect of treatment on body weight gain.

In the 13-week study, the thyroid hormones T3 and TSH levels were decreased in high dose females; however, there was no histological correlate and T4 levels were unaffected. Consistent with its mechanism of action, there was a trend toward an increase in CD4+ and CD8+ effector and central memory T cells, in the high dose group animals of the 13-week study. Exposures (AUC_{0-336}) in the 13-week study were up to 42-fold higher than the anticipated clinical AUCτ of 25500 µg*hr/mL when nivolumab is administered on a Q2Wk regimen.

The pattern of histological binding of nivolumab was assessed in normal cadaveric tissues obtained from both humans and cynomolgus monkeys. A broad pattern of immunoreactivity was observed in lymphocyte populations of many tissues evaluated, particularly circulating blood, breast, gut associated lymphoid tissue (GALT) of the small intestine, kidney, liver, lung, lymph node, spleen, ovary, pancreas, peripheral nerve, prostate, thymus, tonsil, urinary bladder, and uterus. The binding patterns were highly concordant between the two species and the pattern was consistent with both the known pattern of PD-1 RNA expression and its established subcellular distribution (membrane-associated). In addition, immunoreactivity was observed in the endocrine cells of the adenohypophysis and the thyroid in both species; however, because the subcellular staining pattern was cytoplasmic in these tissues, the physiological relevance of this finding is unclear.

The Applicant performed a number of studies to characterize the immunological consequences of chronic PD-1 deficiency in animals. A bronchopharyngeal ovalbumin challenge assay was conducted in WT and PD-1 deficient mice to evaluate the potential for PD-1 inhibition to exacerbate pulmonary reactivity following peripheral sensitization. In this study, there was an increase in airway reactivity of OVA-treated PD-1 deficient mice relative to WT OVA-treated mice, as measured by increased cellularity of the BALF (particularly of eosinophils, lymphocytes and neutrophils). This effect was statistically significant at 24 hours and persisted for at least 72 hours. Increased BALF cellularity was correlated with increases in TNFα, Ccl2, Ccr1, Ccl4, and IFN-γ, at 24 hours. Also correlated with the increases in BALF cytokines and cellularity in PD-1-deficient animals were increased levels of IgG_1 relative to OVA-exposed WT animals; however, the level of IgE in BALF was not affected by genotype in this study. It is noteworthy that levels of PD-1 ligand expression (especially PD-L1) were also

preferentially increased by OVA treatment in PD-1 KO mice relative to WT mice, as were levels of the anti-inflammatory cytokine, IL-10.

The Applicant evaluated potential nivolumab-associated effects on reproduction in an expanded pre- and postnatal development study (EPPND) in the cynomolgus monkey. Forty-eight experimentally naïve, pregnant dams (16/group) received saline or nivolumab (10 or 50 mg/kg/dose) twice weekly beginning on GD20, 21, or 22 (depending on the day of pregnancy confirmation by ultrasound) and continuing until parturition or pregnancy loss. Dams were allowed to give birth naturally and raise their infants through Postpartum Day 182±1.There were no effects of nivolumab treatment on maternal viability, clinical signs, feed consumption, body weight, or clinical pathology parameters. There were no histopathological changes associated with nivolumab administration in dams that were euthanized due to pregnancy loss; dams that survived to the end of the study (PPD 182±1) were returned to the holding colony and were not euthanized.

Treatment of monkeys with nivolumab did result in dose-related increases in first- and third-trimester pregnancy losses relative to concurrent and/or historical controls, and an increase in the incidence of infant loss among dams in the 10 mg/kg dose group compared with either concurrent or historical controls. When adjusted for the difference in dosing interval, maternal exposures (AUC) in this study were between 9.1 (at the 10 mg/kg dose level) and 42-fold (at the 50 mg/kg dose level) greater than those anticipated clinically when administered at the recommended dose of 3 mg/kg every 2 weeks and fetal exposures were between 2.3 and 9.6-fold above anticipated peak exposures of 116 µg/mL when administered on the 3 mg/kg Q2Wk schedule.

There were no malformations observed and aside from one finding of thyroid follicular hypertrophy/hyperplasia in a fetus in the 10 mg/kg dose group that was aborted on GD124, there were no gross or histopathological lesions in infants that died prior to scheduled termination. The cause of death for infants in the 10 mg/kg dose group was ascribed to prematurity and failure to thrive.

In surviving infants, there were no effects of prenatal nivolumab exposure on neurobehavioral, immunological, or clinical pathology parameters throughout the postnatal observation period, and no gross or histopathological findings associated with nivolumab administration at scheduled termination. Prenatal exposure to nivolumab did not affect attainment of immunity to either HBsAg or TT when infants were inoculated during the neonatal period, and there was no effect of nivolumab exposure on the lymphocyte subsets in circulating tissues or lymphoid organs. Interestingly, there was a consistent dose-dependent trend towards an increased antibody recall response to HBsAg following the 2nd antigen exposure in animals from nivolumab treated dams versus controls; while this finding was not indicative of statistically significant changes it does suggest the potential for heightened recall responses in nivolumab-treated patients.

The Applicant also evaluated the effect of nivolumab administration on the attainment of immunity in the cynomolgus monkey following administration of three different antigens, hepatitis B surface antigen (HBsAg; IM), DNP-Ficoll (ID) and SKMel cells (SC). While animals treated with nivolumab appeared to mount a slightly greater antibody response to SKMel than control (saline)-treated animals, the magnitude of the difference was small, and the response of nivolumab-treated animals to HBsAg was comparable to that of controls. There was no response to DNP-ficoll in any group. Immunophenotyping revealed that nivolumab treatment increased levels of memory CD4+ T cells and decreased levels of naïve CD4+ T cells relative to controls, which is consistent with the proposed mechanism of action.

While data in monkeys suggests that nivolumab did not suppress their ability to mount an immune response to certain challenges, data in PD-1-deficient animal models raise concerns about the use of nivolumab in patients with chronic infections. In many models of chronic infection (particularly viral infection models), PD-1 expression is associated with T cell anergy and increased susceptibility; however, in other contexts, loss of PD-1 is associated with heightened susceptibility and increased mortality. PD-1-deficient mice (C57BL/6) infected with *M. tuberculosis* exhibited a dramatic decrease in survival (Figure 44 upper L panel), which correlated with uncontrolled bacterial proliferation (Figure 44, upper R panel; dark bars = WT) and a larger inflammatory response in the lungs of PD-1-deficient mice compared with wild type controls (Figure 44, lower panel; dark bars = WT). Thus, PD-1 appears to be required to control infection and the inflammatory responses in the lungs of mice infected with M. tuberculosis (Lazar-Molnar, et al., 2010); however, the pathogenesis of this observation has not been clearly-defined. In particular, it is unclear whether the decreased survival reflects rampant bacterial growth resulting from an inability to mount appropriate antibacterial responses and/or whether it is a failure to downregulate the immune reaction that leads to massive tissue destruction and organ failure.

Figure 42: Decreased survival, increased bacterial proliferation and increased inflammation in PD-1-deficient mice infected with M. tuberculosis

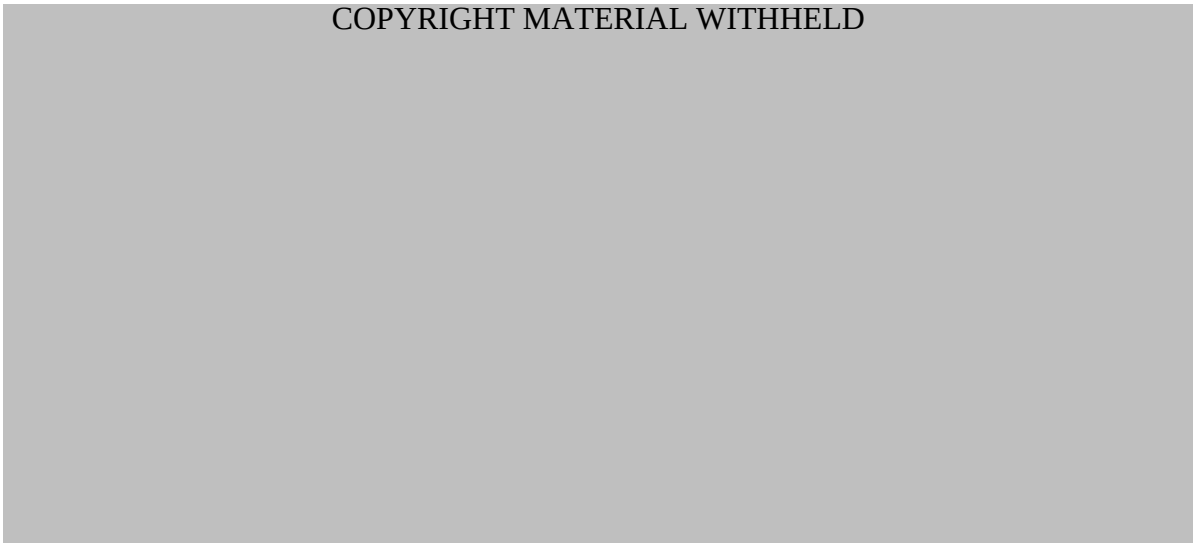

Derived from: Lazar-Molnar, et al., 2010.

The potential for increased toxicity in the presence of nivolumab may also be a concern following viral infection. In mouse models of LCMV infection the absence of PD-1 pathway signaling resulted in fatal CD8+ T cell mediated pathology due to killing of virally infected endothelial cells resulting in cardiovascular collapse (Frebel et. al., 2012; Mueller et. al., 2010). These data suggest that administration of nivolumab to patients with acute or chronic viral infections may result in stronger immune reactions and increased toxicity compared to uninfected patients.

12. References

Amaranth, S., *et al*., 2011. The PDL1-PD1 Axis Converts Human TH1 Cells into Regulatory T Cells. Sci. Transl. Med. 3(111):1-13.

Fife, B.T., and J. A. Bluestone, 2008. Control of peripheral T-cell tolerance and autoimmunity via the CTLA-4 and PD-1 pathways. Immun. Rev. 224:166-182.

Frebel, H., *et. al.*, 2012. Programmed death 1 protects from fatal circulatory failure during systemic virus infection of mice. J. Exp. Med., 209(13):2485-2499.

Keir, ME. *et al*., 2008. PD-1 and its ligands in tolerance and immunity. Ann. Rev. Immunol. 26:677-704.

Lazar-Molnar, *et al*., 2010. Programmed death-1 (PD-1)–deficient mice are extraordinarily sensitive to tuberculosis. PNAS. 107(30):13402-13407.

Mueller, S.N., *et. al*., 2010. PD-L1 has distinct functions in hematopoietic and nonhematopoietic cells in regulating T cell responses during chronic infection in mice. J. Clin. Invest. 120:2508-2515.

Okazaki, T and Honjo, T, 2007. PD-1 and PD-1 ligands: from discovery to clinical application. International Immunology. 19(7):813–824.

Rosignoli, G., et al., 2009. Programmed death (PD)-1 molecule and its ligand PD-L1 distribution among memory CD4 and CD8 T cell subsets in human immunodeficiency virus-1-infected individuals. Clin Exp Immunol. 157(1):90-97.

Sharpe, AH, *et al*., 2007. The function of programmed cell death 1 and its ligands in regulating autoimmunity and infection. Nature Immunology. 8(3):239-245.

Wang, *et al*., 2011. Phenotype, effector function, and tissue localization of PD-1-expressing human follicular helper T cell subsets. BMC Immunology. 12:53.

Wong, *et al*., 2007. Programmed death 1 blockade enhances expansion and functional capacity of human melanoma antigen-specific CTLs. Int Immunol. 19:1223-1234.

This is a representation of an electronic record that was signed electronically and this page is the manifestation of the electronic signature.

/s/

SHAWNA L WEIS
12/04/2014

ALEXANDER H PUTMAN
12/04/2014

WHITNEY S HELMS
12/04/2014

PHARMACOLOGY/TOXICOLOGY FILING CHECKLIST FOR NDA/BLA or Supplement

NDA/BLA Number: 125,554 **Applicant: Bristol-Meyers Squibb** **Stamp Date: 30 July 2014**

Drug Name: Nivolumab **BLA Type:Priority**

On **initial** overview of the NDA/BLA application for filing:

	Content Parameter	Yes	No	Comment
1	Is the pharmacology/toxicology section organized in accord with current regulations and guidelines for format and content in a manner to allow substantive review to begin?	X		
2	Is the pharmacology/toxicology section indexed and paginated in a manner allowing substantive review to begin?	X		
3	Is the pharmacology/toxicology section legible so that substantive review can begin?	X		
4	Are all required (*) and requested IND studies (in accord with 505 b1 and b2 including referenced literature) completed and submitted (carcinogenicity, mutagenicity, teratogenicity, effects on fertility, juvenile studies, acute and repeat dose adult animal studies, animal ADME studies, safety pharmacology, etc)?	X		
5	If the formulation to be marketed is different from the formulation used in the toxicology studies, have studies by the appropriate route been conducted with appropriate formulations? (For other than the oral route, some studies may be by routes different from the clinical route intentionally and by desire of the FDA).	X		No issues were identified to date. This will be assessed during the review.
6	Does the route of administration used in the animal studies appear to be the same as the intended human exposure route? If not, has the applicant submitted a rationale to justify the alternative route?	X		
7	Has the applicant submitted a statement(s) that all of the pivotal pharm/tox studies have been performed in accordance with the GLP regulations (21 CFR 58) or an explanation for any significant deviations?	X		Individual reports state compliance with US GLP regulations, and deviations from GLP regulations were noted. The impact of any GLP deviations will be assessed during the review.
8	Has the applicant submitted all special studies/data requested by the Division during pre-submission discussions?	X		

PHARMACOLOGY/TOXICOLOGY FILING CHECKLIST FOR NDA/BLA or Supplement

	Content Parameter	Yes	No	Comment
9	Are the proposed labeling sections relative to pharmacology/toxicology appropriate (including human dose multiples expressed in either mg/m2 or comparative serum/plasma levels) and in accordance with 201.57?	X		
10	Have any impurity – etc. issues been addressed? (New toxicity studies may not be needed.)	X		To date, no impurities have been identified that require pharm/tox input.
11	Has the applicant addressed any abuse potential issues in the submission?			Not applicable
12	If this NDA/BLA is to support a Rx to OTC switch, have all relevant studies been submitted?			Not applicable

IS THE PHARMACOLOGY/TOXICOLOGY SECTION OF THE APPLICATION FILEABLE? ____YES____

If the NDA/BLA is not fileable from the pharmacology/toxicology perspective, state the reasons and provide comments to be sent to the Applicant.

Please identify and list any potential review issues to be forwarded to the Applicant for the 74-day letter.

Reviewing Pharmacologist Date

Team Leader/Supervisor Date

File name: 5_Pharmacology_Toxicology Filing Checklist for NDA_BLA or Supplement 010908

This is a representation of an electronic record that was signed electronically and this page is the manifestation of the electronic signature.

/s/

SHAWNA L WEIS
09/11/2014

WHITNEY S HELMS
09/11/2014